NON-MARKOVIAN DYNAMICS OF OPEN QUANTUM SYSTEMS

by
Carole Addis

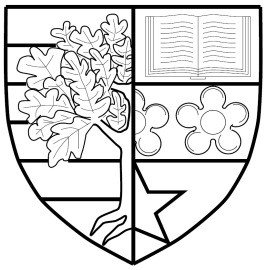

Submitted for the degree of
Doctor of Philosophy

Institute of Photonics and Quantum Sciences
School of Engineering and Physical Sciences
Heriot-Watt University

May 2016

Abstract

This thesis is centred around the striking phenomenon of non-Markovianity which emanates from exact dynamical descriptions of open quantum systems. Non-Markovianity is associated with the existence of memory effects in the environment and leads to a partial recovery of information of the system, temporarily counteracting the deleterious effect of the surrounding environment. We devote this thesis to addressing two fundamental questions surrounding the topic of non-Markovianity. The first is concerned with how to evaluate the extent to which a specific dynamics is non-Markovian, in terms of a physically meaningful and easily computable measure. In literature, the desire to quantify non-Markovianity has motivated a plethora of measures which provide unique, albeit potentially contradicting, interpretations of memory effects. In an attempt to consolidate the literature, we introduce and critically compare several recently proposed non-Markovianity measures for single qubit and two qubit systems in both pure dephasing and dissipative scenarios. The second question explores the natural optimism of the usefulness of non-Markovianity as a resource in quantum information protocols. In more detail, we study whether memory effects combined with external control techniques offer a possibility to exploit non-Markovianity for an overall superior technique to combat decoherence. The standard approach for Markovian dynamics involves the critical assumption of dissipative dynamics which are fixed in the presence of control. We expose the serious pitfalls in experimentally implementing such a strategy in realistic non-Markovian scenarios and accentuate the importance of using exact approaches in non-Markovian control theory. Using an exact description of a pure dephasing system subject to dynamical decoupling protocols, we demonstrate that contrary to intuitive reasoning, non-Markovianity is not trivially a resource.

Acknowledgements

I would like to first thank my supervisor Prof. Sabrina Maniscalco for her never-ending encouragement, advice, enthusiasm and friendship throughout these past few years. I realise how incredibly lucky I am to have had a supervisor such as you throughout this experience and you have inspired me massively in many, many ways, even ways outside of physics. You are someone I hope I will always have in my life. Also, a huge thanks goes to Pinja, Elsi, Massimo, Suzanne and Stephen. You have been big sisters and brothers to me throughout this experience and I appreciate all the support and encouragement you have given me. Particularly, I am very fortunate to have had not one but four amazing women, Sabrina, Elsi, Pinja and Suzanne to look up to. I know too well how rare an experience this is in physics and I am so grateful to know each of you.

This work is dedicated to my family, Joshua, mum, dad and Sarah as without each of you, I never would have completed it. Thank you for being there during all the hard times which are inevitable when completing a Ph.D. and never failing to support me through them. Particularly, to my husband, mum and dad, I can not begin to thank you enough for the constant love and encouragement you have given me from school, to undergraduate years to postgraduate years. To my dad, I started physics because you studied physics and I always wanted to be like you from as long as I can remember so really, this thesis exists because of you. I am lucky to also have very close friends I count as family who have supported me massively throughout these years, Jasmyn, Jenna, Elle and Stewart.

Thanks also goes to all the friends I have made along the way and who have joined me on this journey, to mention a special few, Lawrence, Jack, Charlotte, Yvan and Ollie. Thank you also to all the collaborators included in the projects which contribute to the work completed during my Ph.D, including Dr. Bogna Bylicka, Prof. Dariusz Chruściński, Dr. Clemens Gneiting, Prof. Massimo Palma, Dr. Francesco Ciccarello, Dr. Göktuğ Karpat, Gregoire Brebner, Prof. Chiara Macchiavello, Dr. Teiko Heinosaari and Dr. Jukka Kiukas. Thank you to Dr. Gabriele de Chiara for hosting me at Queens University, Belfast just prior to beginning my Ph.D., the discussions we had during this time helped me immensely in the years to follow. I also would like to thank Prof. Ian Galbraith for stepping in to be my "Edinburgh supervisor" in these past years and for the kind support that has come with that. Lastly, I would like to thank the Scottish Doctoral Training Centre in Condensed Matter Physics for the financial support of this Ph.D., particularly I extend a huge thanks to Dr. Julie Massey and Christine Edwards for their careful organisation of everything Ph.D. related and genuine care and support throughout these years.

List of Publications

This thesis consists of an introductory review and the following publications [1]-[4]:

i C. Addis, B. Bylicka, D. Chruściński and S. Maniscalco, *Comparative study of non-Markovianity measures in exactly solvable one and two qubit models*, Physical Review A **90**, 052103 (2014).

ii C. Addis, E-M Laine, C. Gneiting and S. Maniscalco, *The problem of coherent control in non-Markovian open quantum systems*, arXiv:1604.07998 (2016), in the process of publication.

iii C. Addis, F. Ciccarello, M. Cascio, G. M Palma and S. Maniscalco, *Dynamical decoupling efficiency versus quantum non-Markovianity*, New Journal of Physics **17**, 123004 (2015).

iv C. Addis, G. Karpat and S. Maniscalco, *Time-Invariant discord in dynamically decoupled systems*, Physical Review A **92**, 062109 (2015).

Other papers published as a postgraduate student but not included in this thesis [5]-[8]:

i C. Addis, P. Haikka, S. McEndoo, C. Macchiavello and S. Maniscalco, *Two-qubit non-Markovianity induced by a common environment*, Physical Review A **87**, 052109 (2013).

ii C. Addis, G. Brebner, P. Haikka and S. Maniscalco, *Coherence trapping and information back-flow in dephasing qubits*, Physical Review A **89**, 024101 (2014).

iii C. Addis, T. Heinosaari, J. Kiukas, E-M. Laine and S. Maniscalco, *Dynamics of incompatibility of quantum measurements in open systems*, Physical Review A **93**, 022114 (2016).

iv C. Addis, G. Karpat, C Macchiavello and S. Maniscalco, *Memory effects in correlated quantum Channels*, arXiv:1607.00134 (2016), accepted for publication in Physical Review A.

v G. Karpat, C. Addis and S. Maniscalco, *Frozen and invariant quantum discord under local dephasing noise*, found in *Lectures on general quantum correlations and their applications*. to be published by Springer (2016).

Contents

1 Introduction **1**

2 The Theory of Open Quantum Systems **5**

2.1 Closed Quantum Systems 5

2.1.1 Density Operator Formulation 6

2.1.2 Bloch Vector Notation 7

2.2 Open Quantum Systems 8

2.3 Markovian Master Equations 9

3 Defining Non-Markovianity **13**

3.1 Non-Markovian Master Equations 13

3.2 Non-Markovianity Measures 15

3.2.1 Rivas, Huelga, Plenio Measure 15

3.2.2 Breuer, Laine, Piilo Measure 16

3.2.3 Luo, Fu, Song Measure 18

3.2.4 Bylicka, Chruściński, Maniscalco Measure 19

3.2.4.1 Entanglement-Assisted Classical Capacity 20

3.2.4.2 Quantum Capacity 20

3.3 Comparison for Pure Dephasing Dynamics 21

3.3.1 Single qubit: The Model 21

3.3.2 Single qubit: The Measures 24

3.3.3 Two qubits: The Model 27

3.3.4 Two qubits in independent environment: The Measures 28

3.3.5 Two qubits in common environment: The Measures 29

3.4 Comparison for the Amplitude Damping Channel 32

3.4.1 Single qubit: The Model 32

3.4.2 Single qubit: The Measures 34

3.4.3 Two qubits: The Model 37

3.4.4 Two qubits in independent environment: The Measures 38

3.5 Discussions 39

3.5.1 Comparison of the Measures 39

3.5.2 Practical Applications of Non-Markovianity 40

3.6 Conclusion . . . 41

4 Optimal Control in Non-Markovian Systems 43

4.1 Markovian Optimal Control . . . 43

4.1.1 Two-Point Cycles . . . 45

4.2 Non-Markovian Optimal Control: Phenomenological Case . . . 47

4.2.1 Optimal Control in a Dephasing Model . . . 47

4.2.2 Generality of Fixed Dissipator Assumption . . . 52

4.3 Non-Markovian Optimal Control: Exact Case . . . 53

4.4 Conclusion . . . 57

5 Dynamical Decoupling in Non-Markovian Systems 58

5.1 Introduction to Dynamical Decoupling . . . 58

5.2 Dynamical Decoupling: The model . . . 59

5.3 Relationship between non-Markovianity and Dynamical Decoupling Protocols . . . 61

5.3.1 Pulse-induced information flow reversal . . . 61

5.3.2 Efficiency versus Non-Markovianity measure . . . 63

5.3.3 Non-Markovianity Engineering by Dynamical Decoupling . . . 66

5.4 Dynamical Decoupling with Quantum Correlations . . . 68

5.4.1 Introduction to Quantum Correlations . . . 68

5.4.1.1 Entanglement . . . 68

5.4.1.2 Quantum Discord . . . 69

5.4.2 Time Invariant Discord . . . 71

5.4.3 Dynamically Decoupled Correlations . . . 75

5.5 Conclusions . . . 76

6 Conclusions 78

Appendices 80

A Further Dynamical Description 81

B Optimisation Evidence 83

Bibliography 85

Chapter 1

Introduction

The idealised description of closed quantum systems comprises pure quantum states evolving according to unitary dynamics, determined by the solution of the Schrödinger equation. However, in reality, it is a simplification to assume a quantum system is entirely isolated from its surrounding environment because this in general is never true. The impossibility of legitimately isolating a quantum system from the environment has led to the theory of open quantum systems distending into all subfields of quantum physics [9]-[11]. The adverse influence of the environment induces the so-called quantum to classical transition, destroying the two defining features of quantum mechanics, namely, quantum superpositions and entanglement [12]. Hence, the obstacle in the development of quantum technologies is only apparent when the effect of the environmental noise is incorporated into the system dynamics. In order for quantum technologies to reach the market, environmental-induced decoherence must be understood and minimised to an acceptable degree below the threshold for quantum error correction. Tremendous progress in quantum technologies has encouraged an endeavour to minimise environment-induced decoherence effects [13]-[18]. Moreover, the role of non-Markovianity in biological systems has been recently identified [19]-[20]. In light of this, we study non-Markovianity from two fundamental points of view. Specifically, the characterisation of non-Markovianity in an easily computable and physically relevant quantifier [1], and also, the possibility of exploiting non-Markovianity as a resource in quantum protocols [2]-[3].

The dynamics of an open quantum system is described by a completely positive and trace-preserving map, known as the dynamical map, and is classified into Markovian and non-Markovian regimes. However, Markovian memoryless dynamics generally rely on the validity of certain assumptions and are often only an approximation of exact non-Markovian descriptions when memory effects are intertwined with the dynamics in a non-negligible way. Indeed, Markovian descriptions imply a continuous loss of quantum information from the system to the environment and fail to describe scenarios with strong system-environment couplings or when the timescales characterising the environment and system are comparable. Non-

Markovian dynamics are derived in the absence of approximations and are marked by revivals of information for intervals of time, temporarily combating the stripping effect of the environment. While the defining features of a Markovian evolution are firmly established, the definition of a non-Markovian evolution has given rise to a heated debate. Specifically, for Markovian dynamics, the non-unitary dynamics must necessarily correspond to a completely positive and trace-preserving dynamical map which can be concatenated into a collection of individual dynamical maps governing respective time intervals. The mathematical property is coined divisibility and corresponds to the physical intuition of memoryless dynamics being independent of past dynamics. In Chapter 3, we introduce several recently proposed measures of non-Markovianity and critically compare the merit of each measure [1]. More specifically we investigate and compare their computability, their physical meaning, their Markovian to non-Markovian crossover, and their additivity properties with respect to the number of qubits. Following the characterisation of Markovian dynamics, it is clear that when the dynamics is divisible any well-founded non-Markovianity measure must take zero value, but the converse is not required to be true. Only the Rivas, Huelga and Plenio (RHP) [21] measure quantifies non-Markovianity as the degree of deviation from divisible dynamics and so entirely characterises every non-divisible dynamics as non-Markovian. Alternatively, non-Markovianity can be based on the non-monotonicity of the evolution of a certain quantum quantity when the dynamics is non-divisible. In this framework, we consider the Breuer, Laine and Piilo (BLP) [22]-[23], Luo, Fu, Song (LFS) [24] measure and the Bylicka, Chruściński, Maniscalco (BCM) [16] measures. We study the qualitative behaviour of the measures for one and two qubit systems for dephasing and dissipative dynamics, particularly focusing on the Markovian/non-Markovian crossover for experimental system parameters. We find for the dephasing models [25]-[27], the measures always agree in terms of crossover but the contrary is not always true for the dissipative models [9],[28]. Our comparison is not motivated by a desire to appoint one measure the single defining measure of non-Markovianity, but to instead bring to light the useful insights of non-Markovianity each measure offers.

Recently, many efficient schemes have been developed which utilise external protocols, such as the quantum Zeno effect [29]-[31], dynamical decoupling strategies [130]-[131] and optimal control [34], [35]-[45], in order to compensate for the harmful noise in quantum systems. Generally, the theoretical description of these techniques in the presence of noise is a daunting task and as a consequence, control techniques have been studied almost exclusively in the so-called Markovian limit. In this limit, the dynamics are either derived using microscopic approaches involving assumptions concerning the type of environments the system is interacting with as well as the typical time-scales or found phenomenologically. It is therefore important to extend the investigation of control protocols in open quantum systems to the non-Markovian

regime, where strong and long lasting memory effects become apparent in the dynamics and play an important role in describing realistic experimental scenarios. Moreover, many have naturally wondered whether memory effects combined with external control techniques offer a possibility to design an overall superior technique to combat decoherence [46]-[48]. The aim of Chapter 4 is to expose the serious pitfall of applying the most widespread assumption in the theoretical description of coherent control strategies to non-Markovian open systems. In more detail, it is common in literature related to control theory, to assume that the description of the dephasing or dissipative dynamics of the system is fixed when we add a unitary control Hamiltonian term. This assumption is always valid in the Markovian limit as it does not change the physicality of the solutions of the master equation but we show the converse is not in general true. In Chapter 4, we first explore the phenomenological case seen in literature for a non-Markovian system, where the dissipator is fixed under the control sequence [2]. In analogy to the control protocol introduced in Ref. [34], we seek a control Hamiltonian that, on average, optimally upholds the coherence between the ground and excited state of a qubit for the time the system markedly evolves. Our results expose the unsurmountable difficulties in implementing such an approach experimentally and further, we show, in general, the origin of the physical uncertainty that exists. Indeed, we are able to link the potential failure of such a strategy directly to the intrinsic defining feature of all non-Markovian dynamics, namely non-divisibility. We show that the only way to avoid this problem is a full microscopic description of the controlled system in the presence of noise. Hence the typical theoretical approaches to quantum control theory cannot be used in the framework of non-Markovian open quantum systems, and only a full microscopic derivation leads to physically meaningful results. In general, it is clear that, in absence of the fixed dissipator approximation, constructing superior trajectories (i.e. trajectories which are optimally controlled with varying degrees of rotation) will never be a feasible task. A possible solution to this impasse might be the discovery of certain special forms of non-Markovian dissipators that may not be changing sensibly in the presence of some specific coherent control schemes, perhaps exploiting specific symmetries of the dissipator and control Hamiltonian.

In Chapter 5, we study an exact description of a purely dephasing qubit subject to dynamical decoupling (DD) protocols [3]-[4], first introduced in Ref. [49]. DD techniques are among one of the most successful control protocols to suppress decoherence in qubit systems [50, 51] and rely on the application of a sequence of external pulses to a system in order to reverse the catastrophic effects of the environment for the duration of the sequence. For the first time, we investigate this model in order to connect the efficiency of dynamical decoupling with the reservoir spectral density through an experimental parameter of the environment, namely the Ohmicity parameter. Specifically, through this parameter, one has the ability

to model both Markovian and non-Markovian dynamics. With this in mind, we are curious to establish the role of non-Markovianity as a resource in DD protocols, quantifying dynamical decoupling efficiency as the average coherence preservation over the pulse sequence. We find that simultaneous use of non-Markovian reservoir engineering and DD protocols is counterproductive for coherence preservation. With a shift in perspective, we further reveal how dynamical decoupling techniques can be harnessed to engineer non-Markovianity and control it. In more detail, any system subject to DD will provide a testbed for further investigation of non-Markovian dynamics, independently of the Ohmicity parameter. With a relationship between DD and non-Markovianity well established, we explore the implications in a quantum information scenario. It has been shown that the use of either DD techniques or non-Markovian effects prolongs the preservation of quantum correlations in the presence of environmental noise [52]-[57]. With this in mind, we consider two qubits undergoing local dephasing and in the spirit of reservoir engineering, attempt to identify the optimal conditions for sustaining quantum correlations. In more detail, we focus on modifying the spectrum to enhance either the efficiency of DD protocols or the non-Markovian character of the dynamics. In particular, we study the creation of time-invariant discord. Quantum discord is a measure for the total quantum correlations in a quantum state, beyond those captured by entanglement and has been shown to be crucial for e.g., distribution of entanglement [58]-[61], quantum locking [62], entanglement irreversibility [63] and many other tasks [64]-[65]. We show that given the choice, DD protocols are capable of creating higher values of time-invariant discord for a wider range of system parameters compared to that achieved with non-Markovianity [66].

In Chapter 7, we summarise and conclude the thesis.

Chapter 2

The Theory of Open Quantum Systems

The impossibility of entirely isolating a quantum system has made the theory of open quantum systems fundamental to developing quantum devices which are robust against the inevitable destructive effects of the environment. This chapter is devoted to introducing the basic principles and mathematical formalism developed for open quantum systems. More specifically, I first introduce the idealised description of closed quantum systems, where the modification of the environment to the dynamics is not included. The open quantum system theory is then constructed by reducing the total closed system dynamics to the description of the system of interest only.

2.1 Closed Quantum Systems

The most complete description of the state of a quantum system at a given time $t = t_0$ is provided by a state vector $|\psi(t_0)\rangle$, belonging to a Hilbert space $\mathcal{H}$ associated to the physical system. According to the superposition principle, any linear superposition of N quantum states is also a quantum state:

$$|\psi\rangle = \sum_{n=1}^{N} a_n |\psi_n\rangle . \tag{2.1}$$

The probability of finding the system $|\psi\rangle$ in the state $|\psi_n\rangle$ after an appropriate measurement is $|a_n|^2$ if $|\psi\rangle$ is normalised and $|\psi_n\rangle$ are orthonormal states so the coefficients a_n satisfy the constrain $\sum_{n=1}^{N} |a_n|^2 = 1$.

The time evolution of the state vector is determined by the solution of the Schrödinger equation,

$$i\hbar \frac{d}{dt} |\psi(t)\rangle = \mathbf{H} |\psi(t)\rangle \tag{2.2}$$

where $\mathbf{H}$ is the Hamiltonian of the system and $\hbar$ is Planck's constant. The dynamics generated by Eq. 2.2 is unitary and the solution may be represented in terms of the

unitary time-evolution operator $\mathbf{U}(t, t_0)$ which transforms the state $|\psi(t_0)\rangle$ at some initial time t_0 to the state $|\psi(t)\rangle$ at time t,

$$|\psi(t)\rangle = \mathbf{U}(t, t_0)\,|\psi(t_0)\rangle\,, \qquad \mathbf{U}^{\dagger}(t, t_0) = \mathbf{U}^{-1}(t, t_0). \tag{2.3}$$

The evolution operator for a time-independent Hamiltonian takes the simple form $\mathbf{U}(t, t_0) = \exp\{-i\mathbf{H}(t - t_0)/\hbar\}$.

2.1.1 Density Operator Formulation

It possible to interpret the wavefunction ψ as a statistical ensemble ϵ of identically prepared quantum systems $S^{(1)}, S^{(2)}, ..., S^{(N)}$ that could possibly result from a specific set of experimental conditions [9],

$$\epsilon = \{S^{(1)}, S^{(2)}, ..., S^{(N)}\}. \tag{2.4}$$

Observations on each individual system define the abstract set of probabilities for the various observables. In realistic situations, where the state preparation is not fully known, it is convenient to consider an ensemble composed of M ensembles $\epsilon_1, \epsilon_2, ..., \epsilon_M$, each described by a normalised state vector ψ_α, $\alpha = 1, 2, ..., M$ in the underlying Hilbert space $\mathcal{H}$. The statistics of the total ensemble is given as a weighted sum of the individual ensembles, where the respective weights w_α satisfy

$$w_\alpha \geq 0, \qquad \sum_{\alpha=1}^{M} w_\alpha = 1. \tag{2.5}$$

In order to describe the total statistical ensemble ϵ, we introduce the density operator,

$$\rho = \sum_{\alpha} w_\alpha\,|\psi_\alpha\rangle\,\langle\psi_\alpha|\,, \tag{2.6}$$

where the states $|\psi_\alpha\rangle$ are not assumed to be orthogonal vectors. The diagonalised form of the density matrix is then given as,

$$\rho = \sum_{i} \lambda_i\,|\Psi_i\rangle\,\langle\Psi_i|\,, \qquad \sum_{i} \lambda_i = 1, \qquad \lambda_i \geq 0, \tag{2.7}$$

with λ_i the non-negative real eigenvalues of the density matrix and $|\Psi_i\rangle$ the associated orthogonal eigenvectors of the Hilbert space $\mathcal{H}$, i.e. $\langle\Psi_i|\Psi_j\rangle = \delta_{ij}$ and $\sum_i |\Psi_i\rangle\,\langle\Psi_i| = \mathbb{I}$ where $\mathbb{I}$ is the identity operator. The strictly positive eigenvalues λ_i are finitely degenerate, and 0 is the only possible infinitely degenerate eigenvalue. The trace of an operator ρ i.e., the sum of the diagonal elements, is given as:

$$\mathrm{Tr}[\rho] = \sum_{i} \langle\Psi_i|\,\rho\,|\Psi_i\rangle = 1, \tag{2.8}$$

and it is straightforward to show that the trace operation is independent of the choice of orthogonal basis. The diagonal elements (coined the populations) $\langle\Psi_i|\,\rho\,|\Psi_i\rangle$ represent the probability of occupying state $|\Psi_i\rangle$. As well as unit trace, the density matrix must be Hermitian $\rho = \rho^\dagger$ and positive $\rho \geq 0$. In more detail, a Hermitian matrix satisfies:

$$\langle\Psi_i|\,\rho\,|\Psi_j\rangle^* = \langle\Psi_j|\,\rho\,|\Psi_i\rangle\,, \tag{2.9}$$

where the complex off-diagonal elements (coined coherences) $\langle\Psi_j|\,\rho\,|\Psi_i\rangle$ represent the quantum interference between the states $|\Psi_j\rangle$ and $|\Psi_i\rangle$. From the condition, 2.9, it is clear that the diagonal elements of the density operator must necessarily be real. The purity of a density matrix is calculated as follows:

$$\mu = \mathrm{Tr}[\rho^2] \leq \mathrm{Tr}[\rho]. \tag{2.10}$$

The system is unambiguously described by the pure state $|\psi_i\rangle$ if one of the probabilities is unit $p_i = 1$ and the purity of the density matrix is then given as $\mu = 1$. Otherwise the density operator is a so-called mixed state and $\frac{1}{d} \leq \mu < 1$ where d is the dimension of the Hilbert space of the system.

The dynamical equations governing the time evolution of the density operator for a closed quantum system is straightforward to obtain from Eq. 2.2 and is known as the von Neumann equation,

$$\frac{d}{dt}\rho(t) = -\frac{i}{\hbar}[\mathbf{H}, \rho] \tag{2.11}$$

where $[A, B] = AB - BA$ is the commutator of operators A and B. The solution is represented as follows,

$$\rho(t) = \mathbf{U}^\dagger(t, t_0)\rho(t_0)\mathbf{U}(t, t_0), \tag{2.12}$$

corresponding to unitary dynamics, preserving the purity of the state throughout the evolution.

2.1.2 Bloch Vector Notation

A qubit refers to a fundamental quantum system ψ, described by a two-dimensional complex vector space, where the two states of the system can be physically realised for e.g., by two spin states of a spin-$\frac{1}{2}$ particle, the vertical and horizontal polarisation states of a single photon or the ground and excited states of an atom. Analogous to the classical bit, i.e., the fundamental concept in classical computation and information theory, the qubit is the building block of quantum information protocols. However, while the qubit can be in either states $|0\rangle$ or $|1\rangle$, contrary to its classical counterpart, it can also be in a superposition of these states. The most general state

of a qubit is given as,

$$|\psi\rangle = \alpha\,|0\rangle + \beta\,|1\rangle \tag{2.13}$$

with $|\alpha|^2 + |\beta|^2 = 1$. Introducing the spherical polar coordinates $0 \leq \theta \leq \pi$ and $0 \leq \phi \leq 2\pi$, any pure state can be equivalently written as:

$$|\psi\rangle = \cos\frac{\theta}{2}\,|0\rangle + \sin\frac{\theta}{2}e^{i\phi}\,|1\rangle\,. \tag{2.14}$$

The parameters θ and ϕ define a point on the surface of a unit three-dimensional sphere called the Bloch sphere. In general, including also the arbitrary mixed state qubit describing points within the Bloch sphere, the density matrix may be written as:

$$\rho = \frac{\mathbb{I} + \vec{r}.\vec{\sigma}}{2}, \tag{2.15}$$

where $\vec{\sigma} = \{\sigma_x, \sigma_y, \sigma_z\}$ is the Pauli vector with,

$$\sigma_x = \begin{pmatrix} 0 & 1 \\ 1 & 0 \end{pmatrix}, \quad \sigma_y = \begin{pmatrix} 0 & -i \\ i & 0 \end{pmatrix}, \quad \sigma_z \begin{pmatrix} 1 & 0 \\ 0 & -1 \end{pmatrix} \tag{2.16}$$

and $\vec{r} = \{r_x, r_y, r_z\}$ is the Bloch vector i.e., a real three-dimensional vector satisfying the condition $||\vec{r}|| \leq 1$ with Bloch vector components,

$$r_x = r\cos\phi\sin\theta, \quad r_y = r\sin\phi\sin\theta, \quad r_z = r\cos\theta. \tag{2.17}$$

2.2 Open Quantum Systems

The observation and experimental control of characteristic quantum properties of physical systems is often strongly hindered by the coupling of the system to a noisy environment [67]. The inevitable environmental interaction creates non-negligible system-environment correlations leading to vanishing quantum features and/or dissipation of energy. Realistic quantum systems are therefore open systems governed by a non-unitary time evolution. In order to take into account the interaction with the environment in the dynamical description of the system, we first consider a closed bipartite environment consisting of the system of interest S and an environment E. Hence, the dynamics can be written as:

$$\rho_{SE}(t) = \mathbf{U}^{\dagger}_{SE}(t, t_0)\rho_{SE}(t_0)\mathbf{U}_{SE}(t, t_0), \tag{2.18}$$

where $\rho_{SE}(t_0)$ is the initial state of the full system plus environment. We can define the state of each subsystem by performing the partial trace operation on the

composite state $\rho_{SE} \in \mathcal{D}(\mathcal{H})$ with $\mathcal{H} = \mathcal{H}_S \otimes \mathcal{H}_E$,

$$\rho_S(t) = \mathrm{Tr}_E[\rho_{SE}] = \sum_j \langle \Psi_j^E | \, \rho_{SE} \, | \Psi_j^E \rangle \tag{2.19}$$

where $\{|\Psi_j^E\rangle, j = 1, 2, ...\}$ is an orthogonal basis in $\mathcal{H}_E$. In this way, one can define the non-unitary dynamics of the reduced state $\rho_S(t)$ as

$$\rho_S(t) = \Phi_{t,t_0} \rho_S(t_0), \tag{2.20}$$

where Φ_{t,t_0} is $t-$parametrised completely positive and trace preserving (CPTP) map, known as the dynamical map [68]-[70]. In contrast to closed system dynamics, the states evolving according to the dynamical map experience decoherence, describing the transformation from coherent superpositions (pure states) to incoherent superpositions, i.e. statistical mixtures (mixed states) [71]-[73]. To restrict the transformations associated with the dynamical map to the space of physical states, the map must be completely positive and trace-preserving, i.e., it must be linear. Complete positivity means that not only is Φ positive, i.e., $\Phi(\rho) > 0$, but also the combined operation $\Phi \otimes \mathbb{I}_d$ for all dimensions d [74]-[75]. Physically, the combined map acts locally on only one of the two separated systems while the second system evolves without effect. The functional form of any completely positive map Φ_{t,t_0} can be characterised by the operator sum representation or the Kraus representation [76],

$$\Phi_{t,t_0} = \sum_{i,j} W_{ij}(t) \rho(t_0) W_{ij}^\dagger(t) \qquad \sum_{i,j} W_{ij}^\dagger(t) W_{ij}(t) = \mathbb{I} \tag{2.21}$$

where from the spectral decomposition of the environment $\rho_E = \sum_i \lambda_i^E \, |\Psi_i^E\rangle \langle \Psi_i^E|$, $\sum_i \lambda_i^E = 1$, the Kraus operators $W_{ij}(t)$ are

$$W_{ij}(t) = \sqrt{\lambda_j^E} \, \langle \Psi_i^E | \, \mathbf{U}_{SE}(t, t_0) \, | \Psi_j^E \rangle \, . \tag{2.22}$$

2.3 Markovian Master Equations

We now examine an equivalent approach to determine the dynamics of the open quantum system, using an equation of motion for the reduced system dynamics, known as the master equation. In more detail, we provide the general microscopic derivation of a local in time master equation, valid for weakly coupled systems [9].

The most general open system model can be described by the following Hamiltonian structure:

$$\mathbf{H} = \mathbf{H_S} \otimes \mathbb{I}_E + \mathbb{I}_S \otimes \mathbf{H_E} + \alpha \mathbf{H_I}(t) \tag{2.23}$$

where $\mathbf{H}_S$ is the system free Hamiltonian, $\mathbf{H}_E$ is the reservoir free Hamiltonian, α is a dimensionless constant and $\mathbf{H}_I(t)$ is the interaction term. For convenience,

we consider the dynamics in the interaction picture where the transformations for interaction Hamiltonian and density matrix of the total system $\rho_{SE}(t)$ are given as,

$$\begin{aligned}\tilde{\mathbf{H}}_{\mathbf{I}}(\mathbf{t}) &= e^{i(H_S+H_E)t}\mathbf{H}_{\mathbf{I}}(\mathbf{t})e^{-i(H_S+H_E)t} \\ \tilde{\rho}_{SE}(t) &= e^{i(H_S+H_E)t}\rho_{SE}(t)e^{-i(H_S+H_E)t}\end{aligned} \tag{2.24}$$

The von Neumann equation in the interaction picture, now dependent only on the interaction Hamiltonian and the state of the system plus environment, reads,

$$\frac{d}{dt}\tilde{\rho}_{SE}(t) = -i\alpha[\tilde{\mathbf{H}}_I(t), \tilde{\rho}_{SE}(t)]. \tag{2.25}$$

A formal integration of the equation of motion above leads to,

$$\tilde{\rho}_{SE}(t) = \tilde{\rho}_{SE}(0) - i\alpha \int_0^t ds\, [\tilde{\mathbf{H}}_I(s), \tilde{\rho}_{SE}(s)]. \tag{2.26}$$

Inserting Eq. 2.26 into Eq. 2.25, we have

$$\frac{d}{dt}\tilde{\rho}_{SE}(t) = -i\alpha[\tilde{\mathbf{H}}_I(t), \tilde{\rho}_{SE}(0)] - \alpha^2 \int_0^t ds\, [\tilde{\mathbf{H}}_I(t), [\tilde{\mathbf{H}}_I(s), \tilde{\rho}_{SE}(0)]] + \mathcal{O}(\alpha^3), \tag{2.27}$$

where we assumed the initial time $t_0 = 0$ without any lack of generality. We assume that the system can be prepared in a state that is not correlated with its environment, i.e. the initial state of the system and the environment is factorised $\tilde{\rho}_{SE}(0) = \tilde{\rho}_S(0) \otimes \tilde{\rho}_E(0)$. Dynamics derived under this assumption describe well realistic experimental scenarios. Indeed, when the initial state is not factorised, complete positivity is only guaranteed for classically correlated initial states [77]-[79]. Further, in some cases, it is not even possible to define a dynamical map as its expression depends on the structure and amount of correlations in the initial state of the system.

In the Markovian regime, we adopt the weak coupling/Born approximation. More precisely, we assume that the coupling between the system and environment is weak $\alpha << 1$, allowing terms higher than second order in Eq. 2.27 to be discarded. Further, in the weak coupling regime, the correlations established between the system and environment do not appreciably affect the reduced dynamics of the open system. Hence, the environment does not significantly evolve i.e. $\tilde{\rho}_E(t) = \tilde{\rho}_E(0) \equiv \tilde{\rho}_E$ for all times $t \geq 0$, i.e., the environment has no memory of past states of the system. Moreover, it is justified, from Eq. 2.26, to replace the initial state of the system with the current state of the system. It follows that the system and environment remain uncorrelated at any successive time so that $\tilde{\rho}_{SE}(t) = \tilde{\rho}_S(t) \otimes \tilde{\rho}_E$, where $\tilde{\rho}_E$ is a stationary state for the environment usually taken to be a thermal state.

To obtain the master equation, we apply the partial trace rule to both sides of

Eq. 2.27, obtaining:

$$\frac{d}{dt}\tilde{\rho}_S(t) = -\int_0^t ds\, \mathrm{Tr}_E\{[\tilde{\mathbf{H}}_I(t), [\tilde{\mathbf{H}}_I(s), \tilde{\rho}_{SE}(0)]]\} \tag{2.28}$$

where $\tilde{\rho}_S(t)$ is the state of the system in the interaction picture and we assumed the condition $\mathrm{Tr}_E\{[\tilde{\mathbf{H}}_I(t), \rho(0)]\} = 0$. For the sake of simplicity, the coupling constant has now been incorporated into the interaction Hamiltonian. Following this, we now obtain the Redfield equation,

$$\frac{d}{dt}\tilde{\rho}_S(t) = -\int_0^t ds\, \mathrm{Tr}_E\{[\tilde{\mathbf{H}}_I(t), [\tilde{\mathbf{H}}_I(s), \tilde{\rho}_S(t) \otimes \tilde{\rho}_E]]\} \tag{2.29}$$

which is a master equation at second order in the interaction and in a time local form, i.e. the solution at time t depends only on the value of the system state at time t.

We now consider the Markov approximation which is concerned with two time scales of the dynamics of the total system. In more detail, we consider the time characterising the decay of the reservoir correlation function of the environment τ_E and the relaxation time τ_R over which the state of the system varies appreciably due to the interaction with the environment. The Markov approximation holds when $\tau_R >> \tau_E$ and amounts to replacing the upper limit of the integration in Eq. 2.29 with infinity. Finally, we perform the secular approximation to eliminate rapidly oscillating terms appearing into the integral of Eq. 2.29. This approximation can be performed when associated time scales of the system τ_S satisfy $\tau_S << \tau_R$. With these approximations and after some calculation, we can transform back to the Schrödinger picture to find the Lindblad master equation [80, 81]:

$$\frac{d\rho_S(t)}{dt} = \mathcal{L}\rho_S(t) = -i[\mathbf{H}_S, \rho_S(t)] + \sum_{k=1}^{d^2-1} \gamma_k (A_k \rho_S(t) A_k^\dagger - \frac{1}{2}\{A_k^\dagger A_k, \rho_S(t)\}), \tag{2.30}$$

where $\{A, B\} = AB + BA$ is the anti-commutator of operators A and B, $\mathbf{H}_S$ is the system free Hamiltonian, A_k are the jump of Lindblad operators, the positive constant coefficients γ_k are called decay rates and $\mathcal{L}$ a superoperator corresponding to the map $\Phi_{t,0} = \Phi_t = e^{\mathcal{L}t}$. The first term in the right hand side represents the unitary dynamics induced by the Hamiltonian of the system $\mathbf{H}_S$ while the second term, coined the dissipator, describes the effect of the environment on the system.

The dynamical map corresponding to the Lindblad master equation in Eq. 2.30 has two interesting properties. Indeed, the map is time-homogenous

$$\Phi_{t_0,t} = \Phi_{t-t_0,0} \equiv \Phi_{t-t_0}, \tag{2.31}$$

and it obeys the semi-group property [80, 81]

$$\Phi_{t+s} = \Phi_t \Phi_s. \tag{2.32}$$

Therefore, from the semi-group property, the dynamical map can be divided into infinitely many time-steps, each identical and independent of the past and future steps [82]. Physically this is an intuitive interpretation of memoryless dynamics.

The Lindblad master equation, given in Eq. 2.30 is the most general form of the generator of a quantum dynamical semi-group for a finite-dimensional Hilbert space, obtained by Gorini, Kossakowki and Sudarshan [81] and Lindblad [80]. This common result (referred to as the GKSL theorem) implies that for every t-parametrised, completely positive map which fulfils the semi-group property (Eq. 2.32), the corresponding generator is of the Lindblad form. Conversely, the theorem implies that if the equation of motion is in the Lindblad form, then the time evolution of the density matrix is always physical. The theorem relies on the assumption that the operators H and A_k are bounded and indeed, a Lindblad theorem for unbounded operators does not exist. However, in physical applications, the Hamiltonian H_S of the reduced system as well as the Lindblad operators are, in general, unbounded, e.g., harmonic oscillators. Nevertheless, all known examples for generators of quantum dynamical semigroups are either of Lindblad form, or with suitable approximations can be recast into the Lindblad form.

While certain physical systems sufficiently satisfy the approximations associated with Eq. 2.30 [83], and therefore are naturally consistent with a Markovian description, other systems are intrinsically non-Markovian. The study of the exact dynamics of open quantum systems is therefore of fundamental importance. It is widely accepted that Lindblad theory fails in describing the open system dynamics in various physical situations, e.g. in solid state systems at low temperature [84], or in superconducting circuits [85], as well as with Photonic Band Gap (PBG) materials [28, 86, 87]. Moreover, recently, a non-Markovian approach has been used to describe a scenario in nature, specifically excitonic energy transfer in large photosynthetic complexes [19]-[20].

Chapter 3

Defining Non-Markovianity

In this chapter, we rigorously explore the boundary between the two different classes of dynamical behaviour, known as Markovian and non-Markovian regimes. While a consistent characterisation of Markovianity exists, it is not possible to quantify non-Markovianity in a single definition [67, 88]. Here, we introduce the concept of non-Markovianity and critically evaluate and compare several recently proposed non-Markovianity measures using models amendable to exact solutions. Specifically, we study the qualitative behaviour[1] of the measures and the Markovian to non-Markovian crossover when certain physical parameters of the model are changed. The results from this chapter are based on those obtained in Publication i [1].

3.1 Non-Markovian Master Equations

The Lindblad master equation and associated semi-group property are conventionally recognised as the prototype of Markovian, memoryless dynamics, following from the Born-Markov approximation [80, 81]. The severe assumption in Markovian descriptions as a result of this approximation is the absence of memory effects in the environment. In many natural processes, such as strong system-environment couplings, structured and finite reservoirs and low temperatures, the Markovian description of the dynamics is no longer justified [84]-[87]. Indeed, in exact (non-Markovian) descriptions, the evolution of future states is influenced by significant memory effects of past states. Hence, while in a Markovian process, an open quantum system irretrievably loses information to the environment, non-Markovian processes feature a partial back flow of information from the environment to the open quantum system. As a non-Markovian generalisation of the Lindblad theorem does not exist, phenomenological master equations can lead to unphysical conditions indicated by the violation of positivity and complete positivity [89, 90]. Therefore, to study dynamics influenced by memory, we must consider the microscopic deriva-

[1] As there is no general monotonicity relation between the different non-Markovianity measures, we do not compare their absolute values and instead renormalise all measures to take values between zero and unity.

tion of the master equation without making the Born-Markov approximation. As a consequence, the equations describing the dynamics of the reduced system are mathematically more complicated and thus become more difficult to handle analytically, often requiring the implementation of numerical algorithms. Exact solutions exist only for simple open quantum systems models such as the well-known Jaynes-Cummings model [91], the quantum Brownian motion model [92], and certain pure dephasing models [25]-[27]. Despite the fact that these models are generally idealised versions of what can be accomplished within present experimental limitations, it is undoubtedly important to fully understand and study these systems and compare the theoretical predictions with experimental implementations. It may be expected that the mathematical formulation of quantum processes describing effects of finite memory times in the system must necessarily involve equations of motion which are non-local in time. Specifically, we refer to memory-kernel master equations which contain an integral over the past history of the system associated to memory effects in the dynamics and hence, in the past, have been considered as synonymous with non-Markovianity [93, 94]. However, it is now known that there exist exact (and hence non-Markovian) master equations having local in time form, i.e. the time derivative of the reduced density matrix at time t depends only on the state of the system at that time and not on the previous history of the system. The ensuing master equation has the same structure as the Lindblad master equation but with time-dependent coefficients $\gamma_k = \gamma_k(t)$:

$$\frac{d\rho(t)}{dt} = -i[\mathbf{H}_S, \rho(t)] + \sum_{k=1}^{d^2-1} \gamma_k(t)(A_k \rho(t) A_k^\dagger - \frac{1}{2}\{A_k^\dagger A_k, \rho(t)\}). \tag{3.1}$$

The corresponding dynamical map is given as $\Phi_t = \mathcal{T}\exp(\int_0^t \mathcal{L}_\tau d\tau)$ where $t \geq 0$ and $\mathcal{T}$ denotes the chronological time-ordering operator. Such a map is no longer time-homogenous and hence, the semi-group property is violated. However, if $\gamma_k(t) > 0$ for each k and $t \geq t_0$, one speaks of time-dependent Markovian master equations, in the sense that at each time instant the master equation is in the Lindblad form. The dynamical map is now divisible, thus can be concatenated into a collection of other dynamical maps and analogously to the semi-group property, this concatenation has the intuitive interpretation of memoryless dynamics ($\forall t' < t$):

$$\Phi_t = \Phi_{t,t'} \Phi_{t',0}. \tag{3.2}$$

Non-divisibility therefore occurs if there exist times t' at which an intermediate map $\Phi_{t,t'}$ is not completely positive and trace preserving (CPTP), defying the composition law and corresponding to $\gamma_k(t') < 0$. The inability to write the dynamical map Φ_t as a concatenation of independent CPTP maps connects with intuitive reasoning of present dynamics being dependent on memory effects. The manifestation of

such memory effects, stemming from long lasting and non-negligible system-reservoir correlations, leads to a partial recovery of quantum quantities previously lost due to the deleterious effects of environmental noise. It is important to note that the dynamical map, and hence the open system dynamics depends, not only on the form of the environmental spectral density but also on the type and strength of coupling between the system and the environment. Therefore, one cannot properly talk of non-Markovian environments because the system-environment interaction Hamiltonian also plays a crucial role.

3.2 Non-Markovianity Measures

Recently, an abundance of non-Markovianity measures have emerged in literature in an attempt to characterise memory effects. In this section, we introduce the mathematical and physical features of several measures. With the exception of the Rivas, Huelga and Plenio measure [21], the non-Markovianity measures described in this chapter capture the non-monotonic time evolution of certain quantities, occurring if the dynamics is non-divisible [22, 24, 16]. Other measures not included in this work, are based on the behaviour of quantities such as fidelity [95], Fisher information [96] and the volume of accessible physical states of the system [97]. While the non-monotonic behaviour of such quantities always implies non-divisibility, the inverse is not true, i.e., there can be non-divisible maps consistent with monotonic dynamics [98]-[100]. In this sense, if one would accept divisibility as the characterisation of non-Markovianity, measures associated to non-monotonicity should be considered as witnesses capturing specific aspects of non-Markovianity.

3.2.1 Rivas, Huelga, Plenio Measure

With the defining attribute of all non-Markovian dynamics in mind, namely the violation of the divisibility property, Rivas, Huelga and Plenio (RHP) constructed a measure based on the Choi-Jamiolkowski isomorphism [74]-[75]. The RHP measure quantifies the non-Markovian character of a quantum evolution avoiding standard optimisation procedures over the state space to exclude dependence of the initial state. Such an independence is crucial in non-Markovian quantifiers as non-Markovianity should be a property associated to only the dynamical map.

According to the Choi-Jamiolkowski isomorphism [74], $\Phi_{t,t'}$ is completely positive iff:

$$(\Phi_{t,t'} \otimes \mathbb{1}) |\Omega\rangle \langle\Omega| \geq 0, \tag{3.3}$$

where $|\Omega\rangle = \frac{1}{\sqrt{d}} \sum_{n=1}^{d-1} |n\rangle |n\rangle$ is a maximally entangled state of dimension d of the open system with an ancilla. Hence, given the trace preserving property of the map,

we can take the following expression as a measure of the non-CP character of $\Phi_{t,t'}$:

$$f_{\mathrm{NCP}}(t,t') = ||(\Phi_{t,t'} \otimes \mathbb{1})(|\Omega\rangle \langle\Omega|)||_1, \tag{3.4}$$

where $||...||_1$ refers to the trace norm and the time elapsed between the time t' and t, denoted ϵ, is infinitesimal. Now, $\Phi_{t,t'}$ is CP iff $f_{\mathrm{NCP}}(t,t') = 1$ and otherwise $f_{\mathrm{NCP}}(t,t') > 1$. To construct the RHP measure, we define the right derivative of $f_{NCP}(t,t')$,

$$g(t) = \lim_{\epsilon \to 0^+} \frac{f_{NCP}(t,t') - 1}{\epsilon}, \tag{3.5}$$

noticing that $g(t) \geq 0$, with $g(t) = 0$ iff $\Phi(t,t')$ is CP. In the limit $\epsilon \to 0$, $\Phi(t,t') \to e^{\mathcal{L}_t \epsilon}$ and so we can write (up to first order),

$$g(t) = \lim_{\epsilon \to 0^+} \frac{||[\mathbb{1} \otimes \mathbb{1} + (\mathcal{L}_t \otimes \mathbb{1})\epsilon] |\Omega\rangle \langle\Omega| \, ||_1 - 1}{\epsilon}. \tag{3.6}$$

Non-Markovianity is then quantified as the extent to which the intermediate map departs from a map which is completely positive [21]:

$$\mathcal{N}_{\mathrm{RHP}} = \int_0^\infty dt \, g(t). \tag{3.7}$$

The measure is most simple to calculate using only the specific form of the master equation or the intermediate dynamical map $\Phi_{t,t'}$. However, the measure is often criticised for not having a clear physical interpretation and for being a mathematical definition rather than a physical one. Here we would like to conjecture, however, that a physical interpretation can be given in terms of the non-Markovian quantum jumps unravelling [101]. It is shown in Ref. [101] that when the decay rates become negative, i.e., the dynamical map is non-divisible and the RHP measure is non-zero, reverse quantum jumps restoring previously lost coherence occur. In this sense reverse jumps would be the physical manifestation[2] of memory effects quantified by the RHP definition.

3.2.2 Breuer, Laine, Piilo Measure

The Breuer, Laine, Piilo (BLP) measure, proposed in Ref. [22], conceptualises the physical nature of non-Markovianity in terms of information exchange between the system and environment. Information flow can be interpreted as the dynamical change of the distinguishability of the states of the system and determined by the time evolution of the trace distance. To understand how trace distance D can be interpreted as distinguishability, we suppose that Alice prepares a quantum state in one of two states ρ_1 and ρ_2, each with a probability $\frac{1}{2}$. Alice then gives her system

[2]Reverse quantum jumps always cancel or undo previously occurred jumps and therefore a jump-reverse jump pair describes a virtual process that is in principle not directly observable.

to Bob who must perform a measurement in order to determine the state. It can be shown that the probability p of Bob successfully identifying the state of the system is given as:

$$p = \frac{1}{2}[1 + D(\rho_1, \rho_2)]. \tag{3.8}$$

The trace distance provides a natural metric on the space $\mathcal{S}(\mathcal{H})$ of physical states and satisfies $0 \leq D \leq 1$ where $D(\rho_1, \rho_2) = 0$ iff $\rho_1 = \rho_2$ while the upper bound is reached i.e. $D(\rho_1, \rho_2) = 1$ iff ρ_1 and ρ_2 are orthogonal. For a Markovian processes, any two quantum states become decreasingly distinguishable under the dynamics, leading to a perpetual loss of information from the environment to the system[3]. For a non-Markovian process the converse is true and information flowing back from the environment has an effect on the later dynamics of the system. We emphasis however, as the BLP definition is based only on quantities defined on the Hilbert space of the system and in no way takes into account the information content of the environment or how it is modified by system-environment correlations, the back flow of information can not be interpreted solely as a recovery of information previously lost in the environment.

The construction of the measure is based on the non-monotonicity of the trace distance, given by

$$D(\rho_1, \rho_2) = \frac{1}{2}\mathrm{tr}|\rho_1 - \rho_2|, \tag{3.9}$$

where $|A| = \sqrt{A^\dagger A}$. The derivative of the trace distance determines the temporal change of information content on the system, i.e. the information flux and is given as:

$$\sigma(t, \rho_{1,2}(0)) = \frac{d}{dt} D(\rho_1(t), \rho_2(t)). \tag{3.10}$$

Dynamics are classified as non-Markovian if, for certain time intervals, $\sigma(t, \rho_{1,2}(0)) > 0$, i.e., information flows back into the system. Following this, the measure of non-Markovianity $\mathcal{N}_{\mathrm{BLP}}$ is found by summing over all periods of non-monotonicity of the information flux, following an optimisation over all pairs of initial states of the system $\rho_{1,2}(0)$:

$$\mathcal{N}_{\mathrm{BLP}}(\Phi_t) = \max_{\rho_{1,2}(0)} \int_{\sigma>0} dt\, \sigma(\rho_{1,2}(0), \Phi_t). \tag{3.11}$$

Proofs of specific mathematical attributes of the optimal state pairs have to some degree eased the numerical challenges of this calculation by eliminating the requirement for optimisation in specific regions of the d-dimensional Hilbert space [102]. Indeed, it has been shown that the states which maximise the measure must lie on the boundary of the space of physical states and must be orthogonal (however, beyond the one qubit case, each state has more than one orthogonal state). Finally, we note that in the spirit of this measure, trace distance is not a unique monotone

[3]The trace distance is preserved under unitary transformations $D(U\rho_1 U^\dagger, U\rho_2 U^\dagger) = D(\rho_1\rho_2)$. The invariance under unitary transformations indicates that information is preserved under the dynamics of closed systems.

distance and one may also use others such as the statistical distance [103].

Any quantum process taking values $\mathcal{N}_{\mathrm{BLP}} \neq 0$, must necessarily be described by a non-divisible dynamical map as a result of the following contraction property, true only for CPT dynamical maps ($t > s$),

$$D(\Phi_t\rho_1(t), \Phi_t\rho_2(t)) \leq D(\Phi_s\rho_1(s), \Phi_s\rho_1(s)). \tag{3.12}$$

The converse is not true however and there exist non-divisible processes which are Markovian in the sense of the BLP definition. Indeed, if the contribution of the decay channels with a negative rate is over compensated by the channels with a positive decay rate, the net information flow will be from the open system to the environment. A rigorous mathematical theory linking the RHP and the BLP measures has been presented in Ref. [104].

3.2.3 Luo, Fu, Song Measure

The Luo, Fu, Song (LFS) measure is based on the monotonic dynamical evolution of the total correlations between system and ancilla, when the dynamics is divisible [24]. Quantum mutual information captures both quantum and classical correlations in a bipartite system ρ_{SA} shared between the system and an arbitrary ancillary system and is given by:

$$I(\rho_{SA}) = S(\rho_S) + S(\rho_A) - S(\rho_{SA}), \tag{3.13}$$

where $\rho_S = \mathrm{tr_A}\rho_{\mathrm{SA}}$ and $\rho_A = \mathrm{tr_S}\rho_{\mathrm{SA}}$ are marginal states of a system and ancilla, respectively, and

$$S(\rho) = -\mathrm{tr}\rho\log_2\rho = -\sum_i \rho_i \log_2(\rho_i), \tag{3.14}$$

is von Neumann entropy of state ρ with eigenvalues p_i. The von Neumann entropy quantifies the mixedness of a state and takes values $0 \leq S(\rho) \leq \log_2 d$ where d is the dimension of the Hilbert space of the system and the lower and upper bound correspond to a pure state and maximally mixed state respectively. The LFS measure is defined as:

$$\mathcal{N}_{\mathrm{LFS}}(\Phi_t) = \max_{\rho^{SA}(0)} \int_{\frac{d}{dt}I>0} \frac{d}{dt} I(\rho_{SA}(t))dt, \tag{3.15}$$

with optimisation over all possible initial states $\rho_{SA}(0)$ with arbitrary Hilbert space of the ancilla and $\rho_{SA}(t) = (\Phi_t \otimes \mathbb{I})\rho_{SA}(0)$. Acknowledging the exhaustive nature of the original optimisation, the authors propose the following reduction,

$$\mathcal{N}_{\mathrm{LFS_0}}(\Phi_t) = \int_{\frac{d}{dt}I>0} \frac{d}{dt} I(\rho_{SA}(t))dt, \tag{3.16}$$

where $\rho_{SA}(t) = (\Phi_t \otimes \mathbb{I})|\Psi\rangle\langle\Psi|$ and $|\Psi\rangle$ is an arbitrary maximally entangled state.

When the initial state $\rho_{SA}(0)$ is pure, and also the initial state of the environ-

ment with which the system is interacting, it is possible to rewrite $I(\rho_{SA})$ as the mutual information between the input and output of the channel defining the system evolution,

$$I(\rho(0), \Phi_t) = S(\rho(0)) + S(\Phi_t\rho(0)) - S(\rho(0), \Phi_t), \tag{3.17}$$

with $S(\rho(0))$ the von Neumann entropy of the input state, $S(\Phi_t\rho(0))$ the entropy of the output state and $S(\rho(0), \Phi_t) = S(\tilde{\Phi}_t\rho(0))$ the entropy exchange, i.e., the entropy at the output of the complementary channel[4], $\tilde{\Phi}_t$. Hence, to generalise Eq. 3.16 but avoid the difficulties faced in Eq. 3.15, we introduce an alternative optimisation considering only the initial state of the system $\rho(0)$,

$$\mathcal{N}_{\mathrm{I}}(\Phi_t) = \max_{\rho(0)} \int_{\frac{d}{dt}I>0} \frac{d}{dt} I(\rho(0), \Phi_t) dt. \tag{3.19}$$

The entropy exchange term in Eq. 3.17 encapsulates the change in the information content of the environment due to the interaction of the system. Hence, the LFS measure in terms of mutual information associates non-Markovianity to a memory-induced restoration of previously lost total (quantum and classical) correlations between an open quantum system and an ancilla. We note that, in analogy to Eq. 3.12, the following inequality for mutual information, i.e. $I(\rho(0), \Phi_t) \leq I(\rho(0), \Phi_s)$ for times $t > s$, is true for CPT dynamical maps.

3.2.4 Bylicka, Chruściński, Maniscalco Measure

The Bylicka, Chruściński and Maniscalco (BCM) measures provide a general theory connecting non-Markovianity to an increase in the efficiency of quantum information processing and communication. Channel capacity quantifies the maximum amount of information (classical or quantum) that can be reliably transmitted along a noisy quantum channel between a sender, Alice and receiver, Bob. The BCM measures capture features of non-Markovianity connected with the non-monotonic evolution of two types of capacities, namely the entanglement assisted capacity C_{ea} and quantum channel capacity Q. From the data processing inequality [105], monotonic evolution of channel capacities always implies divisible channels, intuitively stating that processing quantum information always reduces the amount of correlations between the input and output. As a consequence, for divisible quantum channels, both the entanglement assisted capacity and quantum capacity decrease monotonically with time. The time t the quantum state encoding the classical or quantum information is subject to a noisy channel is incorporated in the quantum channel

[4] Physically the complementary channel Φ_t^C captures the environment's view of the channel, and is defined by taking the partial trace on the composite system $\rho_{SE} \in \mathcal{D}(\mathcal{H})$ with $\mathcal{H} = \mathcal{H}_S \otimes \mathcal{H}_E$,

$$\Phi_t^C(\rho) = \mathrm{Tr}_S U \rho_{SE} U^\dagger \tag{3.18}$$

Φ_t. In experimental implementations of quantum protocols e.g. with trapped ion systems, this time t is the duration of the experiment and is connected to the length of the channel, i.e. the length of an optical fibre in optical systems. Therefore, the revivals of quantum channel capacities physically measure the total increase, due to memory effects, of the maximum rate at which information can be transferred in noisy channels for a fixed time interval or a fixed length of the transmission link.

The BCM measures expose the potential enhancement in quantum information processing and communication protocols attained for non-Markovian maps. While Markovian dynamical maps prompt irretrievable deterioration of the channel capacity as the length of the channel increases, non-Markovian dynamical maps may lead to i) increase of the channel capacities for a given channel length, ii) revivals of the channel capacities, hence increasing the length of the channel over which capacities are non-zero, iii) length-independent finite capacity channels (residual channel capacities), i.e., channels for which the quantum and/or entanglement assisted capacity takes non zero positive values after a certain threshold length [16].

3.2.4.1 Entanglement-Assisted Classical Capacity

The entanglement-assisted classical capacity, C_{ea}, sets a bound on the amount of classical information that can be transmitted along a quantum channel when one allows Alice and Bob to share an unlimited amount of entanglement [106]. It is defined in terms of the quantum mutual information $I(\rho(0), \Phi_t)$ between the input and the output of the channel, as given by Eq. 3.17, with an optimisation over all initial states $\rho(0)$,

$$C_{ea}(\Phi_t) = \max_{\rho} I(\rho(0), \Phi_t). \tag{3.20}$$

Revivals in the entanglement-assisted classical capacity indicate violation of the divisibility property and can be considered a witness of non-Markovianity. In light of this, the following measure can be introduced:

$$\mathcal{N}_{\mathrm{C}}(\Phi_t) = \int_{\frac{dC_{ea}(\Phi_t)}{dt}>0} \frac{dC_{ea}(\Phi_t)}{dt} dt, \tag{3.21}$$

where the integral is extended to all time intervals over which dC_{ea}/dt is positive and the optimisation is performed over only one input state $\rho(0)$. Calculating the measure for n identical independent channels can be found directly as a consequence of the additivity property of mutual information, i.e., $\mathcal{N}_{\mathrm{C}}(\Phi_t^{\otimes n}) = n\mathcal{N}_{\mathrm{C}}(\Phi_t)$.

3.2.4.2 Quantum Capacity

The quantum capacity gives the limit to the rate at which quantum information can be reliably sent down a quantum channel and is defined in terms of the coherent information I_c between the input and output of the quantum channel $I_c(\rho(0), \Phi_t)$.

For n successive uses of the channel, the quantum channel capacity is defined as,

$$Q(\Phi_t) = \lim_{n\to\infty}[\max_{\rho_n} I_c(\rho_n, \Phi_t^{\otimes n})]/n, \tag{3.22}$$

with coherent information [107],

$$I_c(\rho(0), \Phi_t) = S(\Phi_t\rho(0)) - S(\rho(0), \Phi_t). \tag{3.23}$$

The associated non-Markovianity measure is then introduced as follows:

$$\mathcal{N}_{\mathrm{Q}}(\Phi_t) = \int_{\frac{dQ(\Phi_t)}{dt}>0} \frac{dQ(\Phi_t)}{dt} dt. \tag{3.24}$$

Contrarily to the entanglement-assisted classical capacity, the quantum channel capacity is in general not additive. However, for degradable channels[5] [108], the general definition coincides with the one-shot capacity, $Q(\Phi_t) = \max_{\rho(0)} I_c(\rho(0), \Phi_t)$, and for identical independent channels, additivity (i.e. $I_c(\rho_n(0), \Phi^{\otimes n}) = nI_c(\rho(0), \Phi)$) holds.

3.3 Comparison for Pure Dephasing Dynamics

We begin our analysis by studying the purely dephasing dynamics of one and two qubits interacting with a reservoir with spectral density of the Ohmic class. A microscopic model of the total system-environment dynamics is presented in Refs. [25]-[27]. For one qubit, the behaviour of all non-Markovianity measures has been studied in Refs. [21]-[22], [96], [109]. In the case of two qubits in both independent and common environments, both BLP and RHP measures have been studied also in this case in Ref. [5], [110]-[111].

We note that further mathematical details of the models, specifically the form of the Kraus operators and complementary map, are found in the Appendix A.1. Moreover, the optimisation evidence is found in the Appendix B.

3.3.1 Single qubit: The Model

The Hamiltonian of the system is given as [26]:

$$H = \omega_0\sigma_z + \sum_k \omega_k a_k^\dagger a_k + \sum_k \sigma_z(g_z a_k + g_k^* a_k^\dagger), \tag{3.26}$$

[5]A classical degraded broadcast channel is a single-sender, two receiver broadcast channel in which one receiver can degrade his/her output to simulate the output of the other receiver. The quantum analogue of this channel was introduced by Devetak and Shor and a channel is degradable if there is another CPT map Ψ such that,

$$\Psi\dot{\Phi} = \Phi^C. \tag{3.25}$$

with ω_0 the qubit frequency, ω_k the frequencies of the reservoir modes, $a_k(a_k^\dagger)$ the annihilation (creation) operators of the bosonic environment and g_k the coupling constant between each reservoir mode and the qubit. In the continuum limit $\sum_k |g_k|^2 \to \int d\omega\, J(\omega)\delta(\omega_k - \omega)$, where $J(\omega)$ is the reservoir spectral density [26, 109]. The dynamics of a purely dephasing single qubit is captured by the time-local master equation [9]:

$$\mathcal{L}_t \rho_t = \gamma_1(t) \left[\sigma_z \rho_t \sigma_z - \rho_t\right], \tag{3.27}$$

with $\gamma_1(t)$ the time-dependent dephasing rate and σ_z the Pauli spin operator. The decay of the off-diagonal elements of the density matrix is described by the decoherence factor $e^{-\Gamma(t)}$, where $\Gamma(t) \geq 0$. For zero-temperature environments we have [26],

$$\begin{aligned} \Gamma(t) &= 2\int_0^t dt'\, \gamma_1(t') \\ &= 2\int d\omega\, J(\omega) \frac{1-\cos(\omega t)}{\omega^2}, \end{aligned} \tag{3.28}$$

with $J(\omega)$ the reservoir spectral density [26, 109]. We consider a reservoir spectral density of the form,

$$J(\omega) = \frac{\omega^s}{\omega_c^{s-1}} e^{-\omega/\omega_c}, \tag{3.29}$$

where ω_c is the cutoff frequency and s is the Ohmicity parameter. Following this, the explicit form of $\Gamma(t)$, given in dimensional units by introducing ω_c^{-1}, is,

$$\Gamma(t) = \frac{2\tilde{\Gamma}[s]}{-1+s}(1-(1+t^2)^{-s/2}(\cos(s\arctan(t)) + t\sin(s\arctan(t))), \tag{3.30}$$

where $\Gamma[x]$ is the Euler gamma function. Ohmic spectrum corresponds to $s = 1$, while super-Ohmic spectra correspond to $s > 1$ and sub-Ohmic to $s < 1$.

Recoherence occurs when $\Gamma(t)$ temporarily decreases for certain time intervals, corresponding to a negative value of the dephasing rate $\gamma_1(t)$. One may analytically determine the times $t \in [a_i, b_i]$ encapsulating non-monotonic intervals of $\Gamma(t)$, i.e. corresponding to $\gamma_1(t) = 0$, with $i = 1, 2, 3, ...$ the number of such time intervals. The extremes of the time intervals, a_i and b_i, will depend on the Ohmicity parameter s, as changing s one changes the form of the reservoir spectral density. We give here the analytical expressions of $\Gamma(t)$ at times a_i and b_i as these will be used in the following.

$$\Gamma(a_1) = \frac{2\tilde{\Gamma}[s][1+\cos^s(\pi/s)]}{s-1} \tag{3.31}$$

$$\Gamma(b_1) = \frac{2\tilde{\Gamma}[s][1-\cos^s(2\pi/s)]}{s-1} \qquad 4 < s \leq 6 \tag{3.32}$$

$$\Gamma(b_1) = 2\tilde{\Gamma}[s-1] \qquad 2 < s \leq 4, \tag{3.33}$$

where $\tilde{\Gamma}[x]$ is the Euler gamma function. In Ref. [66] it is shown that, for $s \leq 2$, $\gamma_1(t) > 0$ at all times, or equivalently $\Gamma(t)$ increases monotonically. For $2 < s \leq 4$: $a_1 = \tan \pi/s, b_1 = \infty$ and for $4 < s \leq 6 : a_1 = \tan \pi/s, b_1 = \tan 2\pi/s$, i.e., we only have one time interval of non-monotonic behaviour. For $s > 6$, $i > 1$, i.e., there are more than one interval of time for which the dephasing rates become negative. For the sake of simplicity we look at values of the Ohmicity parameter in the interval $0 \leq s \leq 6$. In this case there is only one interval of negativity of the decay rates and the only values needed are $\Gamma(a_1)$ and $\Gamma(b_1)$, defined in Eqs. 3.31-3.33

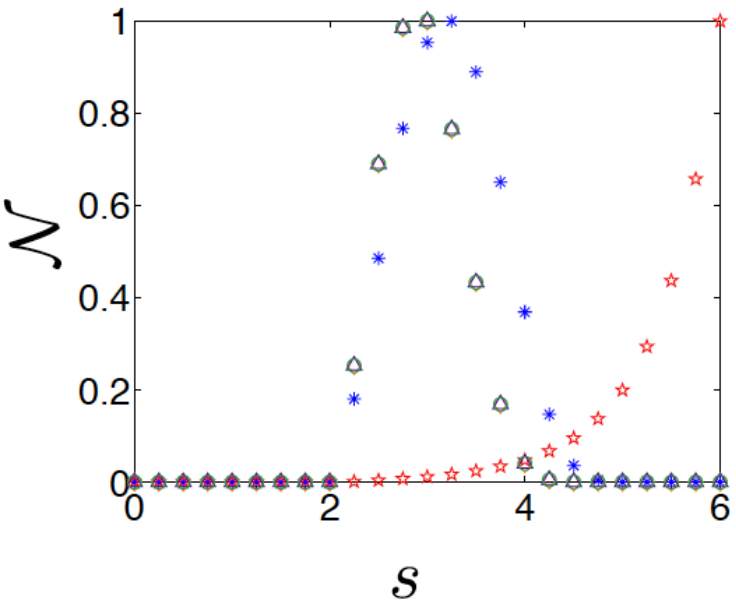

Figure 3.1: Non-Markovianity measures for a single purely dephasing qubit as a function of the Ohmicity parameter s. We show the RHP Measure (red star), the BLP (blue asterisk), the LFS measure (green circle), the quantum capacity measure (purple triangle) and the entanglement-assisted capacity measure (orange diamond). Note that the last three measures in this case coincide. All the measures in this case are normalised to unity. Note that the value of all measures for $s > 2$ is always non-zero, even if all measures except RHP take very small values for $s > 4$.

3.3.2 Single qubit: The Measures

RHP Measure

It is straightforward, from the form of the master equation, to immediately obtain the analytical expression for the RHP non-Markovianity measure. In more detail, the calculation involves inserting the master equation, given in Eq. 3.27 into Eq. 3.6 and using Eq. 3.7. We obtain the simple expression:

$$\mathcal{N}_{\text{RHP}} = -2 \int_{\gamma_1(t)<0} dt\, \gamma_1(t) = \sum_i (\Gamma(a_i) - \Gamma(b_i)). \tag{3.34}$$

In Fig. 3.1, we plot the measure $\mathcal{N}_{\text{RHP}}$ as a function of the Ohmicity parameter s (red stars). From the plot, it is immediate to see, that for $s > 2$, the RHP measure monotonically increases for higher and higher values of s. More precisely, the measure captures, for increasing s, the increasing area of the region of negativity of the dephasing rate $\gamma_1(t)$.

BLP Measure

Recalling the properties of the density matrix it is simple, for a single qubit, to define the density matrix in terms of two independent parameters, specifically a diagonal and off-diagonal element, ρ_{jj} and ρ_{jk} respectively with $(j, k = 1, 2)$. From this, a

simple expression for the BLP measure $\mathcal{N}_{\text{BLP}}$ follows,

$$\mathcal{N}_{\text{BLP}} = -2 \max_{m,n} \int_{\gamma_1<0} dt\, \gamma_1(t) \frac{|n|^2 e^{-2\Gamma(t)}}{\sqrt{m^2 + |n|^2 e^{-2\Gamma(t)}}}, \tag{3.35}$$

where the only two independent elements are defined as $m = \rho^1_{11}(0) - \rho^2_{11}(0)$ and $n = \rho^1_{12}(0) - \rho^2_{12}(0)$, with $\rho^i_{11}(0)$ the diagonal element of the initial density matrices of the pair and $\rho^i_{12}(0)$ their off diagonal element, with $i = 1, 2$. Following the simple characterisation of this model, it is possible to analytically solve the optimisation problem of Eq. 3.35 [112]. The pair of states optimising the increase of the trace distance are antipodal states lying on the equatorial plane, e.g., the states $|\pm\rangle = \frac{1}{\sqrt{2}}(|0\rangle \pm |1\rangle)$, with $|0\rangle$ and $|1\rangle$ the two states forming the qubit. The BLP measure is then defined as:

$$\mathcal{N}_{\text{BLP}} = -2 \int_{\gamma_1<0} dt\, \gamma_1(t) e^{-\Gamma(t)}. \tag{3.36}$$

This expression shows immediately that $\sigma(t) > 0$ iff $\gamma_1(t) < 0$; i.e $\mathcal{N}_{\text{BLP}} \neq 0$ only when the dynamical map is non-divisible [22]. Solving Eq. 3.36, we have:

$$\mathcal{N}_{\text{BLP}} = \sum_i (e^{-\Gamma(b_i)} - e^{-\Gamma(a_i)}), \tag{3.37}$$

where again $t \in [a_i, b_i]$ indicates the time intervals when $\gamma_1(t) < 0$.

Figure 3.1 shows the behaviour of $\mathcal{N}_{\text{BLP}}$ for different s values (blue asterix). The measure remains non-zero for increasing values of s but, contrarily to the RHP measure it starts decreasing, taking increasingly small but finite values for $s > 3.2$.

LFS Measure and BCM Measures

We merge the discussions of the LFS and BCM measures based on the knowledge that for the case of a single pure dephasing qubit, all three measures coincide. Following extensive numerical optimisation to identify the optimising states, an explicit analytical relation between all three measures can be attained. Numerical evidence establishes that the time-independent optimising state for all three measures is the maximally mixed state $\frac{\mathbb{I}}{2}$ [16]. For the pure dephasing single qubit model, the mutual information for the maximally mixed state is given as:

$$I\left(\frac{\mathbb{I}}{2}, \Phi_t\right) = 2 - H_2\left(\frac{1}{2} + \frac{e^{-\Gamma(t)}}{2}\right), \tag{3.38}$$

where $H_2(X) = -X \log_2 X - (1-p)\log_2(1-p)$ is the binary Shannon entropy. The LFS measure is the time-derivative of this expression:

$$\mathcal{N}_{\text{I}} = -\frac{1}{2} \int_{\frac{d}{dt} I\left(\frac{\mathbb{I}}{2}, \Phi_t\right) > 0} \gamma_1(t) e^{-\Gamma(t)} \log_2 \left(\frac{1 + e^{-\Gamma(t)}}{1 - e^{-\Gamma(t)}}\right). \tag{3.39}$$

It is clear that the measure $\mathcal{N}_{\mathrm{I}}$ takes non zero values iff $\gamma(t) < 0$, capturing non-Markovianity for all non-divisible dynamics. The explicit expression for the measure $\mathcal{N}_{\mathrm{I}}$ is written as

$$\mathcal{N}_{\mathrm{I}} = \sum_i \left[H_2\left(\frac{1}{2} + \frac{e^{-\Gamma(a_i)}}{2}\right) - H_2\left(\frac{1}{2} + \frac{e^{-\Gamma(b_i)}}{2}\right)\right]. \tag{3.40}$$

We mention, that for the dephasing channel, $\mathcal{N}_{\mathrm{I}} = \mathcal{N}_{\mathrm{LFS}_0}$.

From the numerical optimisation, it is immediate to see that the classical entanglement assisted capacity is $C_{ea}^{D} = I(\frac{\mathbb{I}}{2}, \Phi_t)$ [113] and so $\mathcal{N}_{\mathrm{C}} = \mathcal{N}_{\mathrm{I}}$. The optimisation is simplified for the quantum capacity for the dephasing channel, which is degradable for all admissible dephasing rates $\gamma(t)$, determined by $\Gamma(t) \geq 0$. With knowledge of the optimising state, one can show $C_{ea}(t) = 1 + Q(t)$ (directly from Eq. 3.17 and 3.23). It follows immediately that $\mathcal{N}_{\mathrm{Q}} = \mathcal{N}_{\mathrm{C}} = \mathcal{N}_{I}$.

In Fig. 3.1 we plot the three equivalent measures $\mathcal{N}_{\mathrm{I}}$, $\mathcal{N}_{\mathrm{C}}$ and $\mathcal{N}_{\mathrm{Q}}$ as a function of s (green circles, purple triangles and orange diamonds respectively). We note that the behaviour of these measures is qualitatively similar to that of $\mathcal{N}_{\mathrm{BLP}}$.

We summarise by restating that, for the single qubit dephasing case, all non-Markovianity measures detect non-divisibility, occurring for $s > 2$. The different qualitative behaviour shown by the RHP measure and measures capturing non-monotonic properties is realised through the analytical expressions shown in Eqs. 3.34, 3.37 and 3.40. Specifically, the RHP measure increases monotonically with s as the number and area of the periods of negativity of the dephasing rate increases and with it, the terms contributing to the sum of Eq. 3.34. Conversely, the other measures depend on the dephasing factors $e^{-\Gamma(t)}$ during time intervals at which the direction of information flow changes i.e. $t = a_i$ and $t = b_i$. For increasing values of s, in the $s \gtrsim 3$ parameter space, however, $e^{-\Gamma(a_i)} \simeq e^{-\Gamma(b_i)}$, hence the values of both $\mathcal{N}_{\mathrm{BLP}}$ and $\mathcal{N}_{\mathrm{I}} = \mathcal{N}_{\mathrm{Q}} = \mathcal{N}_{\mathrm{C}}$ decreases, as one can easily see from Eqs. 3.37 and 3.40. Physically, we can interpret the qualitative behaviour in terms of reverse jumps and information back flow. Specifically, while the number of reverse jumps always increases with s, the information back flow has a maximum for a certain value $s \simeq 3$ and then decreases due the fact that the amplitude of the oscillations in the decay rates becomes increasingly small.

3.3.3 Two qubits: The Model

The Hamiltonian which describes the two qubits i, j for the purely dephasing case is as follows: [26]:

$$H = \omega_0^i \sigma_z^i + \omega_0^j \sigma_z^j + \sum_k \omega_k a_k^\dagger a_k + \sum_k \sigma_z^i (g_k^i a_k^\dagger + g_k^{i*} a_k) + \sum_k \sigma_z^j (g_k^j a_k^\dagger + g_k^{j*} a_k). \tag{3.41}$$

We consider the dynamics for both the following scenarios. The first is a purely dephasing bipartite system consisting of two qubits, A and B, individually coupled to their own identical and non-correlated environments. Their dynamics are governed by the dynamical map given by $\Phi_t^{AB} = \Phi_t^A \otimes \Phi_t^B$. The master equation is simply the sum of two identical Lindblad terms of the form of Eq. 3.27, describing the dynamics of each qubit, both characterised by the same dephasing rate $\gamma_1(t)$. We then consider the scenario of both qubits occupying a common environment, specifically the model described in Ref. [26]. The deviation of the dynamics is encapsulating in a single "cross-talk" term, denoted $\gamma_2(t)$ which acts as an effective reservoir-mediated interaction between the qubits. Intuitively one would expect that the presence of this term may affect the additivity property of the measures and additivity is more likely to be realised for qubits in individual environments. In the common scenario, the density matrix at time t takes the form [26],

$$\rho_t = \begin{pmatrix} 1 & e^{-\Gamma(t)} & e^{-\Gamma(t)} & e^{-\Gamma_-(t)} \\ e^{-\Gamma(t)} & 1 & e^{-\Gamma_+(t)} & e^{-\Gamma(t)} \\ e^{-\Gamma(t)} & e^{-\Gamma_+(t)} & 1 & e^{-\Gamma(t)} \\ e^{-\Gamma_-(t)} & e^{-\Gamma(t)} & e^{-\Gamma(t)} & 1 \end{pmatrix} \circ \rho(0), \tag{3.42}$$

where $\circ$ is the Hadamard product and,

$$\begin{aligned} \Gamma_\pm(t) &= 2\Gamma(t) \pm \delta(t) \\ &= 8 \int d\omega \, J(\omega) \frac{1 - \cos(\omega t)}{\omega^2} \left(1 \pm \cos \omega t_s\right), \end{aligned} \tag{3.43}$$

with $\Gamma(t)$ given by Eq. 3.28 and

$$\delta(t) = 4 \int_0^t dt' \, \gamma_2(t'). \tag{3.44}$$

The transit time t_s describes the time it takes for a wave propagating at the characteristic speed of sound to travel from one qubit to the other, given that the qubit distance is R [26]. As before, for the sake of simplicity, we consider only the zero temperature reservoir case. The expression for the "cross-talk" term $\delta(t)$ is given below:

$$\begin{aligned}\delta(t) &= \frac{2\Gamma[s]}{-1+s}(\{(1+t_s^2)[1+(t_s-t)^2]\}^{-\frac{s}{2}}\{[1+(t_s-t)^2]^{\frac{s}{2}} \\ &\times \cos[s\arctan(t_s)] + t_s[1+(t_s-t)^2]^{\frac{s}{2}}\sin[s\arctan(q)] \\ &- (1+t_s^2)^{\frac{s}{2}}(\cos[s\arctan(t_s-t)] + (t_s-t)\sin[s\arctan(t_s-t)])\} \\ &+ \{(1+t_s^2)[1+(t_s+t)^2]\}^{-\frac{s}{2}}\{[1+(t_s+t)^2]^{\frac{s}{2}} \\ &\times \cos[s\arctan(t_s)] + t_s[1+(t_s+t)^2]^{\frac{s}{2}}\sin[s\arctan(t_s)] \\ &- (1+t_s^2)^{\frac{s}{2}}[\cos[s\arctan(t_s+t)] + (t_s+t)\sin\{s\arctan(t_s+t)\}]\}). \quad (3.45)\end{aligned}$$

The master equation describing the dynamics of the composite system comprising two qubits, a and b, is given by [114]:

$$\begin{aligned}\frac{d\rho(t)}{dt} &= \frac{\gamma_+(t)}{2}\left[(\sigma_z^a-\sigma_z^b)\rho(\sigma_z^a-\sigma_z^b) - \frac{1}{2}\{(\sigma_z^a-\sigma_z^b)(\sigma_z^a-\sigma_z^b),\rho\}\right] \\ &+ \frac{\gamma_-(t)}{2}\left[(\sigma_z^a+\sigma_z^b)\rho(\sigma_z^a+\sigma_z^b) - \frac{1}{2}\{(\sigma_z^a+\sigma_z^b)(\sigma_z^a+\sigma_z^b),\rho\}\right], \quad (3.46)\end{aligned}$$

where $\gamma_\pm(t) = \gamma_1(t) \pm \gamma_2(t)$. Dynamics associated to independent environments emerge in the limit, $R \to \infty$ corresponding to $\delta(t) \to 0$.

3.3.4 Two qubits in independent environment: The Measures

RHP Measure

The master equation, consisting of two single qubit Lindblad terms, immediately implies the RHP measure is additive i.e. the measure is exactly twice that of one qubit. In general for pure dephasing, the measure has a simple analytical expression for any form of spectral density with a corresponding dephasing rate $\gamma_1(t)$.

BLP Measure

Contrary to the analytical optimisation achieved for the single qubit channel, for two qubits in independent identical environments the numerical optimisation is non-trival. In this case, the pair maximising the trace distance is dependent on the form of the environmental spectral density. We chose the entire time interval over which the system markedly evolves and perform extensive numerical optimisation using random pairs of states. We have compelling evidence that the optimal states in this case are $|\pm\pm\rangle\langle\pm\pm|$, i.e., product states of the single qubit optimal pairs. For com-

parison purposes, we recall in passing, the pure dephasing model we studied in Ref. [5]. Despite the identical pure dephasing operational form of this model, the optimal pair is instead a pair of Bell states, highlighting the strong dependence on the spectral density. Specifically, in this study, the spectral density is one corresponding to the Bose-Einstein condensate reservoir [115].

Having the optimal state in mind, and recalling the form of the dynamical map Φ_t^{AB}, one immediately can see the non-apparent change of the information flux as a result of an additional qubit. Specifically, the BLP measure for two independent qubits is exactly that of one qubit, i.e., it is given by Eq. 3.37. Nonetheless, this result is physically counterintuitive and contrary to what one would expect. We stress once again that this result relies on the specific form of the decoherence factors that we have calculated for the Ohmic class of reservoir spectral densities. On the contrary, for the pure dephasing model previously mentioned of Ref. [5], the measure is sub-additive.

LFS Measure and BCM Measures

Once again, we find that the LFS and BCM measures are equivalent for the case of two qubits in independent environments and moreover additive in all cases. Numerical evidence indicates that the optimising state, for the measure $\mathcal{N}_{\mathrm{I}}$, is the product state of states optimising the single qubit channel, i.e., the two-qubit maximally mixed state. With this knowledge, one can realise easily that the additivity property is satisfied. As with the single qubit case, we have again $\mathcal{N}_{\mathrm{LFS}_0} = \mathcal{N}_I$. Both measures based on capacities of quantum channels are additive for any number of n qubits interacting with n independent identical environments. The additivity property is straightforward to realise as the dephasing channel is degradable for all values of parameters.

We conclude by observing that for two qubits in independent environments the qualitative behaviour of all renormalised measures is identical to that of one qubit and we observe no new features. Moreover, all measures we study are additive, except for the BLP measure which is identical to that of one qubit.

3.3.5 Two qubits in common environment: The Measures

RHP Measure

For two qubits occupying a common purely dephasing environment, the RHP measure is found, directly from the form of the master equation:

$$\mathcal{N}_{\mathrm{RHP}} = -2\int_{\gamma_+(t)<0} dt\,\gamma_+(t) - 2\int_{\gamma_-(t)<0} dt\,\gamma_-(t). \tag{3.47}$$

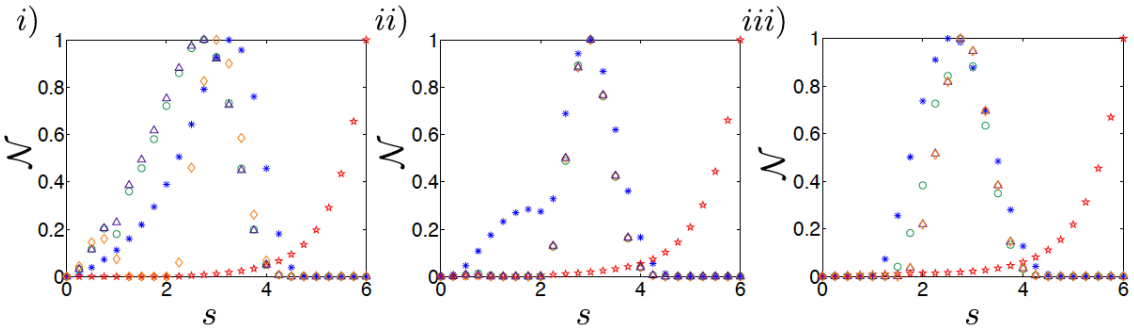

Figure 3.2: Non-Markovianity measures for two-qubit systems interacting with a common pure dephasing environments for transit times t_s i) 0.25, ii) 2 and iii) 6. We plot the RHP measure (red star), the BLP measure (blue asterisk), the LFS measure (green circle), the quantum capacity measure (purple triangle) and the entanglement-assisted capacity measure (orange diamond). All the measures in this case are normalised to unity and plotted against the Ohmic parameter s.

For pure dephasing, the form of the RHP measure shown in Eq. 3.47 is general. On the contrary, the additivity of the measure must be studied numerically for specific spectral densities. In more detail, for our analysis of Ohmic class spectral densities, we numerically prove that the measure is super-additive for any value of s.

In Fig. 3.2 we plot $\mathcal{N}_{\text{RHP}}$ versus s (red stars) for increasing values of separation between the qubits. Although not clearly visible from the plots, there exists a critical value, denoted s_c, marking the Ohmicity parameter for which the dynamics change from Markovian to non-Markovian. This value depends on the distance between the qubits, specifically, numerically we show that the critical value s_c is $\simeq 6.5 \times 10^{-2}$ for case i), $\simeq 6.6 \times 10^{-2}$ for case ii) and $\simeq 6.9 \times 10^{-2}$ for case iii) where the time interval is the time over which the system markedly evolves. We notice s_c increases for increasing values of distance between the qubits, attaining its maximum value $s_c = 2$ for $R \to \infty$ when $\delta(t) \to 0$ and we re-obtain the case of independent environments. Therefore, for $R \to \infty$, the measure is additive in the sense that the measure of the two qubit case is equal to twice the measure for each individual qubit.

BLP Measure

The common dephasing environment involves optimisation dependent on system parameters, illustrating the complexities connected to calculating the BLP measure for higher dimensional systems. In this case, we prove numerically that the optimising pair depends on both the value of s and on the distance R between the qubits i.e., the parameters included in the effective spectrum seen by the qubits. More precisely, the changes in the optimising pair stem from the complex evolution of the cross-talk term $\delta(t)$. We show that the maximising states in this case are either the super or sub-decoherent Bell states $|\Psi_\pm\rangle = \frac{1}{\sqrt{2}}(|01\rangle \pm |10\rangle)$ and $|\Phi_\pm\rangle = \frac{1}{\sqrt{2}}(|00\rangle \pm |11\rangle)$, depending on s and R, for any finite value of R. From the form of the dynamical

map in Eq. 3.42, the decoherence factors of the super- and sub-decoherent states are $\Gamma_+(t)$ and $\Gamma_-(t)$, respectively. The analytical expression for the BLP measure can be written as:

$$\mathcal{N}_{\mathrm{BLP}} = \max\{\mathcal{N}_\Phi, \mathcal{N}_\Psi\}, \tag{3.48}$$

where $\mathcal{N}_\Phi = \sum_i e^{-\Gamma_-(b_i)} - e^{-\Gamma_-(a_i)}$ is the measure if the sub-decoherent Bell states form the maximising pair and $\mathcal{N}_\Psi = \sum_i e^{-\Gamma_+(b_i)} - e^{-\Gamma_+(a_i)}$ is the measure if the super-decoherent Bell states form the maximising pair. Time intervals $t \in [a_i, b_i]$ again indicate the periods of information back flow, manifested as $d\Gamma_\pm(t)/dt \sim \gamma_\pm(t) < 0$.

From the analytic expression of $\mathcal{N}_{\mathrm{BLP}}$ one sees immediately that, also in this case, BLP non-Markovianity coincides with non-divisibility. However, the qualitative behaviour of the BLP measure when changing the reservoir spectrum is different from that of $\mathcal{N}_{\mathrm{RHP}}$, as shown in Fig. 3.2. Numerical investigation also shows that the measure is super-additive as a result of the qubit dephasing collectively through environment-mediated interactions, in contrast to the independent-environment case. For $R \to \infty$ the measure reverts to the independent case with optimal pairs $|\pm\pm\rangle\langle\pm\pm|$ and super-additivity is lost.

BCM and LFS Measures

The effect of the cross-talk term present in the common scenario influences the measures, most severely when the qubits are closer together, $t_s = 0.25$ (see Fig. 3.2, i) compared to when the qubits becoming increasingly separated, $t_s = 2, 6$ (see Fig. 3.2, ii) and iii)). Indeed, the qualitative difference between the two channel capacity measures and the LFS measure is most distinct for the case of $t_s = 0.25$, particularly for the classical capacity measure $\mathcal{N}_{\mathrm{C}}$. Specifically, the $\mathcal{N}_{\mathrm{C}}$ measure has two peaks, a large one for $s \simeq 3$ and a small one for $s \simeq 0.75$. However, as the distance between the qubits increases, the amplitude of the small peak decreases and eventually vanishes, while the bigger peak moves towards the value typical of the independent environments case, i.e., $s = 2.75$.

We now reveal the influence of the cross-talk term which is reflected in the states optimising the relevant quantities. Numerical investigation reveals that when the qubits are close-by (Fig. 3.2, i)), the optimising states of all three measures are of rank 2 with eigenvalues $\lambda_{1,2} = 0.5 \pm \epsilon$, where $\epsilon \in [0, 0.1)$. The corresponding values of $\mathcal{N}_{\mathrm{LFS}}$ and $\mathcal{N}_{\mathrm{Q}}$ differ significantly from the values obtained if the maximally mixed state was optimal. On the contrary, due to the presence of the term $S(\rho(0))$ in the definition of the entanglement assisted capacity, $\mathcal{N}_{\mathrm{C}}$ takes a value similar to the one obtained if the maximally mixed state was the optimising state. As the presence of the cross-talk term decreases, i.e., for $t_s = 2, 6$, the BCM measures are optimised by the states identified in the independent scenario, i.e., the maximally mixed two qubit state for all values s (see Fig. 3.2, ii) and iii)). On the other hand, while the optimal state is close to the maximally mixed state, for the $\mathcal{N}_{\mathrm{LFS}}$, the optimising

states are states of rank 4 with eigenvalues given by $0.25 \pm \epsilon_i$, where $\epsilon_i \in [-0.1, 0.1)$ for $i = 1, ..., 4$ are such that the normalisation condition is satisfied. Hence, for increasing transit times, or equivalently, increasing separation between the qubits, the closer the model is to the independent environment case and the closer the optimising states become to the maximally mixed state. Numerically we can show, that similarly to the BLP measure, the LFS and BCM measures are super-additive.

3.4 Comparison for the Amplitude Damping Channel

We now consider a quantum system which exchanges both energy and information with the surrounding environment, resulting in dissipative open system dynamics. As in Sec. 3.3, we focus on an exemplary open system model amenable to an exact analytical solution as this allows us to gain a solid understanding of the physical phenomena associated with reservoir memory. In more detail, we consider a single qubit interacting with a quantised bosonic field with both Lorentzian and Photonic Band Gap (PBG) spectra. For the single qubit Lorentzian case, both the BLP and BCM measures have been studied numerically in Refs. [16] and [22], respectively. For the Photonic Band Gap model, the BCM measure has been investigated in Ref. [16]. We then discuss for the first time, for both models, the generalisation to the case of two qubits immersed in two independent identical environments. The common environment scenario is not considered here because both the LFS and quantum capacity measures present a high level of difficulty in this case. For the BCM measures, the complexity of the optimisation is amplified by the fact that it should be performed at each time instant of the evolution.

We note that further mathematical details of the models, specifically the form of the Kraus operators and complementary map, are found in the Appendix A.2. Moreover, the optimisation evidence is found in the Appendix B.

3.4.1 Single qubit: The Model

The following microscopic Hamiltonian model describing a two-state system interacting with a bosonic quantum reservoir at zero temperature is given by [9]

$$H = \omega_o \sigma_z + \sum_k \omega_k a_k^\dagger a_k + \sum_k (g_k a_k \sigma_+ + g_k^* a_k^\dagger \sigma_-). \tag{3.49}$$

As usual, $\sigma_\pm$ are standard raising and lowering operators respectively. The dynamics of a single amplitude damped qubit is captured by the time-local master equation [9]:

$$\frac{d\rho_t}{dt} = \gamma_1(t) \left[\sigma_- \rho_t \sigma_+ - \frac{1}{2} \{ \sigma_+ \sigma_-, \rho_t \} \right], \tag{3.50}$$

where

$$\gamma_1(t) = -2\Re\frac{\dot{G}(t)}{G(t)}. \tag{3.51}$$

The state of the density matrix of the qubit at time t can be written in terms of the initial density matrix elements ρ_{ij} $(i,j=1,2)$ as follows

$$\rho_t = \begin{pmatrix} |G(t)|^2\rho_{11} & G(t)\rho_{12} \\ \\ G^*(t)\rho_{12}^* & 1-|G(t)|^2\rho_{11} \end{pmatrix}. \tag{3.52}$$

The function $G(t)$ depends on the form of the reservoir spectral density[6]. We consider first the case of a Lorentzian spectrum

$$J(\omega) = \frac{\gamma_M\lambda^2}{2\pi[(\omega-\omega_c)^2+\lambda^2]}, \tag{3.53}$$

with γ_M an effective coupling constant, λ the width of the Lorentzian and ω_c the peak frequency. When the qubit frequency, denoted ω_0, coincides with ω_c (resonant Jaynes-Cummings model), the dynamical map is non-divisible for $r > r_{\text{crit}} = 0.5$, with $r = \gamma_M/\lambda$ [9]. Then, the function $G^L(t)$ takes the form:

$$G^L(t) = e^{-\frac{(\lambda-i\Delta_L)t}{2}}\left[\cosh\left(\frac{\Omega t}{2}\right) + \frac{\lambda-i\Delta_L}{\Omega}\sinh\left(\frac{\Omega t}{2}\right)\right], \tag{3.54}$$

with

$$\Omega = \sqrt{\lambda^2 - 2i\Delta_L\lambda - 4\varpi^2} \tag{3.55}$$

where $\varpi = \gamma_M\lambda/2 + \Delta_L^2/4$ and $\Delta_L = \omega_0 - \omega_c$.

For $\Delta_L = 0$, one obtains the following solution,

$$G^L(t) = e^{-\lambda t/2}\left[\cosh\left(\sqrt{1-2r}\frac{\lambda t}{2}\right) + \frac{1}{\sqrt{1-2r}}\sinh\left(\sqrt{1-2r}\frac{\lambda t}{2}\right)\right] \tag{3.56}$$

with $r = \gamma_M/\lambda$.

For the Photonic Band Gap model, the specific form of $G^P(t)$ is as follows [28]:

$$\begin{aligned} G^P(t) &= 2v_1x_1e^{\beta x_1^2+i\Delta_P t} + v_2(x_2+|x_2|)e^{\beta x_2^2 t+i\Delta_P t} \\ &- \sum_{j=1}^{3} v_j|x_j|[1-\Phi(\sqrt{\beta x_j^2}t)]e^{\beta x_j^2 t+i\Delta_P t}, \end{aligned} \tag{3.57}$$

where $\Delta_P = \tilde{\omega}_0 - \omega_e$ is the detuning of the qubit frequency from the edge frequency ω_e of the band gap spectrum, set to equal zero as we consider only the resonant case and $\Phi(x)$ is the error function, whose series and asymptotic representations are

[6]We note, that $G(t)$ satisfies the non-local equation $\dot{G}(t) = -\int_0^t f(t-t')G(t')dt'$ with initial condition $G(0)=1$, and $f(t)$ is the reservoir correlation function which is related via the Fourier transform with a spectral density $J(\omega)$.

given in Ref. [116]. In addition:

$$\begin{aligned} x_1 &= (A_+ + A_-)e^{i(\pi/4)}, \\ x_2 &= (A_+ e^{-i(\pi/6)} - A_- e^{i(\pi/6)})e^{-i(\pi/4),} \\ x_3 &= (A_+ e^{i(\pi/6)} - A_- e^{-i(\pi/6)})e^{i(3\pi/4)}, \end{aligned} \tag{3.58}$$

$$A_\pm = \left[\frac{1}{2} \pm \frac{1}{2}\left[1 + \frac{4}{27}\frac{\Delta_P^3}{\beta^3}\right]^{1/2}\right]^{1/3}, \tag{3.59}$$

$$v_1 = \frac{x_1}{(x_1 - x_2)(x_1 - x_3)} \tag{3.60}$$

$$v_2 = \frac{x_2}{(x_2 - x_1)(x_2 - x_3)}, \tag{3.61}$$

$$\beta^{3/2} = \tilde{\omega}_0^{7/2} d^2 / 6\pi\epsilon_0 \hbar c^3. \tag{3.62}$$

The coefficient β is defined as the characteristic frequency, ϵ_0 the Coulomb constant and d the atomic dipole moment. We have defined in our results $z = \Delta_P/\beta$.

For the PBG model [28], the Markovian to non-Markovian crossover is defined in terms of the reservoir parameter $z = \Delta_P/\beta$. Positive values of z correspond to the case in which the qubit is outside the band gap region while negative values of z correspond to the qubit in the band gap region. In the latter case the well-known phenomenon of population trapping occurs as the emission of energy in the reservoir is strongly inhibited. In the asymptotic long time limit and for $z \ll z_{\rm crit}$, population trapping leads to small amplitude oscillations between positive and negative values which persist in the asymptotic limit $t \to \infty$. This eventually leads to divergency in all non-Markovianity measures which, by definition, aim to encapsulate information back flow for the entire time interval the system markedly evolves. For this reason, we aim to study a practical experimental time interval which is finite. The time interval we use is longer compared to the typical times of the system but shorter than the system reservoir correlation time which in this case is ∞.

3.4.2 Single qubit: The Measures

RHP Measure

For master equations in the Lindblad form with time-dependent coefficients and corresponding to amplitude damped dynamics, the RHP measure is straightforward to calculate for a generic spectral density [117]:

$$\mathcal{N}_{\rm RHP} = -\int_{\gamma_1(t)<0} dt\, \gamma_1(t). \tag{3.63}$$

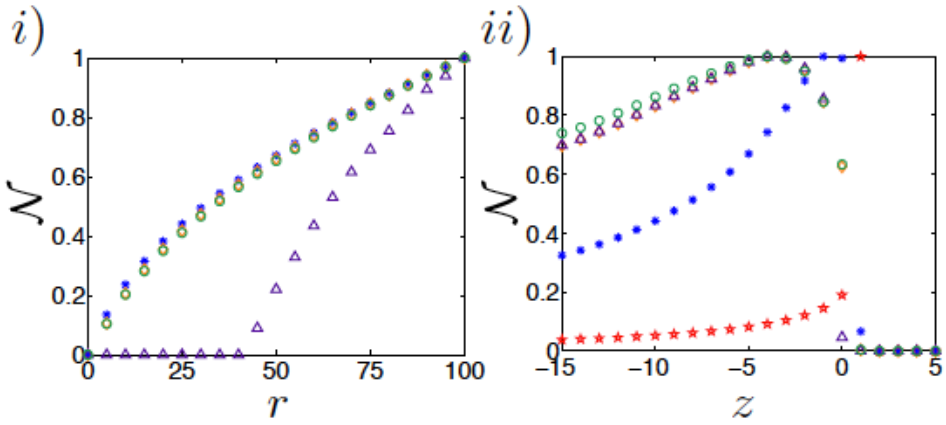

Figure 3.3: Non-Markovianity measures for a qubit undergoing amplitude damping for i) Lorentzian spectrum and ii) Photonic Band Gap model. We plot the RHP measure (red star), the BLP measure (blue asterisk), the LFS measure (green circle), the quantum capacity measure (purple triangle) and the entanglement-assisted capacity measure (orange diamond). All the measures in this case are normalised to unity. We consider the following times periods: i) $0 \leq \lambda t \leq 40$ and ii) $0 \leq \beta t \leq 20$. For the Lorentzian spectrum, the RHP measure is zero for $r \leq 0.5$ while it diverges for $r > 0.5$.

For the Lorentzian spectrum, the dynamical map is non-divisible for $r = r_{\text{crit}} > 0.5$. Above this critical value, $\mathcal{N}_{\text{RHP}}$ diverges as a direct consequence of the divergent behaviour of the decay rate $\gamma_1(t)$. Conversely, in the Markovian regime, $r < 0.5$, the decay rate is positive at all times and hence the channel is always divisible and the RHP measure is zero.

In the Photonic Band Gap (PBG) model, the critical value corresponding to the crossover in regimes is given by $z_{\text{crit}} = 1.7$, where for $z < z_c$, the map is non-divisible. In Fig. 3.3 ii) we plot the RHP measure (red stars) for the PBG reservoir as a function of the parameter z. The measure has a sudden peak at values of z close to the edge $z = 0$, reaching its maximum value for $z = 1.0$ before vanishing for $z = 1.7$. For increasingly negative values of z under the critical point, the measure decreases to small but finite values. This is due to the decreasing amplitude of the oscillations in the decay rate.

BLP Measure

Analytically, the BLP measure $\mathcal{N}_{\text{BLP}}$ takes the form [117]:

$$\mathcal{N}_{\text{BLP}} = -\max_{m,n} \int_{\gamma_1<0} dt\, \gamma_1(t) \frac{|G(t)|^3 m^2 + 0.5|G(t)||n|^2}{\sqrt{|G(t)|^2 m^2 + |n|^2}}, \tag{3.64}$$

where $m = \rho^1_{11}(0) - \rho^2_{11}(0)$ and $n = \rho^1_{12}(0) - \rho^2_{12}(0)$ are coefficients to be optimised. We have compelling numerical evidence that the maximising states are the orthogonal states $|+\rangle\langle+|$ and $|-\rangle\langle-|$ for both the Lorentzian and the PBG spectral densities,

hence, we have:

$$\mathcal{N}_{\rm BLP} = -\frac{1}{2}\int_{\gamma_1<0} dt\, \gamma_1(t)|G(t)|. \tag{3.65}$$

We see immediately that the BLP measure coincides with non-divisibility and takes non-zero values only for $\gamma_1(t) < 0$.

Figure 3.3 shows $\mathcal{N}_{\rm BLP}$ (blue asterisk) for different values of i) r and ii) z for the Lorentzian and PBG spectra, respectively. For the PBG model, the behaviour is qualitatively similar to the one of the RHP measure but with the peak of non-Markovianity slightly shifted towards more negative values of z. In Ref. [118], the BLP measure and RHP witness are calculated for quantum harmonic oscillators in a band gap showing that both measures are sensitive to the edge of the gap, which is what we also observe.

BCM and LFS Measures

For the amplitude damping channel, the optimisation procedure for the entanglement-assisted classical and quantum capacities identifies optimal states which are time-dependent [119, 120]. One finds [121] the following:

$$C_{ea} = \max_{p\in[0,1]} \Big\{ H_2(p) + H_2(|G(t)|^2 p) - H_2([1-|G(t)|^2]p) \Big\}, \tag{3.66}$$

$$Q = \max_{p\in[0,1]} \Big\{ H_2(|G(t)|^2 p) - H_2([1-|G(t)|^2]p) \Big\}, \tag{3.67}$$

which require optimisation over the probability $p \in [0,1]$. The latter formula holds only for $|G(t)|^2 > \frac{1}{2}$, otherwise $Q \equiv 0$. This is due to the fact that the amplitude damping channel is degradable for $|G(t)|^2 > \frac{1}{2}$, while for $|G(t)|^2 \leq \frac{1}{2}$ is anti-degradable with zero quantum capacity.

Numerically, it can be proved that for both the Lorentzian reservoir spectrum and the PBG model, the measures $\mathcal{N}_{\rm C}$ and $\mathcal{N}_{\rm I}$ take non-zero values if and only if the amplitude damping channel is non-divisible (see. Fig. 3.3). Both measures based on quantum mutual information ($\mathcal{N}_{\rm I}$ and $\mathcal{N}_{\rm C}$) take very close values to each other, however no mathematical relation exists between them for the amplitude damped model. We notice a strong dependence on the form of the environmental spectrum through these two measures. In more detail, in the case of the Lorentzian spectrum we have $\mathcal{N}_{\rm C} > \mathcal{N}_{\rm I}$, while in the PBG model the opposite relation holds (see Fig. 3.3 i) and 3.3 ii), respectively).

From Fig. 3.3, it is immediate to notice the difference in the behaviour of $\mathcal{N}_{\rm Q}$ for the Lorentzian reservoir. In more detail, unlike the other measures, $\mathcal{N}_{\rm Q}$ is equal to zero even when the channel is non-divisible and instead, detects non-Markovianity only in the very strong coupling regime, i.e. for $r > 43$. This is due to the fact that the amplitude damping channel is anti-degradable for $|G(t)|^2 < \frac{1}{2}$ so, from

a quantum information processing point of view, only revivals that occur in the region $|G(t)|^2 > \frac{1}{2}$ are important. This result is consistent with the intuitive idea that the transmission of quantum information along a quantum channel is more sensitive to noise than the transmission of classical information (although assisted by entanglement shared between Alice and Bob). Once again however, this conclusion is spectrum-dependent. For the PBG model, it is possible to set the system parameter z such that the noise in the channel has almost the same effect on both kinds of information. This occurs for $z < 0$ as $|G(t)|^2$ in this regime oscillates only above the value $\frac{1}{2}$ but is no longer possible for $0 \leq z < 2$ as shown in Fig. 3.3 ii), the biggest difference occurring for $z = 0$.

3.4.3 Two qubits: The Model

For the amplitude damped channel, we consider the Hamiltonian:

$$H = \omega_o \sigma_z^A + \omega_o \sigma_z^B + \sum_k \omega_k a_k^\dagger a_k + \sum_k (g_k a_k \sigma_+^A + g_k^* a_k^\dagger \sigma_-^A) + \sum_k (g_k a_k \sigma_+^B + g_k^* a_k^\dagger \sigma_-^B). \tag{3.68}$$

For two qubits interacting with identical non-correlated environments the time evolution can still be calculated analytically [122]. The diagonal elements of the amplitude damping channel $\Phi_t^{A,B}$ are written as follows [123]:

$$\begin{aligned}
\rho_{11}(t) &= |G(t)|^4 \rho_{11}(0) \\
\rho_{22}(t) &= |G(t)|^2 \rho_{11}(0)(1 - |G(t)|^2) + \rho_{22}(0)|G(t)|^2 \\
\rho_{33}(t) &= |G(t)|^2 \rho_{11}(0)(1 - |G(t)|^2) + \rho_{33}(0)|G(t)|^2 \\
\rho_{44}(t) &= 1 - (\rho_{11}(t) - \rho_{22}(t) - \rho_{33}(t))
\end{aligned} \tag{3.69}$$

For the off-diagonal elements, we have:

$$\begin{aligned}
\rho_{12}(t) &= |G(t)|^2 G(t) \rho_{12}(0) \\
\rho_{13}(t) &= |G(t)|^2 G(t) \rho_{13}(0) \\
\rho_{14}(t) &= G(t)^2 \rho_{14}(0) \\
\rho_{23}(t) &= |G(t)|^2 \rho_{23}(0) \\
\rho_{24}(t) &= \rho_{13}(0) G(t)(1 - |G(t)|^2) + \rho_{24}(0) G(t) \\
\rho_{34}(t) &= \rho_{12}(0) G(t)(1 - |G(t)|^2) + \rho_{34}(0) G(t)
\end{aligned} \tag{3.70}$$

It is straightforward to confirm that, as for the pure dephasing case, the corresponding master equation can be written as the sum of two Lindblad-like terms, describing the dynamics of each qubit respectively, with time-dependent coefficient $\gamma_1(t)$ given

by Eq. 3.51.

3.4.4 Two qubits in independent environment: The Measures

RHP Measure

Directly from the form of the master equation, we immediately can show that

$$\mathcal{N}_{\text{RHP}} = -2 \int_{\gamma_1(t)<0} dt\, \gamma_1(t). \tag{3.71}$$

For the general operative form of the amplitude damping channel, the measure is additive, hence, for the PBG model, the renormalised measure behaves identically to the single qubit cases of Fig. 3.3. On the other hand, for the Lorentzian spectrum, $\mathcal{N}_{\text{RHP}} = \infty$ when the dynamical map is non-divisible as it is in the one qubit case.

BLP Measure

For the Lorentzian spectrum, we conjecture that the maximising pair is $|\pm\pm\rangle\langle\pm\pm|$. Following this, we obtain the following expression for the BLP measure,

$$\mathcal{N}_{\text{BLP}} = -\int_{\gamma_1<0} dt\, \gamma_1(t) \frac{|G(t)| - 2|G(t)|^3 + 1.5|G(t)|^5}{\sqrt{2 - 2|G(t)|^2 + |G(t)|^4}}. \tag{3.72}$$

Numerically, we prove that the measure is sub-additive in this case, however, we notice that the qualitative behaviour as r changes is exactly that of the one qubit case. Hence the renormalised value of the BLP measure for two qubits in independent environments gives exactly the same curve as the one shown in Fig. 3.3 i) (blue asterisk).

The Photonic Band Gap model presents a number of difficulties and we do not identify precisely the optimal state in this case. Indeed, in this model, the pair of states maximising the increase in trace distance is very strongly dependent on the time interval chosen. Numerical investigation shows that the measure is maximised for initial pairs of mixed and pure states (blue dots) for $-15 \leq z \leq -3$, maximally entangled (purple dots) for $-2 \leq z \leq -1$, pure (pink dots) for $z = 0$ and the tensor product state $|\pm\rangle\langle\pm|$ (yellow dots) for $z = 1$. We have not been able to exactly identify the states for which the increase in trace distance is maximal, even for a fixed time interval. By comparing the numerical value of $\mathcal{N}_{\text{BLP}}$ with the single qubit case of Fig. 3.3 ii), we see however that also in this case the renormalised quantity has the same qualitative behaviour for one and two qubits. In this case we have verified that the BLP is super-additive for $-15 \leq z \leq -2$ and sub-additive for $-1 \leq z \leq 1$. Moreover, the measure is zero if and only if the channel is divisible.

LFS Measure and BCM Measures

For two qubits in independent environments for the amplitude damped channel, we

realise the LFS and BCM measures are additive. Compelling numerical evidence identifies the state optimising the LFS measure, for both the Lorentzian and PBG spectral densities, as $\rho^*_{AB} = \rho^* \otimes \rho^*$ where ρ^* is the maximising state for the one-qubit channel. Therefore, the renormalised measure for two qubits is identical to the measure of one qubit, shown in Fig. 3.3. Having in mind that whenever the amplitude damping channel is not degradable it is anti-degradable, and hence has zero quantum capacity, one can clearly see that the measures $\mathcal{N}_{\mathrm{C}}$ and $\mathcal{N}_{\mathrm{Q}}$ are additive and therefore display identical behaviour with respect to the system parameters as the one discussed in the one qubit scenario, shown in Fig. 3.3.

3.5 Discussions

3.5.1 Comparison of the Measures

We now discuss the qualitative behaviour of the measures for the single and composite scenarios we have studied in this chapter. It is evident that in general, the behaviour of the RHP measure is different from measures capturing non-monotonic quantum quantities (see. Figs. 3.1, 3.2, and 3.3 ii)). Indeed, in the non-divisible regime, the behaviour of the RHP measure is generally monotonically increasing, while for the other measures studied, there exists specific system parameters for which the memory effects peak. This behaviour can be traced back to the definition of the RHP measure, which counts and sums the areas of negativity of the time-dependent decay rates in the master equation. Precisely, as the environment becomes increasingly structured, the number of negativity intervals increase and subsequently the RHP measure increases. Physically, as the RHP measure increases, the number of reverse jumps increase, leading to greater recoherence. While the measure is easily computable, indeed amendable to analytical expressions in all models we have studied, we find the measure diverges for the Lorentzian spectrum. The problematic divergent behaviour is a direct consequence of the decay rate diverging when the dynamics is non-divisible. Moreover, the measure is additive in all models for independent reservoirs (and finite decay rates) and the qualitative behaviour for two qubits in either independent and common (dephasing) environments is the same.

We now discuss the measures based on the non-monotonic time evolution of certain quantum properties. All measures, excluding the BLP measure, i.e. LFS and BCM measures, are additive for two qubits interacting in independent environments. This demonstrates the difficulties in optimising the BLP measure for higher dimensional systems, and in fact calculations for systems comprising even three qubits are most likely impractical. In the pure dephasing cases, Fig. 3.1 (single qubit and two qubits in independent environment) and Fig. 3.2 (two qubits in common environment), the behaviour of all non-monotonic measures is similar, in the sense that

they all have a maximal value in the parameter range $2 < s < 4$. Hence, the manifestations of memory in terms of increase of information on the system, increase of system-ancilla total correlations, or in terms of increase of channel capacities arise in a similar way when modifying the form of the spectrum. In the common environment case of Fig. 3.2, contrarily to the RHP measure, the other measures show a stronger sensitivity to the distance between the qubits, which in turn is connected to the cross-talk term, i.e. the environment mediated interaction that is known to contribute to the overall memory effects [124]. The BLP, LFS and BCM measures seem to show a narrower peak as the distance is increased, consistently with the independent qubit case of Fig. 3.1.

The amplitude damping case presents clear differences and, interestingly, contrary to the pure dephasing case, the measures do not always detect non-Markovianity for the full range of system parameters corresponding to the non-divisible regime. Specifically, for the Lorentzian case, the quantum channel capacity measure takes non-zero values only when the coupling of the system with the environment is sufficiently strong. Our result is intuitive, as quantum information is more sensitive to environmental noise than classical information, hence a much stronger memory effect is required for a partial increase to occur in the maximum rate of information transfer for increasing times or length of channel. The presence of energy exchange between the system and the environment introduces a new relevant time scale, or frequency, i.e. the Bohr frequency ω_0 of the two-level system forming the qubit. In the dephasing case the structure of the spectral density and the presence of peaks in resonance with ω_0 is not related to the occurrence of non-Markovian dynamics. Rather, it is the form of the spectrum at the origin $\omega = 0$ that dictates the presence or not of re-coherence and revivals of information [66]. The situation is clearly different in the dissipative case where the qubit is more likely to interact with environmental modes of the same frequency of ω_0. A clear sign of this behaviour is shown in Fig. 3.3 ii) for the Photonic Band Gap case. Here all non-Markovianity indicators display the same key feature, i.e., they have their maximum around $\omega_0 = \omega_e$, where the coupling between the qubit and the modes is the strongest [91]. In this case, indeed, the qubit exchanges periodically energy with the environment and its population shows Rabi oscillations. Consistently, memory effects associated to the energy exchange between system and environment also lead to oscillations of the information content of the system (back flow of information), total correlations between system and ancilla, and channel capacities.

3.5.2 Practical Applications of Non-Markovianity

The simulation of open quantum systems in both Markovian and non-Markovian regimes can now be realised within modern experimental limitations [125]-[128]. Theoretically, it is therefore important to define non-Markovian quantifiers from an

experimental perspective with the minimum practical requirements possible. In this chapter, all non-Markovianity measures are not defined in terms of observables of the system. Indeed, at present, all proposed witnesses of non-Markovianity rely on the full knowledge of the density matrix at all times t [129]. Hence, for experimental detection, quantum process tomography, i.e., a practical process for constructing the density matrix, must be performed. On the one hand, the RHP measure is the only quantifier which does not require optimisation over the space of states, however assumes the knowledge of either the dynamical map or the explicit form of the master equation. On the other hand, the BLP, LFS and BCM measures do not in principle require an assumption on the specific model of open quantum system dynamics if one decides to instead perform the heavy optimisation experimentally. Indeed, in this case, every quantum state in the state space should be prepared and subject to the environment whilst quantum state tomography is performed at all times. In this way, the non-monotonicity of certain quantum properties would be determined for all states and the optimal identified. Alternatively, one may assume the validity of a given model and solve the optimisation problem either numerically or analytically. Hence, experimentally, it is then sufficient to only prepare the optimal state(s) and perform process tomography once to acquire the evolution of the density matrix. From this more realistic perspective the requirements for experimental implementation are comparable for all measures. At present, the BLP and the RHP measures have been experimentally observed in optical experiments simulating pure dephasing environments [25]-[27].

The potential advantage of non-Markovianity as an exploitable resource in quantum technologies is a non-trivial focus of ongoing research. Recent results have shown that, in certain circumstances, the manipulation of reservoir spectral properties may lead to improvements in certain quantum technologies [13]-[18]. The improvements demonstrated for quantum metrology [13] and for quantum key distribution [14] are realised also when the dynamical map is divisible and so can not be attributed to the presence of memory effects. Other results work instead in the specific case of correlated dephasing environments, where the effect of the noise is known, such as the quantum teleportation scheme of Ref. [15]. Generally, the connection between certain quantum technologies and non-Markovian memory effects is found in Ref. [16] and was indeed the motivation behind the introduction to the channel capacity measures.

3.6 Conclusion

In this chapter, we have presented an extensive comparative study of several measures of non-Markovianity through calculations for one and two qubits subject to purely dephasing and amplitude damped dynamics. The emerging picture is that,

despite the obvious differences between the measures, their corresponding physical mechanisms contributing to memory effects often appear correlated and show a similar connection with the reservoir spectral features. The insights gained from each measure can be compared to the perceptions found in the old Indian tale of the "Blind Men and the Elephant". The story illustrates how perception is based on what a person is able to see or touch, specifically blind men touching an elephant and determining what they think the elephant is. In our case the elephant is non-Markovian dynamics and the blind men are the different measures. Although each man touches the same animal, his determination of the elephant is based only on what he is able to perceive or, in our terms, on what physical phenomenon stemming from reservoir memory the measure is revealing. In conclusion, the non-Markovianity measures give different perspectives on the same complex physical process, a full understanding of which requires them all.

Chapter 4

Optimal Control in Non-Markovian Systems

In this chapter, we investigate the potential usefulness of non-Markovianity for advancing quantum protocols aimed at optimally counteracting decoherence. Efficient schemes for compensating harmful noise in quantum systems have been developed utilising the quantum Zeno effect [29, 30], dynamical decoupling strategies [130, 131] and optimal control [34]-[45]. Generally, the theoretical description of these techniques in the presence of noise is a daunting task, therefore they are typically studied under a number of assumptions concerning the type of environments the system is interacting with as well as the typical time-scales. Specifically, optimal control techniques have been so far studied, almost exclusively, in the so-called Markovian limit, that is whenever the system-environment interaction is weak and the correlations short living. In this case the master equations describing the open system dynamics are found phenomenologically or derived with microscopic approaches using numerous approximations [34]-[45]. However, in order to understand control theory with realistic experimental scenarios [9],[132]-[136] in mind, Markovian descriptions must be replaced with non-Markovian descriptions. Moreover, intuitively, one may wonder whether the ability of non-Markovian systems to retrieve information previously lost to decoherence can be exploited in quantum information tasks by means of reservoir engineering techniques [13]-[18]. The results from this chapter are based on the those obtained in Publication ii [2].

4.1 Markovian Optimal Control

For the sake of concreteness, we focus on a novel approach to optimal control, recently proposed in Ref. [34]. In this context, the aim is to seek a control Hamiltonian that optimally upholds, on asymptotic time scales, a given target property (e.g. coherence, entanglement or fidelity w.r.t. a target state) [34]. The feasibility of this approach crucially relies on the fact that it is physically admissible to fix the

dissipative part of the master equation. Specifically, that one can assume that the dissipative dynamics is governed by external circumstances only and does not change in the presence of a control Hamiltonian. In order to identify the control Hamiltonian that optimally counteracts the detrimental effect of decoherence, an indirect method of optimisation must be found. The complexity of the optimisation arises from the fact that the space of Hamiltonians can not be efficiently parametrised and so the problem must be approached from a different perspective. Instead, we aim to identify the optimal asymptotic cycle compatible with a given dissipator. More precisely, we sample in the set of stabilizable cycles $\mathcal{S}^{\circlearrowleft}$ which comprises all closed trajectories of arbitrary period T, for which a suitable Hamiltonian $H(t)$ exists that turns the trajectory into a solution of the following Markovian master equation ($\hbar = 1$),

$$\dot{\rho} = -i[H(t), \rho] + \mathcal{D}(\rho), \tag{4.1}$$

with a fixed dissipator $\mathcal{D}(\rho) = \sum_k \gamma_k [L_k \rho L_k^\dagger - \frac{1}{2}\{L_k^\dagger L_k, \rho\}]$ composed of Lindblad operators L_k and time independent decay rates γ_k. The crucial insight behind this is that physically admissible trajectories in state space are exclusively constrained by the dissipative part $\mathcal{D}$ of the dynamics alone. In light of this, given an asymptotic cycle $\rho(t) \in \mathcal{S}^{\circlearrowleft}$, the corresponding Hamiltonian $H(t)$ which stabilises the cycle can be determined in terms of $\rho = \sum_\alpha p_\alpha |\alpha\rangle \langle\alpha|$, where p_α and $|\alpha\rangle$ denote the instantaneous eigenvalues and eigenstates of $\rho(t)$, i.e., at time instant t:

$$H(t) = \sum_{p_\alpha \neq p_\beta} \frac{i \langle\alpha| (\mathcal{D}(\rho) - \dot{\rho}) |\beta\rangle}{p_\alpha - p_\beta} |\alpha\rangle \langle\beta| . \tag{4.2}$$

It is straightforward, directly from Eq. 4.1, to define a simple criterion, for which a time-dependent control Hamiltonian $H(t)$ exists such that $\rho(t)$ solves the master equation:

$$\forall t \; \forall n : \mathrm{Tr}[\rho^{n-1}(t)\mathcal{D}(\rho(t))] = \frac{1}{n}\delta_t \mathrm{Tr}[\rho(t)^n], \tag{4.3}$$

which holds for any $\rho(t)$ with non-degenerate eigenvalues and $n \in \{2, .., d\}$, with $d = \dim\mathcal{H}$ the dimension of the system [34]. The criteria in Eq. 4.3 implies that only the dissipative dynamics can modify the spectrum μ_n of the density matrix ρ, defined as,

$$\mu_n = \mathrm{Tr}(\rho^n) = \sum_{\alpha=1}^{d} (p_\alpha)^n. \qquad n, 1, 2...d \tag{4.4}$$

More precisely, the temporal change of μ_n exclusively depends on the quantity

$$f_n(\rho(t)) = n.\mathrm{Tr}(\rho(t)^{n-1}\mathcal{D}(\rho(t))), \tag{4.5}$$

identifying $f_n(\rho(t)$ as a dissipative flux generated at the time instant t at the specific point $\rho(t)$ in the state space, i.e. $f_n(\rho(t)) = \dot{\mu}_n(\rho(t))$. In order to satisfy the criteria

set in Eq. 4.5, μ_n must necessarily increase (decrease) if $\rho(t)$ occupies a region of state space corresponding to positive (negative) flux. If $\rho(t)$ occupies points of vanishing flux, $\mu_n(\rho(t))$ must remain constant.

To explicate these concepts, we focus on the simplest case of a single qubit. The desirable objective to optimise in this case is the coherence between the ground and excited state, i.e., the capability of ρ to show interference phenomena in the $|0\rangle$ / $|1\rangle$ basis:

$$\mathcal{C}(\rho) = 2|\langle 0|\rho|1\rangle|. \tag{4.6}$$

In Bloch notation, the Bloch vector $\vec{r}$ of single qubit state ρ is given as $\vec{r} = \mathrm{tr}(\vec{\sigma}\rho)$ and coherence can be geometrically interpreted as the distance of Bloch vector from the z-axis, $\mathcal{C}(\rho) = \sqrt{r_x^2 + r_y^2}$. Immediately, Eq. 4.5 simplifies, imposing only a constraint on the evolution of the purity $\mu_2 = \mathrm{tr}(\rho^2)$ of the state, defined in Bloch notation as $\mu_2 = \frac{1}{2}(|\vec{r}|^2 + 1)$. In Bloch notation, an admissible trajectory $\{\rho(t) : t \in [0, T)\}$, or $\{\vec{r}_t\}$ in the Bloch ball, must then satisfy at all times the following criterion [34]:

$$\underbrace{\vec{r}_t.(\mathfrak{D}\vec{r}_t + \vec{\delta})}_{f(\vec{r}_t)} = \underbrace{\frac{1}{2}\delta_t|\vec{r}_t|^2}_{\dot{\mu}(\vec{r}_t)}, \tag{4.7}$$

where the term $\mathfrak{D}\vec{r} + \vec{\delta}$ reflects the dissipative part of the dynamics, precisely:

$$(\mathfrak{D})_{ij} = \mathrm{tr}(\sigma_i \mathcal{D}(\sigma_j))/2, \qquad (\vec{\delta})_i = \mathrm{tr}(\sigma_i \mathcal{D}(\mathbb{I}))/2. \tag{4.8}$$

Hence, Eq. 4.7 implies that only the dissipative flux can change the radial component of the Bloch vector $\vec{r}_t$. The challenge now remains to identify the cycle that optimises the time average $\bar{\mathcal{O}}(\rho)$ of an objective $\mathcal{O}(\rho(t))$,

$$\bar{\mathcal{O}}(\rho) = \frac{1}{T}\int_0^T dt\ \mathcal{O}(\rho(t)), \tag{4.9}$$

where T is the period of the cycle. Despite the simplification achieved with the characterisation of stabilizable cycles, the complexity of the remaining optimisation over the vast and unstructured set $\rho(t) \in \mathcal{S}^{\circlearrowleft}$ still requires further reduction to be feasible.

4.1.1 Two-Point Cycles

In Ref. [34], it is shown that the optimisation over all stabilizable cycles can be reduced to the tractable class of *two point cycles* (TPC). The validity of this statement is twofold. Without loss of generality, it must be possible to limit the investigation to specific cycles, which undergo a single monotonic purity gain (loss) followed by an equivalent monotonic loss (gain). Moreover, nontrivially, the physical feasibility of implementing a TPC relies on the ability to reduce a full cycle to a cycle containing

a pair of Bloch vectors of purity p and experiencing a flux equivalent to that of the full cycle. To explain in detail, we will briefly outline the formalism of TPCs, with the full explanation given in Ref. [137]. For cycles undergoing a single purity increasing stage during the time interval $[t_0, t_1]$, followed by a single purity decreasing during the time interval $[t_1, T]$, the cycle can be purity parametrised and just as well described by the following pair $\vec{r}_\pm$,

$$\vec{r}(t) \quad \text{with} \quad t \in [t_0, T] \rightarrow (\vec{r}_+(p), \vec{r}_-(p)) \quad \text{with} \quad p \in [p_0, p_1], \tag{4.10}$$

where p_0 (p_1) dictates the minimum (maximum) purity obtained in the cycle. With this in mind, it is possible to define the following inequality [137],

$$\bar{\mathcal{O}}[\vec{r}] = \frac{\int_{p_0}^{p_1} \left(\frac{\mathcal{O}(\vec{r}_+(p))}{|f(\vec{r}_+(p))|} + \frac{\mathcal{O}(\vec{r}_-(p))}{|f(\vec{r}_-(p))|} \right) dp}{\int_{p_0}^{p_1} \left(\frac{1}{|f(\vec{r}_+(p))|} + \frac{1}{|f(\vec{r}_-(p))|} \right) dp} \leq \max_p \bar{\mathcal{O}}_{\text{TPC}}(\vec{r}_+(p), \vec{r}_-(p)), \tag{4.11}$$

where,

$$\bar{\mathcal{O}}_{\text{TPC}}(\vec{r}_+(p), \vec{r}_-(p)) = \frac{\mathcal{O}(\vec{r}_+(p))|f(\vec{r}_-(p))| + \mathcal{O}(\vec{r}_-(p))|f(\vec{r}_+(p))|}{|f(\vec{r}_+(p))| + |f(\vec{r}_-(p))|}. \tag{4.12}$$

The inequality can be interpreted as follows: The time-averaged objective function $\bar{\mathcal{O}}[\vec{r}]$ of a general cycle, with purity values in $[p_0, p_1]$, is equal to, or smaller than the quantity $\bar{\mathcal{O}}_{\text{TPC}}(\vec{r}_+, \vec{r}_-)$, evaluated for the pair $\vec{r}_\pm(p)$ at the optimal intermediate purity value p [137]. Hence any stabilizable cycle is always outperformed by one of the TPCs that it contains. The TPC is understood as a minimalistic cycle, which instantaneously jumps back and forth between $\vec{r}_\pm(p)$, dwelling in the neighbourhood of each point for a time $\delta t_\pm \rightarrow 0$. This is always possible with sufficiently strong Hamiltonian control, capable of generating purity-preserving unitary "kicks" on timescales smaller than the time scales related to the system. In spite of this limit, it is always possible to define Eq. 4.12, as the ratio of the dwell times remains finite,

$$\frac{\delta t_+}{\delta t_-} = \frac{\delta p / |f(\vec{r}_+(p))|}{\delta p / |f(\vec{r}_-(p))|} = \frac{|f(\vec{r}_-(p))|}{|f(\vec{r}_+(p))|}. \tag{4.13}$$

Hence, optimisation over TPCs involves identifying only the optimal pair of equal purity Bloch vectors $\vec{r}_\pm(p)$ which occupy purity increasing (decreasing) regions of the state space, i.e. $f(\vec{r}_+) > 0$ and $f(\vec{r}_-) < 0$ respectively. In this new framework, the sampling, now restricted to the subset of TPCs, becomes a manageable task.

We now briefly discuss the generality of the inequality Eq. 4.11, specifically, the feasibility of implementing a TPC for time-dependent decay rates. In Ref. [34], the optimal control protocol is applied to a single qubit, exposed to the three most common incoherent processes: decay of the excited state, absorption from the ground state and dephasing between ground and excited state. For time-independent

and positive (Markovian) decay rates, they find that the optimal TPC degenerates to a single point, implying periodic Hamiltonians offer no advantage compared to stationary ones. Therefore, in this limit, the optimal value of coherence achievable is equal to $\sqrt{1/2}$. In Ref. [137], an artificially modified decay rate is proposed in order to achieve superior optimal values. In more detail, by applying a time-dependent amplification to the incoherent dynamics, occurring when the cycle transverses a purity-increasing region, the incoherent rates γ_k must temporarily increase, in a control manner, by a factor $\alpha > 1$. It can be easily seen that the purity flux $f(\vec{r}_+(p))$ will be rescaled by the same factor α, and hence we can write [137]:

$$\bar{\mathcal{O}}_{\mathrm{TPC}}(\vec{r}_+(p), \vec{r}_-(p)) = \frac{\mathcal{O}(\vec{r}_+(p))|f(\vec{r}_-(p))| + \alpha\mathcal{O}(\vec{r}_-(p))|f(\vec{r}_+(p))|}{\alpha|f(\vec{r}_+(p))| + |f(\vec{r}_-(p))|} \tag{4.14}$$

The optimal pair is now dependent on α and in the extreme case of infinite amplification $\alpha \to \infty$. the TPC effectively reduces to a single point of perfect coherence $\vec{r} = (1, 0, 0)$ [137]. More in general, for arbitrary time-dependent decay rates excluding this special case, it is straightforward to convince ones self that the two-fold statement for the validity of Eq. 4.11 is no longer true. Hence, one must complete full cycle optimisation in this case.

Nevertheless, in light of the astonishingly simple characterisation of optimal control schemes in the present of fixed dissipation given in Eq. 4.7, the following question stands: Is it possible to determine a time-dependent control Hamiltonian for a fixed non-Markovian dissipator (with temporarily negative decay rates) to optimise some target property?

4.2 Non-Markovian Optimal Control: Phenomenological Case

4.2.1 Optimal Control in a Dephasing Model

In order to tackle this question, we concentrate on a simple example of a single qubit in a dephasing environment. We begin by exploring the phenomenological case, where the qubit dissipator is fixed under the control sequence. In contrast to Ref. [34], we seek a control Hamiltonian that, on average, optimally upholds the coherence of the single qubit for the time T the system markedly evolves rather than for asymptotic time scales. The natural dephasing of the system ends for $t \geq T$ and in the absence of control, when the Hamiltonian vanishes, the states cease to evolve. For the single qubit, an admissible trajectory $\{\rho(t) : t \in [0, T)\}$, or $\{\vec{r}_t\}$ in the Bloch ball, must then satisfy at all times the criterion of Eq. 4.7 [34].

For a Markovian dephasing process, for which the dynamics is generated by the

dissipator

$$\mathcal{L}_t\rho_t = \frac{\gamma(t)}{2}(\sigma_z\rho_t\sigma_z - \rho_t), \tag{4.15}$$

with $\gamma(t) > 0$, the dissipative dynamics in Bloch notation is (from Eq. 4.8):

$$\mathfrak{D}(t) = -\begin{pmatrix}\gamma(t) & & \\ & \gamma(t) & \\ & & 0\end{pmatrix}, \quad \vec{\delta}(t) = \begin{pmatrix}0\\0\\0\end{pmatrix}. \tag{4.16}$$

Hence, we obtain at all times negative purity flux $f(\vec{r},t)$ generated by:

$$f(\vec{r},t) = \vec{r}.(\mathfrak{D}(t)\vec{r} + \vec{\delta}(t)) = -\gamma(t)(r_x(t)^2 + r_y(t)^2). \tag{4.17}$$

Moreover, recognising that the flux and coherence are independent of the azimuthal angle contained in r_x and r_y, we choose $\theta = 0$ and Eq. 4.17 becomes,

$$f(\vec{r},t) = -\gamma(t)(r\sin\phi)^2 < 0 \tag{4.18}$$

where $r \in \{0,1\}$ and $\phi \in \{0,\pi\}$ is the polar angle. From Eq. 4.18, trajectories with purity-increasing sections are physically inconsistent in a purely dephasing Markovian system. As a consequence, any trajectory will, after sufficient evolution, inevitably be devoid of coherence, irrespective of any conceivable coherent control strategy. To achieve positive purity flux, it is necessary to utilise non-Markovian dynamics where, for intervals of time, the decay rates take negative values. As the entire state space can be governed by negative and positive flux for separate intervals of time, one may naively assume that optimal control trajectories may now be implemented anywhere in the Bloch sphere.

Let us assume that there exists an implementation strategy, where we choose a non-Markovian dephasing process which is fixed in the presence of control. We consider a decay rate of the form[1]

$$\gamma(t) = [1+t^2]^{-s/2}\Gamma[s]\sin[s\arctan(t)], \tag{4.19}$$

which is obtained in the exact model of a qubit interacting with a bosonic zero temperature environment with the following spectral density [25]-[27],

$$J(\omega) = \frac{\omega^s}{\omega_c^{s-1}}e^{-\omega/\omega_c}, \tag{4.20}$$

where s is the Ohmicity parameter and ω_c a cutoff frequency. The form of spectral density can be modified through the parameter s. Specifically, for $s > 2$, the decay rate takes temporarily negative values for certain time intervals [66] which temporar-

[1] $\Gamma[x]$ is the Euler gamma function.

ily reverses the direction of the purity flux $f(\vec{r},t)$. The purity flux associated to this model is shown in Fig. 4.1 for intervals of time when the decay rate is positive (i) and negative (ii) respectively and choosing $s = 3$ for illustrative purposes.

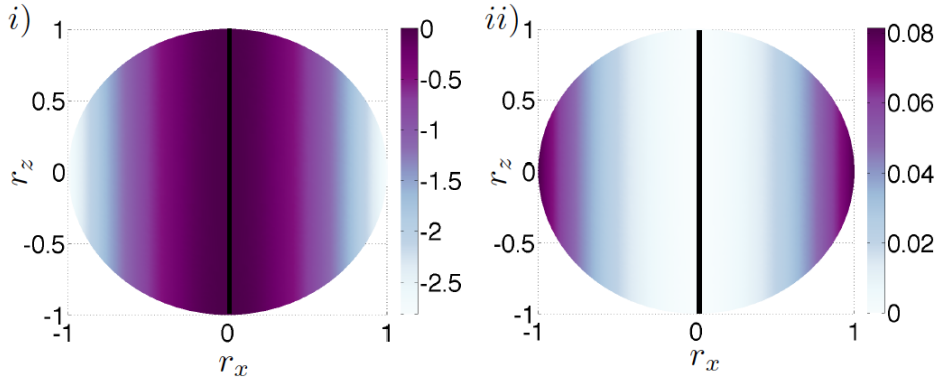

Figure 4.1: Snapshots of the purity flux $f(\vec{r})$ for the purely dephasing dynamics (4.15) with the non-Markovian rate (4.19) for $s = 3$ and time instances corresponding to positive (i) and negative (ii) values of the decay rate. The set of stabilizable states $\mathcal{S}$ [35] corresponding to vanishing purity flux is time-independent and forms a line along $r_x = 0$ (shown in black). For $\gamma(t) > 0$, it is immediate to see that $f(\vec{r},t) < 0$ (i). On the contrary, $f(\vec{r},t) > 0$ whenever $\gamma(t) < 0$ (ii).

In order to achieve an optimal control protocol, it is sufficient to restrict to trajectories containing two intervals of free evolution (evolution without control), interrupted by a single unitary rotation at the instant $\tilde{t}$ at which the decay rate changes sign. In more detail, the trajectories consist of an initial period of positive decay rate for which $f(\vec{r},t) < 0$, followed by a single time period in which the decay rate is negative, and hence $f(\vec{r},t) > 0$. For this reason, we study the Ohmicity range $2 < s \leq 5$ where information back flow occurs in the time interval $t \in [t_1, t_2]$ and $t_1 = \tan(\pi/s)$ and $t_2 = \infty(\tan(2\pi/s)$ for $2 < s \leq 4$ and $4 < s \leq 5$ respectively. We note in passing, that in general, decay rates with n intervals of information back flow (associated with Ohmicity values $s > 6$), can be implemented as n cycles through a series of unitary transformations. Our strategy is in close analogy to the two-point cycles considered in [34], i.e. a "two-point cycle" with finite dwell times. We assume the single rotation interrupting the trajectory is instantaneous, i.e. fast compared to the incoherent dynamics so that no purity is lost in that instant. This is a satisfactory assumption provided the duration of the pulse is much shorter than any other time scale relevant to the system [138, 139]. Moreover, we perform the fixed-dissipator assumption, assuming that for times $t > \tilde{t}$, the dynamics can still be described with the original Lindbladian $\mathcal{L}_t$, shown in Eq. 4.15.

In order to indicate the apparent drastic improvement that can be achieved with the control protocol described above, we compare in Fig. 4.2, for various values of s, the best possible average coherence $\bar{\mathcal{C}}(s)$ that is achievable in the presence and absence of control.

The initial Bloch vectors of the trajectory are as follows: $r_x(0) = \sin\phi_{\text{in}}(s), r_y(0) =$

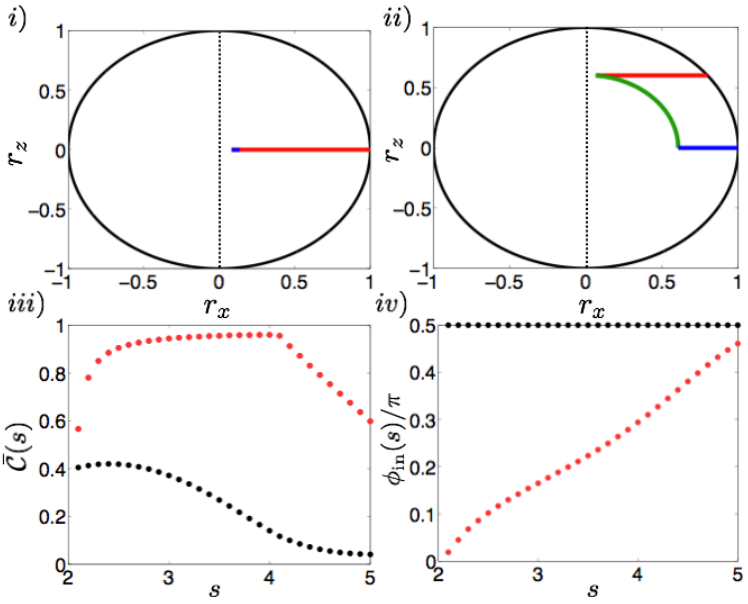

Figure 4.2: Comparison of the optimal trajectories without i) and with ii) coherent control pulses. In the upper panel, we illustrate, for $s = 4$, the trajectories in the stages $t < \tilde{t}$ (red line) and $t > \tilde{t}$ (blue line), where $\gamma(\tilde{t}) = 0$. The unitary rotation in the controlled trajectory is shown in green. In the lower panel, we show the optimal average coherence $\bar{\mathcal{C}}(s)$ (iii) and corresponding azimuthal angle $\phi_{\rm in}(s)$ for the initial Bloch vectors, $r_x(0)$, $r_y(0) = r_y(t) = 0$, $r_z(0)$ (iv) for the uncontrolled (black) and controlled (red) evolution. For $2 < s \leq 4$, we consider a finite dephasing interval $0 \leq \omega_c t \leq 30$. For $4 < s \leq 5$, the decay is naturally bound by a time T determined by the Ohmicity parameter s. One can clearly see the coherence enhancement obtained in the controlled case.

$r_y(t) = 0$, $r_z(0) = \cos\phi_{\text{in}}(s)$ where the evolution of $r_x(t)$ and $r_z(t)$ is determined by the dynamics given in Eq. 4.15 . While the respective initial polar angle $\phi_{\text{in}}(s)$ varies in the controlled case, in the uncontrolled case, the optimal initial state is always an eigenstate of σ_x, for all values of s. It is not possible to obtain on the Bloch ball, regions of weak flux corresponding to high values of coherence, i.e., the two desired quantities exist as a trade-off. The physical intuition behind the control protocol is to initially "kick" the state into the region of weak flux for the time it is exposed to detrimental purity-decreasing dynamics, and to return it to the equator region of maximal flux when it undergoes supportive purity-increasing dynamics. Strictly speaking, the initial "kick" is equivalent to a different initial state preparation process so is not included in Fig. 4.2. It is immediate to see from Fig. 4.2 iii), that the optimal controlled trajectories are superior in obtaining higher average coherence values as compared to the optimal uncontrolled evolution. In the Ohmicity range $2 < s \leq 4$, recalling the long time nature of dephasing in this range, we choose to consider optimal trajectories confined to a finite time interval $0 \leq t \leq T > \tilde{t}$ where $\gamma(t \geq T) \approx 0$. We note that for longer times T, the values of optimal average coherence increase but retain the same dependence on the Ohmicity parameter s. Naturally, the non-Markovian revivals are weak in a sense that they will never be strong enough to fully regain the initial state, i.e., the initial state is only reached asymptotically (see Fig. 4.2, i). We choose the intermediate rotation to optimally compensate for the weak non-Markovian revivals, ensuring that the purity lost in the red stage is fully regained in the blue stage. Moreover, with optimal coherence in mind, we choose to always start the cycle from the surface of the Bloch sphere ($|r(0)| = 1$). The optimal average coherence $\bar{\mathcal{C}}(s)$ and corresponding initial angle $\phi_{\text{in}}(s)$ (fixed by the constraint $|r(0)| = |r(T)| = 1$) increase with s as the strength of the purity flux increases and $\tilde{t}$ decreases. For $4 < s \leq 6$, the initial angle ϕ_{in} continues to increase (due to the increasing purity flux) but the average coherence $\bar{\mathcal{C}}(s)$ decreases (see Fig. 4.2 iii, iv)) at T decreases. For $t \geq T$, the state remains at the surface of the Bloch sphere with perfect coherence. Hence, for asymptotic timescales, coherence can be maximally exploited as a resource.

These results illustrate the enhanced ability of coherent control schemes to achieve high values of average coherence as a consequence of non-Markovian noise. However, the corresponding trajectories are admissible only if the fixed-dissipator assumption is satisfied and such protocols are experimentally realisable. The purely dephasing model is particularly remarkable as the scheme can not even be applied in any form in the Markovian case. On the other hand, for incoherent processes where the method does work in the Markovian case, a wider portion of the state space becomes available for trajectories in the presence of memory effects. In more detail, in Ref. [34], for the incoherent dynamics studied, positive and negative flux exist simultaneously, separated by a boundary of zero flux. Hence, admissible trajectories

must necessarily pass through both spaces, restricting the set of all possible trajectories. For the same incoherent processes, but with time-dependent non-Markovian decay rates, a wider portion of the state space becomes available for trajectories in the presence of memory effects as the direction of the flux on each side of the zero flux boundary corresponds to the change of sign of the decay rate.

4.2.2 Generality of Fixed Dissipator Assumption

Unfortunately, the promise of utilising non-Markovian dynamics to achieve such high average coherence values can never be reached experimentally. To demonstrate the problem, let us now examine the physical feasibility of the above strategy by critically examining the fixed dissipator assumption in full generality.

We consider a fixed dissipator $\mathcal{D}_t$ generating, in the absence of any coherent control, a t-parametrised family of completely positive and trace preserving (CPTP) maps $\{\Phi_t\}$, such that,

$$\rho(t) = \Phi_t \rho(0). \tag{4.21}$$

Explicitly, non-divisibility implies that the propagator $\Phi_{t,s} = \Phi_t \Phi_s^{-1}$, defined via the relation $\Phi_t = \Phi_{t,s}\Phi_s$, is not completely positive. Since Φ_t is, however, CPTP, one should conclude that on a restricted space of initial states (space of accessible states) defined by $\rho(s) = \Phi_s \rho(0)$ the intermediate map $\Phi_{t,s}$ is completely positive. Now, if we use the widespread assumption that the dissipator remains fixed under a unitary (coherent) interruption U of the dynamics at time s, we can write the dynamical map in the controlled case as $\tilde{\Phi}_t = \Phi_{t,s} U \Phi_s = \Phi_t \Phi_s^{-1} U \Phi_s$. Unless the original dynamical maps are covariant, i.e., $U\Phi_t = \Phi_t U$, the object $\tilde{\Phi}_t$ is no longer guaranteed to be a CP map because the unitary can move the intermediate state $\rho(s)$ outside the space of accessible states. Loosing complete positivity of the dynamical map means that the dynamics is never physical or, stated another way, no physical implementation of the master equation exists. It is worth noticing that, for Markovian and therefore divisible dynamics this problem does not occur because the intermediate propagator $\Phi_{t,s}$ is always CP and therefore the modified map $\tilde{\Phi}_t$ in presence of coherent control unitaries is always CP and therefore physical.

Thus, in general, knowing the open system dynamics in the absence of control does not give enough information to construct a physically meaningful open system dynamics in the presence of control, even if the control field is completely known. In general, the full exact dynamics of the system plus the environment needs to be solved, taking into account the control field in the microscopic derivation, in order to tackle the problem of optimal control in the non-Markovian case.

4.3 Non-Markovian Optimal Control: Exact Case

To illustrate the physical relevance of our result, we return to the exact pure dephasing model, and determine the system dynamics following an instantaneous rotation [25]-[27]. The exact nature of the microscopic derivation is not threatened by assuming instantaneous control, if the pulse duration is much shorter than any other time scale relevant to the system. Our aim is to show how the presence of even a single unitary rotation drastically alters the form of the dissipator in a non-negligible way. We compare the correct microscopically derived dynamics with the phenomenological approach using the fixed dissipator assumption.

In the absence of control the dynamics are described by the dissipator in Eq. 4.15 with the decay rate given by Eq. 4.19. The decay rate is related to the decoherence function $\Gamma(t)$, defined by $\rho_{ij}(t) = \rho_{ij}(0)e^{-\Gamma(t)}$ $(i \neq j)$, through the relation $\gamma(t) = \frac{d\Gamma(t)}{dt}$. For the Ohmic class of spectral densities here considered the decoherence function takes the form,

$$\Gamma(t) = \frac{\Gamma[s]}{s-1}[1-(1+t^2)^{-s/2} \times (\cos(s\arctan(t)) + t\sin(s\arctan(t)))]. \quad (4.22)$$

We now derive the new resultant dynamics once control has been applied in the form of a single pulse, inducing an instantaneous rotation of polar angle ϕ around the y-axis. The initial state, composed by the qubit and the field is given by,

$$|\Psi(0)\rangle = (c_e|e\rangle + c_g|g\rangle) \otimes |0\rangle, \quad (4.23)$$

with $|0\rangle = \bigotimes_k |0\rangle_{\mathbf{k}}$.The system evolves for $0 < t < \tilde{t}$ as follows [25]-[27]:

$$\begin{aligned} |\Psi(t)\rangle &= U(t,0)|\Psi(0)\rangle \\ &= c_e|e\rangle \otimes |\Psi_e(t)\rangle + c_g|g\rangle \otimes |\Psi_g(t)\rangle, \end{aligned} \quad (4.24)$$

with $|\Psi_e\rangle = \bigotimes_k U_e(t,0)|0_{\mathbf{k}}\rangle$ and $|\Psi_g\rangle = \bigotimes_k U_g(t,0)|0_{\mathbf{k}}\rangle$. The time evolution operator (in the interaction picture) takes the form:

$$\begin{aligned} U(t) &= \exp\left\{-i\int_0^t \sum_k \sigma_z(g_k b_k^\dagger e^{i\omega_k t'} + g_k^* b_k e^{-i\omega_k t'})dt'\right\} \\ &= \exp\left\{\sigma_z \frac{1}{2}\sum_k (b_k^\dagger \xi_k(t) - b_k \xi_k^*(t))\right\}, \end{aligned} \quad (4.25)$$

with

$$\xi_k(t) = 2g_k \frac{1-e^{i\omega_k t}}{\omega_k}. \quad (4.26)$$

Here, $U(t)$ can be described as a conditional displacement operator, the sign of the

displacement being dependent on the logical value of the qubit, denoted U_e and U_g for the respective values. In particular, for any pure state $|\Phi\rangle$ of the field:

$$\begin{aligned} U(t)\,|g\rangle \otimes |\Phi\rangle &= |g\rangle \otimes \prod_k D\left(-\frac{1}{2}\xi_k(t)\right)|\Phi\rangle \\ U(t)\,|e\rangle \otimes |\Phi\rangle &= |e\rangle \otimes \prod_k D\left(\frac{1}{2}\xi_k(t)\right)|\Phi\rangle \end{aligned} \tag{4.27}$$

where the displacement operator $D(\xi_k)$ is defined as:

$$D(\xi_k) = \exp\{b_k^\dagger \xi_k - b_k \xi_k^*\}, \tag{4.28}$$

and where $|\frac{1}{2}\xi_k(t)\rangle$ is a coherent state of amplitude $\frac{1}{2}\xi_k(t)$. If a rotation occurs at $\tilde{t}$, we have:

$$\begin{aligned} |\Psi(\tilde{t})\rangle &= R_y(\theta)\,|\Psi(\tilde{t})\rangle \\ &= |e\rangle \otimes [c_e \cos\left(\frac{\theta}{2}\right) U_e(\tilde{t},0)\,|0\rangle - c_g \sin\left(\frac{\theta}{2}\right) U_g(\tilde{t},0)\,|0\rangle] \\ &+ |g\rangle \otimes [c_e \sin\left(\frac{\theta}{2}\right) U_e(\tilde{t},0)\,|0\rangle + c_g \cos\left(\frac{\theta}{2}\right) U_g(\tilde{t},0)\,|0\rangle]. \end{aligned} \tag{4.29}$$

and $R_y(\theta) = e^{-i\frac{\theta}{2}\sigma_y} = \cos\frac{\theta}{2}\mathbb{I} - i\sin\frac{\theta}{2}\sigma_y$. For times $t > \tilde{t}$, the combined system evolves according to:

$$\begin{aligned} U(t,\tilde{t})R_y(\theta)U(\tilde{t},0)\,|\Psi(0)\rangle &= |e\rangle \otimes [c_e \cos\left(\frac{\phi}{2}\right)|\Psi_{ee}(t)\rangle - c_g \sin\left(\frac{\phi}{2}\right)|\Psi_{eg}(t,\tilde{t})\rangle] \\ &+ |g\rangle \otimes [c_e \sin\left(\frac{\phi}{2}\right)|\Psi_{ge}(t,\tilde{t})\rangle + c_g \cos\left(\frac{\phi}{2}\right)|\Psi_{gg}(t)\rangle], \\ &, \end{aligned} \tag{4.30}$$

where we have:

$$\begin{aligned} |\Psi_{ee}(t)\rangle = U_e(t,\tilde{t})U_e(\tilde{t},0)\,|0\rangle\,,\ |\Psi_{ge}(t,\tilde{t})\rangle = U_g(t,\tilde{t})U_e(\tilde{t},0)\,|0\rangle\,, \\ |\Psi_{eg}(t,\tilde{t})\rangle = U_e(t,\tilde{t})U_g(\tilde{t},0)\,|0\rangle\,,\ |\Psi_{gg}(t)\rangle = U_g(t,\tilde{t})U_g(\tilde{t},0)\,|0\rangle\,. \end{aligned} \tag{4.31}$$

The matrix elements of the reduced density matrix of the qubit are defined as:

$$\rho_{ij}(t,\tilde{t}) = \langle i|\,\mathrm{Tr}_E U(t,\tilde{t})R_y(\Phi)U(t,0)\rho(0)U^\dagger(t,0)R_y^\dagger(\Phi)U^\dagger(t,\tilde{t})\,|j\rangle\,. \tag{4.32}$$

We have,

$$\begin{aligned}\rho_{ee}(t,\tilde{t}) &= |c_e|^2\cos^2\left(\frac{\phi}{2}\right)+|c_g|^2\sin^2\left(\frac{\phi}{2}\right)\\ &- (c_e c_g^*\langle\Psi_{eg}(t,\tilde{t})|\Psi_{ee}(t)\rangle + c_e^* c_g\langle\Psi_{ee}(t)|\Psi_{eg}(t,\tilde{t})\rangle\sin\left(\frac{\phi}{2}\right)\cos\left(\frac{\phi}{2}\right)\end{aligned} \tag{4.33}$$

$$\begin{aligned}\rho_{eg}(t,\tilde{t}) &= \cos\left(\frac{\phi}{2}\right)\sin\left(\frac{\phi}{2}\right)(|c_e|^2\langle\Psi_{ee}(t)|\Psi_{ge}(t,\tilde{t})\rangle - |c_g|^2\langle\Psi_{eg}(t,\tilde{t})|\Psi_{gg}(t)\rangle)\\ &+ c_e^* c_g\cos^2\left(\frac{\phi}{2}\right)\langle\Psi_{ee}(t)|\Psi_{gg}(t)\rangle - c_e c_g^*\sin^2\left(\frac{\phi}{2}\right)\langle\Psi_{eg}(t,\tilde{t})|\Psi_{ge}(t,\tilde{t})\rangle.\end{aligned} \tag{4.34}$$

where $\rho_{gg}=1-\rho_{ee}$ and $\rho_{ge}=\rho_{eg}^*$. After some simple calculations we get (after a rotation of angle θ around the y-axis) the resultant Bloch vectors:

$$\begin{aligned}r_x(t,\tilde{t}) &= r_z(0)\sin(\theta)e^{-\Gamma(t-\tilde{t})}\cos[y(t)] + r_x(0)e^{-\Gamma(t)}\\ &\times [\cos^2\left(\frac{\theta}{2}\right)-\sin^2\left(\frac{\theta}{2}\right)e^{2[\Gamma(t)-\Gamma(\tilde{t})-\Gamma(t-\tilde{t})]}],\end{aligned} \tag{4.35}$$

$$\begin{aligned}r_y(t,\tilde{t}) &= r_z(0)\sin(\theta)e^{-\Gamma(t-\tilde{t})}\sin[y(t)] + r_y(0)e^{-\Gamma(t)}\\ &\times [\cos^2\left(\frac{\theta}{2}\right)-\sin^2\left(\frac{\theta}{2}\right)e^{2[\Gamma(t)-\Gamma(\tilde{t})-\Gamma(t-\tilde{t})]}],\end{aligned} \tag{4.36}$$

$$r_z(\tilde{t}) = r_z(0)\cos(\phi) - r_x(0)\sin(\phi)e^{-\Gamma(\tilde{t})}. \tag{4.37}$$

where $y(t)=\mathrm{Im}(\tilde{\Gamma}(t)-\tilde{\Gamma}(\tilde{t})-\tilde{\Gamma}(t-\tilde{t}))$ and

$$\begin{aligned}\tilde{\Gamma}(t) &= 4\Gamma[s-1]\\ &\times (1-t^2)^{-s/2}[\sin(s\arctan(t)) - t\cos(s\arctan(t)].\end{aligned} \tag{4.38}$$

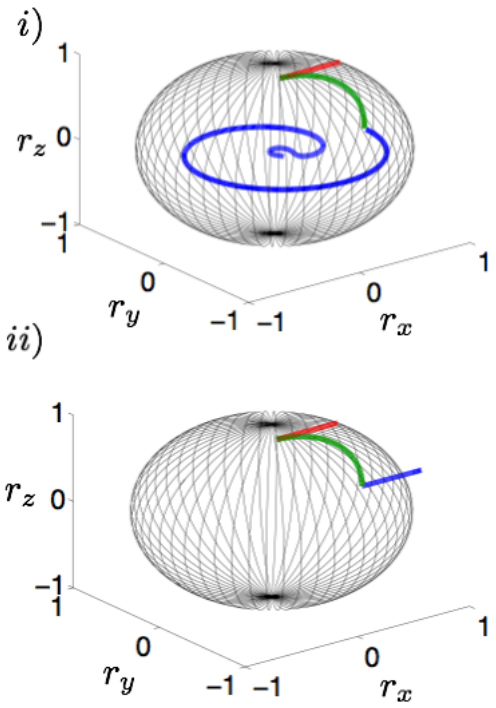

Figure 4.3: Dynamics of the qubit obtained from i) the exact model in the presence of a control pulse and ii) assuming a fixed dissipator. The trajectory is divided into three stages: $t < \tilde{t}$ (top red line), $t > \tilde{t}$ (bottom blue line) and the unitary jump between the two (middle green line). For illustrative purposes, we have chosen $s = 4$ and initial polar angle $\Phi_{\text{in}}(s) > \tilde{\Phi}_{\text{in}} = 0.2\pi$.

In Fig. 4.3 i), we plot the true evolution of the system, when the dissipator is not fixed but instead the unitary rotation is incorporated into the microscopic derivation. The dynamics remain purely dephasing as r_z remains time-independent but a new time-dependence in the y-direction results in a spiral evolution. The purity flux is therefore not reversed, but the dephasing is altered after the control pulse such that no advantage can be obtained with respect to the Markovian case. This dynamics should be contrasted with the corresponding trajectory on the Bloch sphere in the fixed dissipator assumption, as shown in Fig. 4.3 ii). The latter dynamics are obviously not CP, since the trajectory falls outside the Bloch sphere. Such trajectories can be achieved, for example, by choosing initial polar angles $\tilde{\phi}_{\text{in}} < \phi_{\text{in}}(s)$, where $\phi_{\text{in}}(s)$ is the angle fixed by the constraint $|r(0)| = |r(T)| = 1$, shown in Fig. 4.2 iv).

To conclude, we briefly comment on the special case in which the fixed dissipator assumption is used but the qubit undergoes a covariant dynamics [140]. It is easy to convince oneself that coherent control will never be useful in such a case, since by definition applying the control pulse before, during, or after the non-unitary evolution leads to the very same state. Hence, choosing a different initial state is equivalent to implementing any coherent control sequence during the evolution.

4.4 Conclusion

Summarising, our results show that the appealing idea of using optimal control strategies in the presence of non-Markovian noise may lead to formidable difficulties. We have revealed that the only physically meaningful description of the reduced purely dephasing dynamics in the presence of control pulses, is the one obtained via an exact microscopic model entailing system plus controlled pulses plus interaction with the environment. If the decay rate in the dissipator changes markedly after each pulse, it is likely that, in general, constructing superior trajectories (i.e. trajectories which are optimally controlled with varying degrees of rotation) will never be a feasible task. A possible solution to this impasse might be the discovery of certain special forms of non-Markovian dissipators that may not be changing sensibly in the presence of some specific coherent control schemes, perhaps exploiting specific symmetries of the dissipator and control Hamiltonian.

Chapter 5

Dynamical Decoupling in Non-Markovian Systems

In Chapter 4, we realised that in order to investigate optimal control protocols in the non-Markovian regime, a full microscopic derivation of the dynamics in the presence of control is required. Now, we turn our attention to an exact dynamical description of unitary control in purely dephasing systems. In more detail, we aim to investigate the relationship between non-Markovianity and the efficiency of dynamical decoupling protocols. In this context, recently many have wondered whether memory effects combined with external control techniques offer a possibility to design an overall superior technique to combat decoherence [46]-[48]. With the relationship firmly established, we provide an example of the connotation of our result for quantum information protocols requiring quantum correlations. The results from this chapter are based on those obtained in Publications iii and iv [3, 4].

5.1 Introduction to Dynamical Decoupling

Dynamical decoupling (DD) techniques for open quantum systems are considered one of the most successful control protocols to suppress decoherence in qubit systems [50, 51]. The scheme is inspired by the idea of coherently averaging unwanted interactions, as established in the nuclear magnetic resonance (NMR) community following the breakthrough discovery of the spin-echo effect [141]. Analogous to the spin-echo effect, dynamical decoupling relies on the application of a sequence of external pulses to the system which induce unitary rotations in order to counter the harmful effects of the environment [130]-[143]. Specifically, "bang bang" periodic dynamical decoupling (PDD) schemes can be exploited to prolong coherence times and restore monotonically decaying correlations in quantum systems which are undergoing decoherence [139]. However, sophisticated control designs have superseded this early scheme involving simple periodic application of pulses [51] and its time-symmetrised version [144]-[147]. Most prominently, periodic "supercycle"

techniques from NMR [148] have been incorporated in "concatenated" DD (CDD) protocols to counter decoherence for general noise scenarios [142, 143]. Moreover, qualitatively different approaches to synthesising pulse sequences which attempt to minimise errors in specific noise settings, including "randomised" DD schemes, have emerged [142] such as the so-called Uhrig DD (UDD) for a single qubit undergoing pure dephasing. It is well known in all these cases, that the performance of the protocol crucially depends on the careful tuning of pulse timings. Moreover, the performance depends on the timescale of the environment correlation function, highlighting the important role played by spectral properties of the noise causing decoherence and introducing errors [149].

In Ref. [31], a formal mathematical equivalence of the quantum Zeno effect (QZE) and "bang-bang" decoupling protocol has been established. Analogously to DD, the quantum Zeno effect (QZE) occurs when frequent observations or "measurements" of a quantum system, in order to ascertain whether the system is still in its initial state, slow down the decay of a quantum state. Conversely, by exploiting first the short-time features of the quantum system, one can accelerate the decay with a series of less frequent measurements, resulting in the inverse quantum Zeno effect (IZE). One can define a characteristic time, the quantum Zeno time τ^*, where for $\Delta t < \tau^*$ one obtains a QZE and conversely for $\Delta t > \tau^*$ one obtains a IZE. Decoherence is suppressed in the former case while it is enhanced in the latter. On the other hand, if $\Delta t = \tau^*$, the system decays naturally as if no measurements were performed.

5.2 Dynamical Decoupling: The model

In this section, we describe the model, originally introduced in Ref. [49], for a single purely dephasing qubit subject to PDD and interacting with a bosonic environment with spectral density of the Ohmic class. In Ref. [49], with reservoir engineering in mind [131], a comparative study was presented regarding the efficiency of certain DD protocols on Ohmic, sub-Ohmic and super-Ohmic environments. In this chapter, we exploit the Ohmic parameterisation of the model to study the efficiency of DD in the presence of memory effects. In particular, we are curious to establish the role of non-Markovianity as a resource in such protocols by considering coherence preservation to be synonymous to dynamical decoupling efficiency in a simple one qubit system.

We now recall the exact dynamics obtained in Ref. [49] which address the qubit behaviour in the presence of an arbitrary sequence of instantaneous bang-bang pulses:

$$\rho_{01}(t) = \rho_{10}^*(t) = \rho_{01}(0)e^{-\Gamma(t)}, \tag{5.1}$$

where $\gamma(t) = d\Gamma(t)/dt$. Each pulse is modelled as an instantaneous π-rotation

around the x-axis. We consider an arbitrary storage time, t, during which a total number of N pulses are applied at instants $\{t_1, ...t_n, ...t_f\}$, with $0 < t_1 < t_2 < ... < t_f < t$. As shown by Uhrig [150, 151], the controlled coherence function $\Gamma(t)$ can be worked out as,

$$\Gamma(t) = \begin{cases} \Gamma_0(t) & t \leq t_1 \\ \Gamma_n(t) & t_n < t \leq t_{n+1}, 0 < n < N \\ \Gamma_N(t) & t_f < t \end{cases}, \tag{5.2}$$

where the exact representation of the controlled decoherence function $\Gamma_n(t)$ for $1 \leq n \leq N$, can be written in the following form:

$$\Gamma_n(t) = \int_0^\infty \frac{J(\omega)}{2\omega^2} |y_n(\omega t)|^2 d\omega, \quad n \geq 0, \tag{5.3}$$

where

$$J(\omega) = \frac{\omega^s}{\omega_c^{s-1}} e^{-\omega/\omega_c}, \tag{5.4}$$

is the spectral density function characterising the interaction of the qubit with the oscillator bath (this is assumed to be at zero temperature) with s the Ohmicity parameter and ω_c a cutoff frequency. Further, from Eq. 5.3, $|y_0(\omega t)|^2 = |1 - e^{i\omega t}|^2$ and for $n > 1$,

$$y_n(z) = 1 + (-1)^{n+1} e^{iz} + 2 \sum_{m=1}^{n} (-1)^m e^{iz\delta_m}, \quad z > 0. \tag{5.5}$$

The expression for $\Gamma_0(t)$ can be calculated analytically[1] and is given by

$$\Gamma_0(t) = \frac{\tilde{\Gamma}[s]}{s-1} \left[1 - (1+t^2)^{-s/2} \cos(s \arctan(t)) + t \sin(s \arctan(t))\right], \tag{5.6}$$

with $\tilde{\Gamma}[s]$ the Euler Gamma function. Ohmic spectrum corresponds to $s = 1$, while super-Ohmic spectra correspond to $s > 1$ and sub-Ohmic to $s < 1$. Here, it is understood that the nth pulse occurs at time $t_n = \delta_n t$ and $0 < \delta_1 < ... < \delta_n < ... < \delta_s < 1$. In order to express the controlled decoherence function $\Gamma_n(t)$ in terms of its uncontrolled counterpart $\Gamma_0(t)$, we simply relate $|y_1(\omega t)|^2$ to $|y_0(\omega t)|^2$ to write,

$$\Gamma_1(t) = -\Gamma_0(t) + 2\Gamma_0(t_1) + 2\Gamma_0(t - t_1). \tag{5.7}$$

[1]We note that Eq. 5.6 is written in dimensionless units by introducing ω_c^{-1} as a time scale.

Upon continuation of this iteration, this yields,

$$\begin{aligned}\Gamma_2(t) &= -\Gamma_1(t) + 2\Gamma_1(t_2) + 2\Gamma_0(t-t_1) \\ &\vdots \\ \Gamma_n(t) &= -\Gamma_{n-1}(t) + 2\Gamma_{n-1}(t_n) + 2\Gamma_0(t-t_n)\end{aligned} \tag{5.8}$$

By relating again, $|y_n(\omega t)|^2$ to $|y_0(\omega t)|^2$, we find the decoherence rate for n pulses,

$$\begin{aligned}\Gamma_n(t) &= 2\sum_{m=1}^{n}(-1)^{m+1}\Gamma_0(t_m) \\ &+ 4\sum_{m=2}^{n}\sum_{j<m}\Gamma_0(t_m - t_j)(-1)^{m-1+j} \\ &+ 2\sum_{m=1}^{n}(-1)^{m+n}\Gamma_0(t-t_m) + (-1)^n\Gamma_0(t).\end{aligned} \tag{5.9}$$

While here, the dynamics have been derived for a qubit interacting with a quantum bosonic bath, the exact representation holds also for arbitrary Gaussian phase randomisation processes. Hence the main conclusions of our study are applicable also to experimental settings such as trapped ions [152, 153] and solid-state qubits [154, 155, 161].

5.3 Relationship between non-Markovianity and Dynamical Decoupling Protocols

5.3.1 Pulse-induced information flow reversal

In this chapter, we choose to quantify non-Markovianity using the BLP measure in order to establish a relationship between dynamical decoupling and information flow between the system and environment. The BLP measure, in terms of the analytical expression for the pure dephasing model, is given as [112].

$$\mathcal{N} = -\int_{\gamma<0} dt\,\gamma(t)e^{-\Gamma(t)}, \tag{5.10}$$

where the integral is extended over the time intervals such that $\gamma(t) < 0$. Further, we recall that for $\Gamma(t) = \Gamma_0(t)$, the onset of non-Markovianity is intimately linked to the form of the spectral density Eq. 5.4 through the Ohmicity parameter, i.e. for $s > 2$ [66].

In order to study the influence of dynamical decoupling on the direction of information flow, we derive a relation connecting $\gamma_n(t_n)$, i.e., $\dot{\Gamma}_n(t_n)$ at the moment t_n when the system is pulsed and the corresponding quantity at the previous instant.

The relation is straightforward to derive from Eq. 5.8 [49],

$$\gamma_n(t_n) = -\gamma_{n-1}(t_n), \tag{5.11}$$

where for $1 \leq n \leq N$,

$$\gamma_n(t) = 2\sum_{m=1}^{n}(-1)^{m+n}\gamma_0(t - t_x m) + (-1)^n\gamma_0(t). \tag{5.12}$$

Interestingly, from Eq. 5.11, an explicit connection between the direction of information flow and DD is apparent. In more detail, simply from noticing the change of sign of the decay rate, one can identify a reversal of information flow occuring at the same time instant the pulse interrupts the free-system dynamics. This result implies that Markovian open system dynamics will always be transformed to a non-Markovian dynamics, although in some cases the resulting BLP measure can take negligible values.

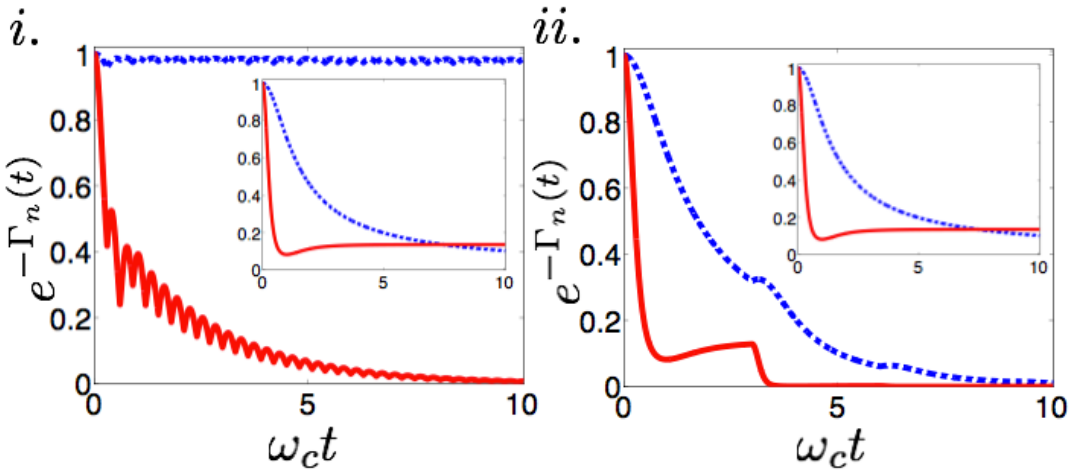

Figure 5.1: Time evolution of the controlled coherence $e^{-\Gamma_n(t)}$ for: i. Δt=0.3 (short pulse spacing regime) and ii. Δt=3 (long pulse spacing regime), in units of ω_c^{-1}. The Ohmicity parameters are $s = 1$ (blue dashed line) and $s = 4$ (red solid line), which are respectively an instance of Markovian and non-Markovian dynamics. In the inset, we display the free uncontrolled coherences $e^{-\Gamma_0(t)}$, which shows in particular that $\tilde{t}$=1 for s=4. All times are expressed in units of ω_c^{-1}.

To study this relationship in detail, we plot in Fig. 5.1, the time evolution of the coherences $e^{-\Gamma_n(t)}$ of the purely dephasing system subject to DD protocols. We determine the efficiency of a DD scheme by the ability of the protocol to preserve coherences over the time interval the system is pulsed. For the sake of simplicity, we restrict our investigation to equally-spaced DD pulses applied at times $t_n = n\Delta t$, which $n = 1, 2, 3, ...$ In the Ohmicity range $2 \leq s \leq 6$, we recall that $\tilde{t} = \tan(\pi/s)$ is the time instant connected to information reversal in the unperturbed dynamics ($\gamma_0(\tilde{t}) = 0$), i.e. the onset of non-Markovianity [66]. In Fig. 5.1, we consider the cases s=1 and s=4 as paradigmatic instances of a Markovian and non-Markovian

(free) dynamics respectively. We first note that, for any time $t < \tilde{t}$, before revivals associated to non-Markovianity occur, the unperturbed coherences are always higher for $s \leq 2$ (Markovian case) than for $s > 2$ (non-Markovian case). We define two pulse intervals with respect to the onset of non-Markovian dynamics. In more detail, short pulse intervals are defined as $\Delta t < \tilde{t}$ and conversely for long pulse intervals. For divisible (Markovian) dynamics in the quantum Zeno regime, i.e. $\Delta t < \tau^*$, the shorter is the interval between the DD pulses, the higher is the efficiency of the DD scheme [29, 30] (see Fig. 5.1 i, blue line). For non-Markovian ones the same holds, if information back flow has not yet occurred, ie. provided that $\Delta t < \tilde{t}$ (see Fig. 5.1 i red line).

From the relation of Eq. 5.11, we conjecture that, in the short-pulsing regime, Markovian environments are more favourable to protect coherences via DD compared to non-Markovian ones. In more detail, as the effect of the pulses is always to reverse information flow, the ideal unperturbed dynamics would be those characterised by information flowing from the system to the environment. Moreover, in the Markovian case, DD inhibits loss of coherence compared to the unpulsed free evolution. This can be proved numerically, confirmed by Fig. 5.1 showing that pulsing is fully successful in inhibiting the coherence decay for the $s=1$ case, while it is not in the $s=4$ case.

Now considering the long-pulsing regime (see Fig. 5.1 ii), we show that the efficiency of the DD scheme here considered is drastically reduced in both the Markovian and non-Markovian case. In this case, the time evolution of the coherence greatly depends on the details of the dynamics, specifically the interplay between the DD and non-Markovian influence on the direction of information flow, and so no general conclusion can be drawn. In particular, in this regime, reversing information flow can have disastrous consequences for non-Markovian environments: If the first pulse occurs during a time of re-coherence (information back flow), it will indeed induce an even faster coherence decay. This effect can be seen in Fig. 5.1 ii, red line, where in particular we study the case $s=4$ for a pulse spacing such that $\Delta t > \tilde{t} = 1$. One can note that the occurrence of the first pulse induces an extremely rapid deterioration of coherences (when compared to the unpulsed free dynamics).

5.3.2 Efficiency versus Non-Markovianity measure

To elucidate the relationship between the non-Markovian character of the free dynamics and the efficiency of dynamical decoupling techniques, we perform a numerical investigation based on their respective measures. In literature, the efficiency of DD is commonly quantified by means of the fidelity function, measuring the overlap between the state at time t and the initial state $\rho(0) = |\Phi(0)\rangle \langle\Phi(0)|$:

$$\mathcal{F}(t) = \langle\Phi(0)| \rho(t) |\Phi(0)\rangle , \tag{5.13}$$

where $1/2 \leq \mathcal{F} \leq 1$. In the weak-coupling approximation, the coherences decay as $\mathcal{C}(t) = e^{-R(t)t}$ where $R(t)$ is the overlap interval of the noise spectral density and the filter function generated by the DD sequence [162]. In this framework, fidelity is defined as:

$$\mathcal{F}(t) = \rho_{11}(0)^2 + \rho_{22}(0)^2 + 2\rho_{12}(0)\rho_{21}(0)e^{-R(t)t}, \tag{5.14}$$

with $\rho_{ij}(0)$ the density matrix elements of the initial state. It is worth stressing that in this chapter, we use an exact approach that allows us to write the most general form of the decoherence factor as $\mathcal{C}(t) = e^{-\Gamma(t)}$, with $\Gamma(t)$ given by Eq. 5.2. In the weak coupling limit $\Gamma(t)$ reduces to $R(t)t$ and one obtains Eq. 5.14. In contrast to this measure, our aim is to instead capture DD efficiency in a quantifier comparable to a non-Markovianity quantifier. In more detail, we require a measure which captures how well the DD sequences protect the system from decoherence *at all times* and *independently of the initial state*. Hence, rather than the fidelity, which is both time-dependent and state dependent, we introduce the following as a new quantifier of DD efficiency:

$$\mathcal{D}(t_f) = \frac{\int_0^{t_f} e^{-\Gamma(t)}}{t_f}\,. \tag{5.15}$$

The measure is bounded between zero (ineffective DD) and unity (ideal DD) and is based only on preserving the evolution of coherence undergoing dynamical decoupling up to some time t_f, which is assumed to be the duration of the DD pulsing scheme.

In Fig. 5.2, we compare the DD efficiency measure $\mathcal{D}(t_f)$, as defined by Eq. 5.15 with $\Gamma(t)$ given by Eq. 5.2, and the non-Markovianity $\mathcal{N}$ of the unperturbed dynamics, as defined by Eq. 5.10 with free decoherence $\Gamma_0(t)$ given by Eq. 5.6, as functions of the Ohmicity parameter s. With optimal DD efficiency in mind, we focus on the short-pulsing regime, specifically, $\Delta t = 0.3\omega_c^{-1}$. We find that the DD efficiency sharply decreases for $s > 2$, corresponding to the onset of non-Markovianity. We note however that the quantity is only sensitive to the Markovian to non-Markovian crossover rather that the specific values of the BLP measure. In more detail, the DD efficiency decreases monotonically for $s > 2$ while the BLP measure has its maximum value at $s \simeq 3.7$. We note in passing, that the RHP measure in this case increases monotonically for $s > 2$ and may be considered to be more closely related to the DD efficiency. For increasingly longer times t_f, the efficiency becomes increasingly sensitive to the onset of non-Markovian dynamics, indeed, for $t_f \to \infty$, we conjecture that $\mathcal{D}$ will decrease to smaller and smaller values for $s > 2$. We have purposely chosen sufficiently large values of t_f to capture properly the dynamical decoupling efficiency dependence on s. Particularly, if t_f is too short, the measure will yield an almost uniform dependence on s, since in this case, the coherences will

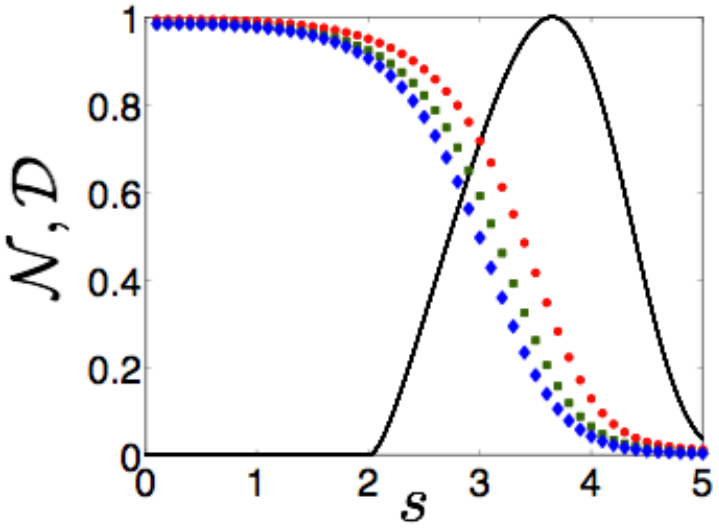

Figure 5.2: Non-Markovianity measure $\mathcal{N}$ of the free (unpulsed) dynamics (black solid line) and dynamical decoupling efficiency $\mathcal{D}$ against the Ohmicity parameter s for $\Delta t = 0.3$ (in units of ω_c^{-1}). Dynamical decoupling efficiency is plotted for $\omega_c t_f = 9.9$ (red dot), 19.8 (green square) and 30 (blue diamond). For comparison purposes, we have rescaled $\mathcal{N}$ to its maximum value.

still be high for any s value. Moreover, we wish to investigate the supreme potential of DD, specifically, the preservation of coherences for long times. Hence, in Fig. 5.2, we have aimed to calculate efficiency for increasingly long times up until the limit of our computational capabilities.

We now widen our investigation to study how the DD efficiency depends on the time spacing between pulses when $\Delta t < \tau^*$ (see Fig. 5.3). While the values of DD efficiency decrease as the pulses become further apart, the dependency on the Ohmicity parameter s remains rather insensitive and we observe similar behaviour to that seen in Fig. 5.2. We have numerically checked that this conclusion is not dependent on the specific value chosen for t_f. In conclusion, our investigation shows that for maximal protection of the coherence, ideally, one would strive for a Markovian unperturbed dynamics, subject to a DD scheme imposing unitary rotations on the system in short succession. In more detail, the maximum efficiency of PDD is obtained for pulse spacings $\Delta t < \tilde{t}$ with Markovian dynamics ($s < 2$). As the formalism used to describe the dynamics holds for any arbitrary Gaussian phase randomisation process, our conclusions hold in general for these types of models [49]. For $\Delta t > \tilde{t}$ and for $s > 2$, non-Markovian effects become relevant in the overall free dynamics and the amount of coherence preservation will depend on a combined effect of both the presence of information back flow connected to the unperturbed dynamics and DD. An intricate dependence on the time interval Δt as well as on t_f emerges in this case from numerical studies. This can be traced back to the fact that for dynamics in the non-Markovian regime, for the Ohmicity range we study, a single time interval exists where information flow is reversed to flow from the en-

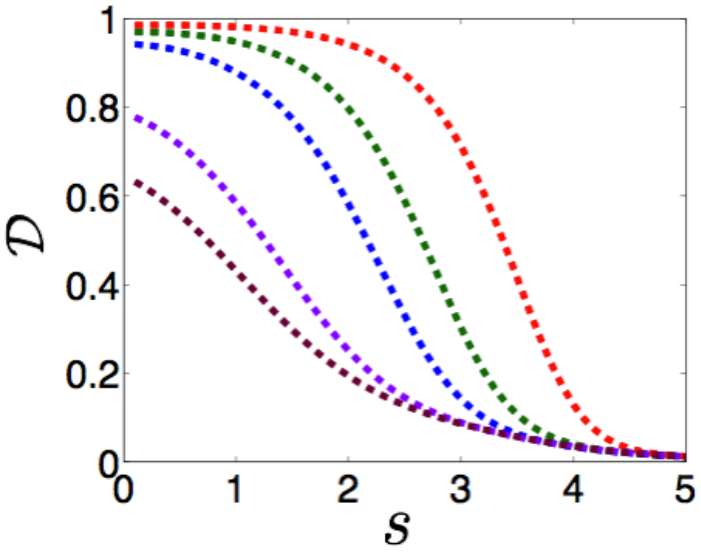

Figure 5.3: Dynamical decoupling efficiency $\mathcal{D}$ against the Ohmicity parameter s for different values of the pulsing period (in units of ω_c^{-1}): Δt =0.3 (red), Δt =0.4 (dark green), Δt =0.5 (blue), Δt =0.8 (purple) and Δt =1 (brown). The final pulse is applied at $\omega_c t_f = N_{\max}\omega_c \Delta t < 10.05$ where $N_{\max}$ is the maximum number of pulses that can be applied within the time interval $0 \leq \omega_c t \leq 10.05$.

vironment to the system. Hence, in the quantum Zeno regime, pulses will either enhance decoherence or preserve coherence depending on whether or not they occur in this time interval of back flow.

5.3.3 Non-Markovianity Engineering by Dynamical Decoupling

While Markovian open quantum systems have been extensively studied and are very well characterised, non-Markovian systems remain relatively unexplored and many fundamental questions remain unanswered. We recall that for Markovian dynamics fulfilling the semigroup property, the Lindblad-Gorini-Kossakowski-Sudarshan theorem identifies the general form of master equation and affirms the physical evolution of the system [80, 81]. However, no such generalisation exists in the non-Markovian regime. Moreover, in the Markovian limit, quantum state diffusion methods allow to unravel the dynamics in terms of homodyne or heterodyne measurements on the environment [163]. Further, the Monte Carlo wave function approach provides both a powerful numerical technique to study the dynamics of Markovian systems and a deep interpretation in terms of quantum jumps for individual quantum systems, like ions or cavity modes [164]. On the other hand, the existence of a measurement scheme interpretation guaranteeing a physical meaning to individual trajectories in the non-Markovian regime is still under investigation. Also, the extension of the Monte Carlo wave function approach to the non-Markovian regime has been determined only for certain classes of time-local master equations [101]. Nevertheless,

the interest in developing techniques for engineering non-Markovian dynamics to be used as testbeds for experimental and theoretical investigations is increasing [25], [125].

From our previous investigations of DD, we have shown that, in addition to its traditional employment as a method to hamper decoherence, DD can also be exploited as a simple tool for engineering non-Markovian dynamics. Independently of system parameters, a Markovian system will always become non-Markovian when subject to PDD. More in general, PDD will change the non-Markovian character of the open system regardless of whether the free dynamics were Markovian or not. The exact degree of the pulse-induced non-Markovianity depends on both the pulsing parameters, i.e. pulse spacing Δt and environmental parameters, specifically in this case, the Ohmicity parameter s. Hence, a testbed for further investigating non-Markovianity is always obtained using PDD. Engineering non-Markovianity here refers specifically to the information-theoretical approach which has been proven useful for quantum technologies [13]-[17]. In this sense, our results should not simply be understood as another variant of the well known idea that DD modifies the reservoir spectrum by making it more structured. On the contrary, they are an exploration on the ability to controllably modify and enhance quantities such as the channel capacities [16], mutual information [24], Fisher information [96], etc. This in turn provides a way to control the efficiency of quantum communication protocols [16], quantum metrology [13], and work extraction [165].

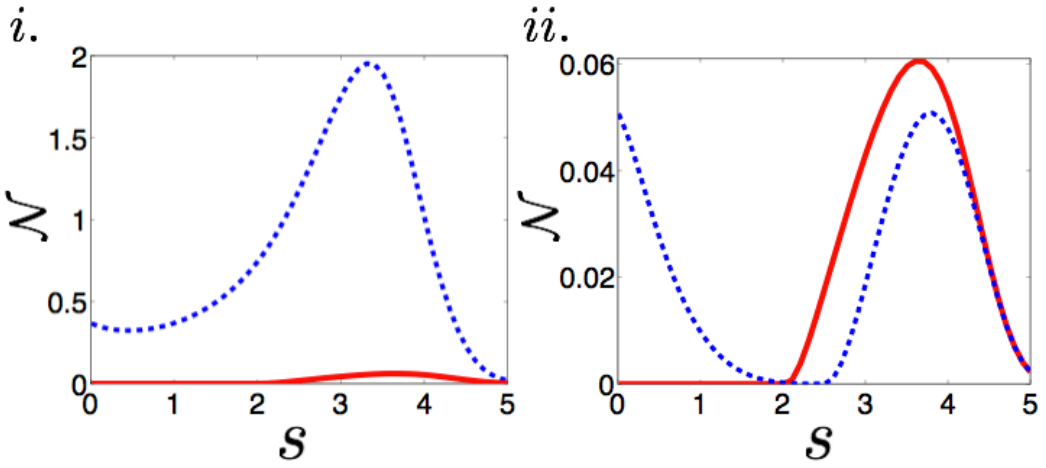

Figure 5.4: Non-Markovianity measure against the Ohmicity parameter for the dynamically decoupled system (blue dotted line) for time intervals i) $\Delta t = 0.3$ and ii. $\Delta t = 3$ (in units of ω_c^{-1}) and the non-Markovianity for the free system (red solid line). The final pulse is applied at time $\omega_c t_f = 9$. We draw attention to the fact that $\mathcal{N} \neq 0$ for all values of s when the system is subject to DD but may take very small values as shown in ii) for $2 \leq s < 2.6$.

In Fig. 5.4, we investigate the non-Markovianity, in terms of the BLP measure, induced by PDD in the absence and presence of pulses and for both the short-pulse and long pulse regimes. In the short pulse regime, for any value of the Ohmicity

parameter s, the effect of the pulses is to create non-Markovianity by inducing information back flow when it is initially absent, or in any case to increase the non-Markovian character (see Fig. 5.4 i). In the long-pulsing regime, the situation is more variegated as pulses can also, under certain conditions, decrease the non-Markovian character of the dynamics as seen in the example of Fig. 5.4 ii.

5.4 Dynamical Decoupling with Quantum Correlations

We now investigate the implications of the relationship between DD techniques and non-Markovianity in a quantum information scenario. It is well known that the use of either DD techniques or non-Markovian effects prolongs the preservation of both entanglement and discord in the presence of environmental noise [52]-[57]. While entanglement has long been established as the principle resource in quantum protocols (for e.g., in quantum cryptography [166], teleportation [167], Shor's algorithm [168]), numerous examples have demonstrated that quantum discord is also crucial for, e.g., distribution of entanglement [58]-[61], quantum locking [62], entanglement irreversibility [63] and many other tasks [64]-[65]. With this in mind, we study the preservation of quantum and classical correlations and the possibility of creating time-invariant discord through PDD techniques in relation to the initial conditions (unperturbed dynamics). On the one hand, the use of either DD techniques or non-Markovian effects prolongs the preservation of both entanglement and discord in the presence of environmental noise [52]-[57]. On the other hand, we have shown that the simultaneous use of non-Markovian reservoir engineering and DD protocols is counterproductive for avoiding decoherence. We now study two qubits experiencing local dephasing with an Ohmic class spectrum and subject to dynamical decoupling protocols. In more detail, we aim to investigate the connection between the preservation of quantum correlations and the direction of information flow between the system and environment, controlled by DD and non-Markovianity.

5.4.1 Introduction to Quantum Correlations

Before presenting the results of this section, we now provide the necessary preliminary introductions to quantum entanglement and time-invariant discord.

5.4.1.1 Entanglement

Entanglement, coined "spooky action at a distance" by Albert Einstein [169] captures a quantum correlation not found in the classical world [170]. The state of a multipartite system is said to be entangled if it is not possible to write the state as the product of its component states. More precisely, the global description given

by the total entangled state of the system, comprises information that the single reduced states do not contain. A bipartite quantum system ρ_{AB} composed of reduced states ρ_A and ρ_B is said to be entangled if it is not possible to write it in the factorised form,

$$\rho_{AB} \neq \sum_k p_k \rho_k^{(A)} \otimes \rho_k^{(B)}, \tag{5.16}$$

with $\{|\Psi_k^{(A),(B)}\rangle\}$ being an orthonormal basis in $\mathcal{H}_{A,B}$.

In this work, we use a well-known measure to quantify entanglement, namely concurrence $C(\rho)$ [171]-[174], defined as follows:

$$C(\rho) = \max\{0, \sqrt{\lambda_1} - \sqrt{\lambda_2} - \sqrt{\lambda_3} - \sqrt{\lambda_4}\}, \tag{5.17}$$

where λ_i are the eigenvalues of the matrix

$$R = \rho(\sigma_y^A \otimes \sigma^B)\rho^*(\sigma_y^A \otimes \sigma^B), \tag{5.18}$$

and with ρ^* the complex conjugate of ρ and $\sigma_y^{A/B}$, the Pauli matrices for the qubits A and B. The quantity is conveniently bound between zero (separable states) and 1 (maximally entangled states). Moreover, for the wide class of states, known as X-states, having the following form,

$$\rho(t) = \begin{pmatrix} a(t) & 0 & 0 & w(t) \\ 0 & b(t) & z(t) & 0 \\ 0 & z^*(t) & c(t) & 0 \\ w^*(t) & 0 & 0 & d(t) \end{pmatrix} \tag{5.19}$$

concurrence attains a simple expression,

$$C(t) = \max\{0, C_1(t), C_2(t)\} \tag{5.20}$$

where

$$\begin{aligned} C_1(t) &= 2|w(t)| - 2\sqrt{b(t), c(t)}, \\ C_2(t) &= 2|z(t)| - 2\sqrt{a(t), d(t)}. \end{aligned} \tag{5.21}$$

In our case, the states are initially as Eq. 5.19 and are preserved in this form for the duration of the time evolution.

5.4.1.2 Quantum Discord

Genuine quantum correlations of a more general type than entanglement are defined as quantum discord [175], originally introduced by Ollivier and Zurek [176] and independently identified by Henderson and Vedral [177]. The definition of quantum

discord is based on the difference between the quantum analogues of two classically equivalent concepts of mutual information of a bipartite system. The classical expressions for mutual information are given, for two classical random variables A and B as follows,

$$I(AB) = H(A) + H(B) - H(AB), \tag{5.22}$$

and

$$J(AB) = H(A) - H(A|B), \tag{5.23}$$

where $H(A)$ and $H(B)$ are Shannon entropies, and $H(A|B)$ is the conditional entropy on A when B is known. The first quantum generalisation of mutual information is the so-called quantum mutual information which quantifies the total amount of classical and quantum correlations in a bipartite system:

$$\mathcal{I}(\rho_{AB}) \;\; = \;\; S(\rho_A) + S(\rho_B) - S(\rho_{AB}), \tag{5.24}$$

where ρ_{AB} and $\rho_{A(B)}$ are the density matrix of the total system and reduced density matrix of subsystem A(B) respectively and $S(\rho) = -\mathrm{Tr}\{\rho \log_2 \rho\}$ is the von Neumann entropy. On the other hand, in Ref. [177], Henderson and Vedral show that the second quantum extension of mutual information can be interpreted as a measure of the classical correlations of the state following a maximisation over all possible sets of measurements. Hence we have,

$$\mathcal{C}(\rho_{AB}) = \max_{\{\Pi_k^B\}} \left\{ S\left(\rho_A\right) - \sum_k p_k S\left(\rho_{A|k},\right) \right\} \tag{5.25}$$

where $\{\Pi_k^B\}$ is a positive operator valued measure (POVM) acting only on the subsystem B, and $\rho_{A|k} = Tr_B(\Pi_k^B \rho_{AB} \Pi_k^B)/p_k$ is the remaining state of the subsystem A after obtaining the outcome k with probability $p_k = Tr_{AB}(\Pi_k^B \rho_{AB} \Pi_k^B)$ in the subsystem B. Therefore, the difference between the quantum mutual information $I(\rho_{AB})$ describing total correlations and the measurement-based definition of quantum mutual information $C(\rho_{AB})$, capturing classical correlations, defines the quantum discord,

$$D(\rho_{AB}) = \mathcal{I}(\rho_{AB}) - \mathcal{C}(\rho_{AB}). \tag{5.26}$$

Analytically, quantum discord is defined for two qubit systems [178, 179], and also continuous variable systems [180, 181]. From this point of view, discord has been studied extensively in literature from a mathematical perspective, particularly the time evolution of discord in the presence of (Markovian and non-Markovian) environments [182]-[185]. In more detail, it has been demonstrated that discord never disappears completely after a finite time [183, 186] while total loss of entanglement is possible, known as the so-called entanglement sudden death phenomenon (ESD)

[187, 188]. Moreover, discord can exhibit sudden transitions if certain parameters characteristic of the system are abruptly changed. The most striking difference which we study in this chapter is the possibility of discord remaining constant for long times, completely unaffected by the presence of the environment. Indeed, quantum discord has been shown to be frozen for a finite time for a certain time interval [189] or even forever [66], depending on the properties of the initial state and the specifics of the interaction with the environment. In particular, for two qubits in Bell-diagonal states and independently interacting with dephasing environments, while frozen discord manifests itself for both Markovian [189] and non-Markovian [190] environments, the emergence of time-invariant discord is more closely related to the presence of memory [66], i.e. occurring for only non-Markovian regimes. A clear merit in creating time-invariant discord is in the execution of quantum protocols based on discord, which become unaffected by noise under the specific conditions.

5.4.2 Time Invariant Discord

We now recall the details of the two relevant studies which motivate this work. Specifically, the first encounter of frozen discord in Markovian environments and further, the complementary non-Markovian generalisation of this work. The mysterious phenomenon of frozen discord was introduced in Ref. [189], for a class of Bell-diagonal states, interacting locally with Markovian dephasing environments. It was demonstrated, that for certain initial states, initial time periods $0 < t < \bar{t}$ exist for which quantum discord remains frozen at finite values while classical correlations decay. For times following $\bar{t} > t$, classical correlations remain constant while discord is subject to noise-induced decay. The transition time $\bar{t}$ can be found analytically and characterised by a single parameter of the initial state. This unanticipated phenomenon, coined the sudden transition between classical and quantum decoherence, is contrary to what one might expect intuitively, i.e. the initial resilience of discord compared to classical correlations in a Markovian environment. For non-Markovian environments, the existence of a transition time $\bar{t}$ crucially depends not only on the initial state of the bipartite system but now, also on the specific properties of the spectral density of the environment [66]. Interestingly, it was demonstrated that for specific parameters of the spectral density, a transition time $\bar{t}$ does not exist and therefore discord remains frozen forever [66].

We now consider reservoir engineering from an additional perspective with the aim of optimally controlling the direction of information flow for the purpose of creating time-invariant discord. In more detail, we consider two types of engineering, one based on a modification of the reservoir density through the Ohmicity parameter in order to change the Markovian character of the dynamics, and secondly, one exploiting dynamical decoupling (which in turn, can also be seen as effective filtering of the spectral density). In order to determine a set of necessary conditions for which

time-invariant discord manifests when the system is periodically pulsed, we focus on initial Bell-diagonal states of the form,

$$\rho_{AB} = \frac{(1+c)}{2} |\Phi^{\pm}\rangle \langle\Phi^{\pm}| + \frac{(1-c)}{2} |\Psi^{\pm}\rangle \langle\Psi^{\pm}| \tag{5.27}$$

where $|\Phi\rangle = (|00\rangle \pm |11\rangle)/\sqrt{2}$ and $|\Psi\rangle = (|01\rangle \pm |10\rangle)/\sqrt{2}$ are the four Bell states and $|c| < 1$. For a more detailed insight, we consider two different cases of local dephasing noise in the presence of DD. Firstly, we consider the scenario where both qubits A and B interact locally with identical dephasing environments with an Ohmic type spectral density. In this case, the expressions for the mutual information $\mathcal{I}(\rho_{AB})$ and classical correlations $\mathcal{C}(\rho_{AB})$ are given by [178]:

$$\mathcal{C}[\rho_{AB}] = \sum_{j=1}^{2} \frac{1+(-1)^j\chi}{2} \log_2[1+(-1)^j\chi(t)], \tag{5.28}$$

$$\begin{aligned}\mathcal{I}[\rho_{AB}(t)] = &\sum_{j=1}^{2} \frac{1+(-1)^j c}{2} \log_2[1+(-1)^j c] \\ &+ \sum_{j=1}^{2} \frac{1+(-1)^j e^{-2\Gamma(t)}}{2} \log_2[1+(-1)^j e^{-2\Gamma(t)}],\end{aligned} \tag{5.29}$$

where $\chi(t) = \max\{e^{-2\Gamma(t)}, c\}$. Secondly, we consider the case where only one of the qubits interacts with the dephasing environment while the other qubit is entirely protected from decoherence. The corresponding expressions for mutual information $\mathcal{I}(\rho_{AB})$ and classical correlations $\mathcal{C}(\rho_{AB})$ are straightforward to obtain from Eq. 5.29 by replacing $e^{-2\Gamma(t)}$ with $e^{-\Gamma(t)}$. It is also important to realise that for one-sided noise, DD pulses are applied only to the qubit experiencing dephasing through the modified dephasing model, while for two-sided noise, both qubits are subject to pulsing. Now, from the expressions given in Eqs. 5.28-5.29, it is straightforward to realise that when $e^{-2\Gamma(t)} > c$, classical correlations decay while the discord, given by the first term in Eq. 5.29, remains constant. The transition time $\bar{t}$, marking the sudden transition phenomenon, exists only if $e^{-2\Gamma(\bar{t})} = c$. Note, the same is true for one-sided noise, again replacing $e^{-2\Gamma(\bar{t})}$ by $e^{-\Gamma(\bar{t})}$.

Without the possibility of analytically or numerically defining continuously pulsed dynamics in the asymptotic time limit, we focus on discord which remains "time-invariant" within a chosen experimental time interval rather than forever. The values of invariant discord are easily found from the difference of Eqs 5.28-5.29 when $\chi(t) = \{e^{-\Gamma(t)}, e^{-2\Gamma(t)}\}$ for one-sided noise and two-sided noise respectively:

$$D = (1+c)\log_2(1+c)/2 + (1-c)\log_2(1-c)/2. \tag{5.30}$$

Immediately from this expression, one can see that discord acquires a significant value for larger values of c. We now study the regions of s and c for which time-

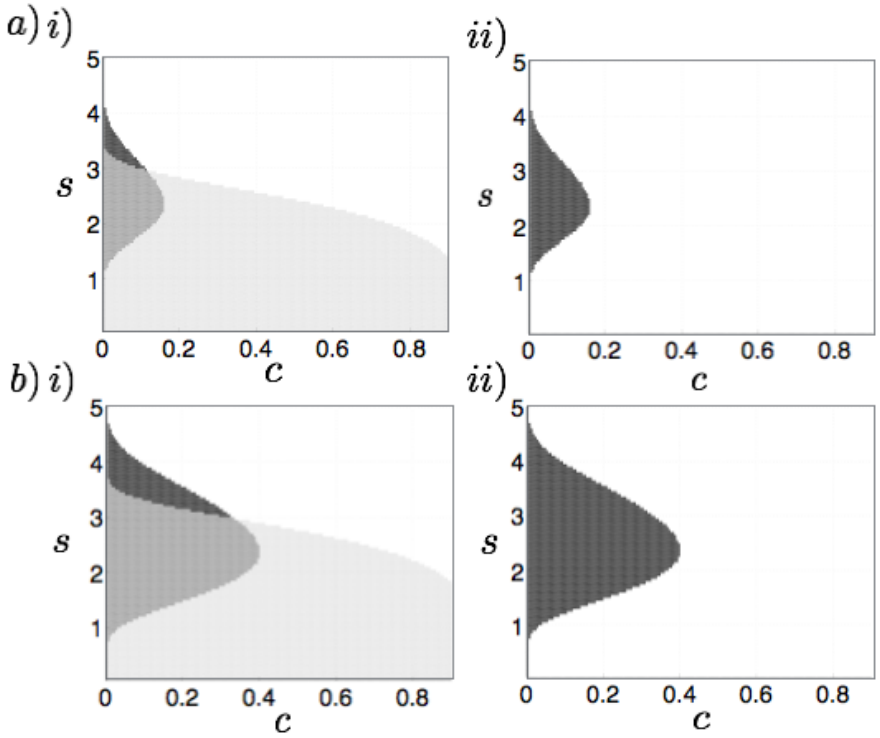

Figure 5.5: The black region shows the range of s and c parameters for which the discord is frozen forever for a free system evolving without pulsing. The grey region shows the range of s and c for dynamical decoupled systems with small interval spacing $\Delta t = 0.3\omega_c^{-1}$ (i) and long interval spacing $\Delta t = 3\omega_c^{-1}$ (ii). The plots in (a) are for the case where both qubits are affected by noise, as the plots in (b) are for single qubit noise. Outside these regions, one will always observe a transition from classical to quantum decoherence and thus no time-invariant discord. The final pulse is applied at $t_f = N_{\max}\Delta t \leq 25\omega_c^{-1}$ where $N_{\max}$ is the maximum number of pulses that can be applied within the time interval $0 \leq t \leq 25\omega_c^{-1}$. Quantities plotted are dimensionless.

invariant discord exists for both the pulsed and unperturbed case. In Fig. 5.5 a i), we show that for two-sided local dephasing noise and short pulse intervals (e.g. $\omega_c\Delta t = 0.3$), time-invariant discord is created for a wider range of both c and s compared to the unperturbed case. Particularly, time-invariant discord is created for sub-Ohmic values of s, ($s < 1$) for up to very high values of c, only when the system is subject for DD. Generally, one can see from the plot, that increasingly significant values of time-invariant discord (corresponding to large values of c), occur for $s < 2$. Numerical investigation proves these conclusions are independent of the specific pulse interval chosen, provided that $\Delta t < \tilde{t}$. Moreover, we conjecture that in the asymptotic long time limit ($t_f \to \infty$), DD will only create time-invariant discord for $s \lesssim 1$. This is based on the knowledge from numerical investigation, specifically, that no degradation of the coherence is shown to occur within computable times. Hence, it is natural to think that in the asymptotic long time limit, coherence is maintained for values close to unity and a transition time therefore will not exist. On the other hand, for $s \geq 1$, as t_f increases, the region of time-invariant discord

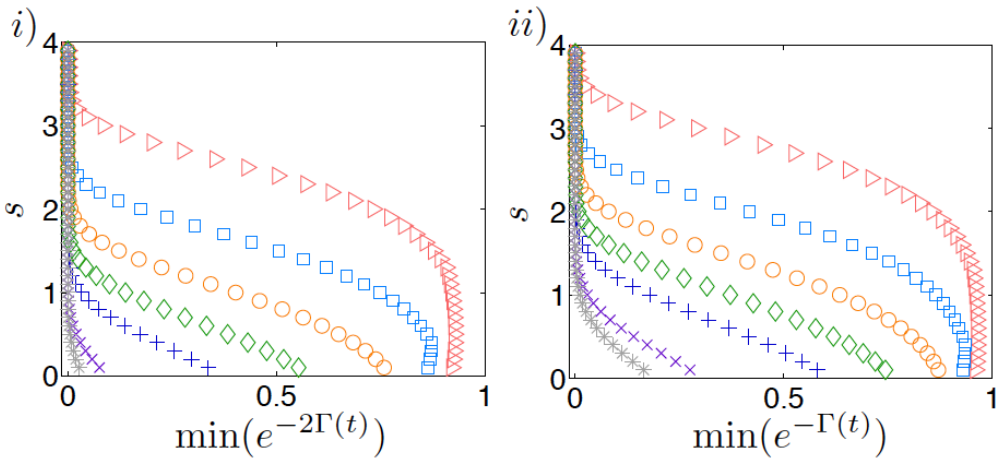

Figure 5.6: The boundary between the sudden transition and the time-invariant discord as a function of the Ohmicity parameter s and the minimum value of decoherence factor throughout the time evolution, for two-sided (i) and one-sided (ii) dephasing noise. We show pulse intervals $\Delta t = 0.3\omega_c^{-1}$ (red triangles), $\Delta t = 0.4\omega_c^{-1}$ (blue squares), $\Delta t = 0.5\omega_c^{-1}$ (orange circles), $\Delta t = 0.6\omega_c^{-1}$ (green diamonds), $\Delta t = 1\omega_c^{-1}$ (blue plus signs), $\Delta t = 1.5\omega_c^{-1}$ (purple crosses) and $\Delta t = 2\omega_c^{-1}$ (grey stars). The final pulse is applied at $t_f = N_{\max}\Delta t \leq 25\omega_c^{-1}$ where $N_{\max}$ is the maximum number of pulses that can be applied within the time interval $0 \leq t \leq 25\omega_c^{-1}$. Quantities plotted are dimensionless.

will decrease as the coherence decays to increasingly small values.

We have so far shown the potential high values of discord that can be achieved if one entirely avoids non-Markovianity and instead exploits dynamical decoupling. However, we now demonstrate the destructive influence of DD on time-invariant discord for large pulse intervals. Indeed, in Fig. 5.5 a ii), we show that time-invariant discord is completely non-existent for large pulse intervals (e.g, $\omega_c\Delta t = 3$) in the case of two-sided noise. Once again, we have extensively investigated this regime numerically to ensure this behaviour is characteristic of large pulse intervals $\Delta t > \tilde{t}$. Our conclusion follows intuitively from the results of Sec. 5.3. Indeed, we find that short pulse interval DD schemes paired with Markovian environments (specifically $s < 1$), are optimal for the creation of time-invariant discord for a larger range of initial states and compared to relying on non-Markovianity alone as a resource.

For the sake of comparison, we show in Fig. 5.5 b i) and b ii) corresponding plots illustrating the same conclusions for when only one of the qubits is affected by dephasing noise. Although we observe similar results to the previous case, in general, we note that the regions of invariant discord, in the absence and presence of control, become larger. Physically, this result is self-evident as in this case, one of the qubits in the pair is fully protected against noise. However, we note that whereas the difference in the regions of s and c between the one-sided and two-sided noise is significant in the case of unpulsed non-Markovian dynamics, the difference is less pronounced when we implement the DD pulses.

Let us now extend our investigation by considering the region of parameters c and s giving rise to time-invariant discord for *intermediate* values of pulse interval Δt. The behaviour of the boundary between the sudden transition and the time-invariant discord for different values of the pulse interval is displayed in Fig. 5.6 (i) and Fig. 5.6 (ii) for two-sided and one-sided local dephasing noise, respectively. We plot the transition boundary: below which, discord is time-invariant and classical correlations decay and above which, the converse is true. Given that $e^{-2\Gamma(0)} = 1$ and considering a fixed value of s, if the initial state parameter $0 \leq c \leq 1$ is chosen so that it is smaller than the minimum value of the decoherence factor $e^{-2\Gamma(t)}$ at any point during the pulsed dynamics, there occurs no sudden transition and consequently, discord remains invariant at all times. On the other hand, if $c > \min(e^{-2\Gamma(t)})$, a sudden transition takes place and discord begins to decay after the critical time instant $\bar{t}$, which can be obtained analytically from the solution of the equation $\min(e^{-2\Gamma(t)}) = c$. For one-sided noise, the same is true, replacing $e^{-2\Gamma(t)}$ with $e^{-\Gamma(t)}$. Therefore, Fig. 5.6 actually demonstrates how the region of parameters s and c creating time-invariant discord are affected as the pulse interval changes between the short and long interval limits. It is clear, that as the pulse interval Δt increases, the overlap between the regions of uncontrolled and controlled time-invariant discord becomes smaller. Following this, one can say that relying only on non-Markovianity as a resource of time-invariant discord becomes more preferable in general as the pulse interval Δt increases.

5.4.3 Dynamically Decoupled Correlations

We conclude this chapter by studying, for a specific initial state, i.e. $c = 0.5$, the time evolution of quantum and classical correlations. Specifically, we are interested in how DD pulses affect the sudden transition and time-invariant discord dynamics for small and large pulse intervals with Markovian/non-Markovian regimes. Moreover, for completeness, we compare the behaviour of discord and classical correlations to the dynamics of entanglement as measured by concurrence:

$$C = \frac{1}{2}\max\{0, |e^{-\Gamma(t)}(1-c)| - 1 - c, |e^{-\Gamma(t)}(1+c)| - 1 + c\}, \tag{5.31}$$

where we assume that only one of the qubits is locally interacting with the environment. In line with results from Sec. 5.3, we observe that for short pulse intervals ($\Delta t < \tan(\pi/s)$), and Markovian dynamics ($s < 2$), both classical correlations and entanglement are well preserved while discord remains invariant at a non-zero value for the experimental time interval considered (see. Fig. 5.7 a (i)). Indeed, we realise that both conditions are necessary and leaving even one unsatisfied leads to vanishing time-invariant discord due to the sudden transition between classical and quantum decoherence. Moreover, we see that entanglement decays to zero. Natu-

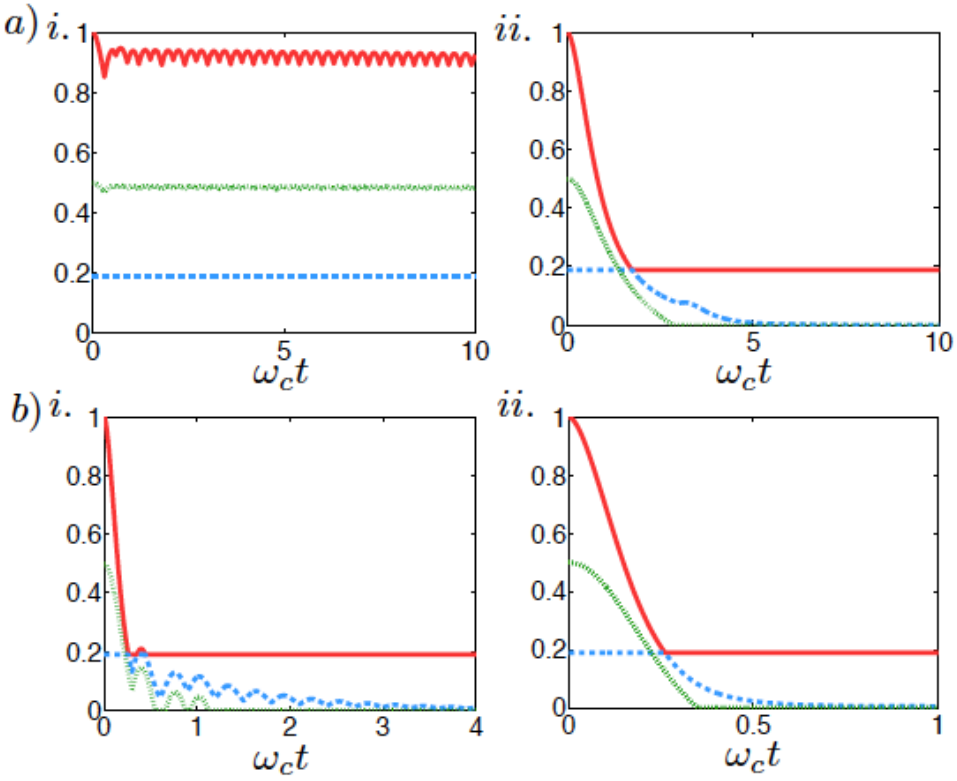

Figure 5.7: Dynamics of entanglement (dotted green), classical correlations (solid red) and quantum discord (dashed blue) for i) short pulse spacing $\Delta t = 0.3$ and ii) long pulse spacing $\Delta t = 3$ (in units of ω_c^{-1}) and a) Markovian environments (s=1.01) and b) non-Markovian environments (s=4). The plots are for local dephasing noise on one qubit and $c = 0.5$. Quantities plotted are dimensionless.

rally, in order to preserve entanglement through dynamical decoupling, a pulse must occur before entanglement decays to zero (see Fig. 5.7 (ii)).

More in general, as one can see from Fig. 5.6, for $c = 0.5$, time-invariant discord only occurs for small pulse spacings, specifically, $\omega_c \Delta t \lessapprox 1$. Moreover, in the most destructive scenario, time-invariant discord can be created in the non-Markovian regime only for pulse spacings satisfying $\omega_c \Delta t < 0.4$. Once discord becomes invariant, the value depends only on the initial state through the parameter c.

5.5 Conclusions

In this chapter, we have studied an exact dynamical description of dynamical decoupling in order to connect the efficiency of DD protocols to the reservoir spectral density. Particularly, we have studied the direction of information flow between the system and environment, determined by the interplay of DD and the unperturbed dynamics. We have explored this connection to shed light on the phenomena responsible for revivals in coherence, specifically, to define the role of non-Markovianity as a resource in such protocols. Contrary to intuitive reasoning, we found that non-Markovianity is not trivially a resource for control protocols and instead, memory

effects are detrimental in the presence of control. Also, in Ref. [48], in the case of amplitude damping channels, the existence of regimes where non-Markovianity can be either beneficial or detrimental to optimal control strategies were revealed. Having efficient error correction in mind, we have focused on the short pulse regime. In this case, we have found that a Markovian environment is necessary to optimise the DD performance. With a shift in perspective, we have shown how dynamical decoupling techniques can be harnessed to engineer and control the non-Markovian character of the dynamics.

Knowing that it is counterproductive to exploit both DD and non-Markovianity simultaneously, we investigated the optimal conditions in a quantum information setting. In more detail, we studied the competition between exploiting non-Markovianity or DD to best preserve quantum correlations. In the absence of control, time-invariant discord mainly occurs in the non-Markovian regime [66]. In this work, we studied the intriguing phenomenon of time-invariant discord with the aim of understanding whether the presence of DD pulses might lead to a wider range of parameters for which it occurs and if, in this way, one can obtain higher values of "protected" discord. We have shown that, in the presence of control, the optimal conditions to achieve significant values of time-invariant discord, persisting for experimental time scales, are obtained for Markovian reservoirs ($s < 2$) in the short pulse regime. Further, we conjecture that for discord to remain invariant to non-zero values forever, i.e. in the limit $t_f \to \infty$, the Ohmicity parameter is further restricted to $s < 1$. On the contrary, utilising large pulse spacing and free non-Markovian dynamics are detrimental to the creation of time-invariant discord, in the pulsed scenario. In order to achieve the maximum values of discord, and given the choice, DD techniques are best compared to relying on non-Markovianity alone as a resource, albeit, for a restricted Ohmicity range ($s < 2$).

Chapter 6

Conclusions

The collection of results presented in this thesis are centralised around the multi-faceted phenomenon of non-Markovianity. The first part of this thesis is devoted to an extensive comparison of the definitions and associated quantifiers of non-Markovianity. The following chapters investigate optimal control in non-Markovian scenarios. Specifically, we exposed the failure of applying the crucial assumption in control theory, to non-Markovian dynamics. Avoiding this assumption in an exact microscopic description of control, we investigated the relationship between dynamical decoupling techniques and non-Markovianity, revealing the detrimental role of non-Markovianity in such schemes. We now examine the conclusions of this thesis in more detail.

In Chapter 3, we revealed distinct aspects of non-Markovianity through several recently proposed definitions and associated quantifiers. Particularly, we studied the RHP, BLP, LFS and BCM measures in relation to their computability, additivity, and physical interpretation. While all measures are associated with a relevant physical interpretation, the additivity and computability properties vary. We found that while all measures excluding the BLP measure are additive (in the sense that the measure for two qubits in independent environments is twice that for one qubit), only the RHP measure can be determined analytically. All other measures require extensive sampling over initial states with formidable difficulties in the optimisation occurring for higher dimensional systems. Despite the variations between the measures, the connection between the memory effects each measure captures and the form of the spectral density is, in most cases, similar. We note, however, that while in the pure dephasing case, all non-Markovian measures detect non-Markovianity for the same range of system parameters, the converse is not true in the amplitude damped case. We conclude our comparison by acknowledging that in order to fully understand the complex physical process, non-Markovianity, each perspective offered by the measures is valuable.

In the following chapters, we investigated the usefulness of non-Markovianity in optimal control protocols. In Chapter 4, we studied a simple optimal control

strategy in the form of a single unitary pulse, in the presence of non-Markovian noise. In this regime, the widespread assumption in control theory, mainly, that the dissipator remains fixed in the presence of control, can lead to physical uncertainty in the resultant dynamics. For pure dephasing dynamics, we found that the only physically meaningful description of the reduced dynamics in the presence of control is the one obtained via a microscopic model including the controlled system plus the environment. In general, if the dissipator changes markedly after each pulse, creating trajectories with superior properties compared to the uncontrolled trajectories will not be possible. The only possible solution to this impasse might be the discovery of certain special forms of non-Markovian dissipators that may not be changing sensibly in the presence of some specific coherent control schemes, perhaps exploiting specific symmetries of the dissipator and control Hamiltonian.

In Chapter 5, we studied an exact dynamical description of a purely dephasing system subject to periodic dynamical decoupling protocols. We explored the relationship between non-Markovianity and DD in terms of information flow to establish the role of non-Markovianity as a resource in such protocols. With sufficient error correction in mind, we focused on defining the optimal conditions in the short pulse regime and demonstrated that a Markovian environment is essential for efficient DD schemes. Indeed, simultaneous use of a non-Markovian dynamics and DD protocols is counterproductive for coherence preservation. With a shift in perspective, we demonstrated how dynamical decoupling techniques can be harnessed to engineer quantum non-Markovianity and control it. With the counterintuitive relationship between non-Markovianity and DD established, we focused on the preservation of quantum correlations with quantum information tasks in mind. While in the unpulsed regime, significant values of time-invariant discord mainly occur in the non-Markovian regime, the converse is true in the pulsed regime, if the spacing between pulses is small. On the other hand, if the space between pulses is large, time-invariant discord is completely destroyed.

Our results contribute to the two central themes related to non-Markovianity regarding its characterisation and role as a resource. While we believe that extending the GKSL theorem to non-Markovian cases may not be easy to achieve in general, the possible means to exploit non-Markovianity as a resource should still be further explored. Indeed, the potential resourcefulness of non-Markovianity in applications useful for quantum technologies remains an open question. A key line of research in this approach lies in realising how nature utilises memory effects to preserve quantum quantities [19, 20].

Appendices

Appendix A

Further Dynamical Description

In this section, we define the Kraus operators and complementary maps required for Chapter 2.

A.1 Pure Dephasing Model

Recalling the operator-sum representation of the dynamical map $\Phi_t(\rho) = \sum_{i=1}^{2} K_i(t)\rho K_i^\dagger(t)$ with time-dependent Kraus operators, we define for the single qubit dephasing maps:

$$K_1(t) = \sqrt{\frac{1+e^{-\Gamma(t)}}{2}}\mathbb{I}$$

$$K_2(t) = \sqrt{\frac{1-e^{-\Gamma(t)}}{2}}\mathbb{I}$$

Knowledge of the Kraus operators allows one to immediately also write the complementary map, needed to calculate both the coherent information and the entropy exchange which appears in the definition of the mutual information of the channel:

$$\begin{aligned}\tilde{\Phi}_t[\rho] &= \frac{1}{2}\left[(1+e^{-\Gamma(t)})\left|1\right\rangle_E\left\langle 1\right| + (1-e^{\Gamma(t)})\left|2\right\rangle_E\left\langle 2\right|\right] \\ &+ \frac{1}{2}\sqrt{1-e^{2\Gamma(t)}}\mathrm{Tr}(\rho\sigma_z)\left(\left|1\right\rangle_E\left\langle 2\right| + \left|2\right\rangle_E\left\langle 1\right|\right). \qquad \text{(A.1)}\end{aligned}$$

For two qubits, the form of the Kraus operators is as follows

$$K_1 = \begin{pmatrix} e^{-\frac{1}{2}\Gamma_-(t)} & 0 & 0 & 0 \\ 0 & e^{-\frac{1}{2}\Gamma_+(t)} & 0 & 0 \\ 0 & 0 & e^{-\frac{1}{2}\Gamma_+(t)} & 0 \\ 0 & 0 & 0 & e^{-\frac{1}{2}\Gamma_-(t)} \end{pmatrix}$$

$$K_2 = (e^{-\Gamma_-(t)} - 1)\sqrt{e^{-\Gamma_-(t)} + 1} \begin{pmatrix} 1 & 0 & 0 & 0 \\ 0 & 0 & 0 & 0 \\ 0 & 0 & 0 & 0 \\ 0 & 0 & 0 & 0 \end{pmatrix}$$

$$K_3 = \sqrt{1 - e^{-\Gamma_-(t)}} \begin{pmatrix} -e^{-\Gamma_-(t)} & 0 & 0 & 0 \\ 0 & 0 & 0 & 0 \\ 0 & 0 & 0 & 0 \\ 0 & 0 & 0 & 1 \end{pmatrix}$$

$$K_4 = (e^{-\Gamma_+(t)} - 1)\sqrt{e^{-\Gamma_+(t)} + 1} \begin{pmatrix} 0 & 0 & 0 & 0 \\ 0 & 1 & 0 & 0 \\ 0 & 0 & 0 & 0 \\ 0 & 0 & 0 & 0 \end{pmatrix}$$

$$K_5 = \sqrt{1 - e^{-\Gamma_+(t)}} \begin{pmatrix} 0 & 0 & 0 & 0 \\ 0 & -e^{-\Gamma_+(t)} & 0 & 0 \\ 0 & 0 & 1 & 0 \\ 0 & 0 & 0 & 0 \end{pmatrix}.$$

We note that for two qubits occupying independent environments, the Kraus operators are of the above form with $\Gamma_\pm(t) \to \Gamma(t)$.

A.2 Amplitude Damped Model

The Kraus representation $\Phi_t(\rho) = \sum_{i=1}^{2} K_i(t)\rho K_i^\dagger(t)$ for the amplitude damping channel is given by

$$K_1 = \begin{pmatrix} 1 & 0 \\ 0 & G \end{pmatrix}$$

$$K_2 = \begin{pmatrix} 0 & \sqrt{1 - |G|^2} \\ 0 & 0 \end{pmatrix}$$

which gives us a complementary map defined by:

$$\begin{aligned} \tilde{\Phi}_t^A(\rho) &= [1 - (1 - |G(t)|^2)\rho_{22}] \, |1\rangle_E \langle 1| \\ &+ (1 - |G(t)|^2)\rho_{22} \, |2\rangle_E \langle 2| \\ &+ \sqrt{1 - |G(t)|^2}(\rho_{12} \, |1\rangle_E \langle 2| + \rho_{21} \, |2\rangle_E \langle 1|). \end{aligned} \tag{A.2}$$

For two independent identical environments, the Kraus operators are the tensor products of Kraus operators of the one qubit case, $K_{ij} = K_i \otimes K_j$, for $i, j = 1, 2$.

Appendix B

Optimisation Evidence

This section contains graphical evidence of the optimisation procedures used in the calculation of the non-Markovianity measures of Chapter 2. The states sampled are shown as single points on the plots with the top points corresponding to the points maximising the measure.

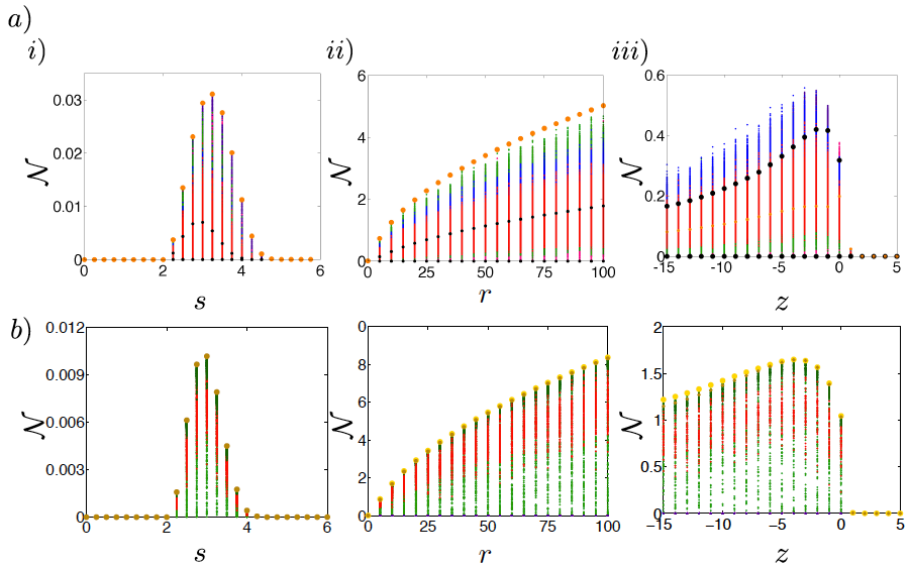

Figure B.1: Non-Markovianity Measure (the largest value in each column for each plot) for independent two qubit systems for the following reservoir spectra: i) Pure dephasing, ii) Lorentzian and iii) Photonic Band Gap model. We define the dynamics using a) the Breuer, Laine, Piilo Measure and b) the Luo, Fu, Song Measure. All the measures are plotted against an environmental parameter which may be modifed. In general, to maximize each measure, random states are used, including maximally entangled (purple), pure (pink), mixed states (red) and product states (green). For the Breuer, Laine and Piilo measure we include combinations of mixed and pure states (blue), Bell states (black) and the tensor product state $|\pm\pm\rangle\langle\pm\pm|$ (yellow). For all other measures we include separable states other than product states (dark green), the maximally mixed state (brown) and tensor product state of the optimizing states for the one qubit case (gold), which is parameter dependent. We consider for the Pure dephasing, Lorentzian and Photonic the following times periods: $t \in [0, 20]$ in units of $\omega_c t$, $t \in [0, 40]$ in units of λt and $t \in [0, 20]$ in units of βt.

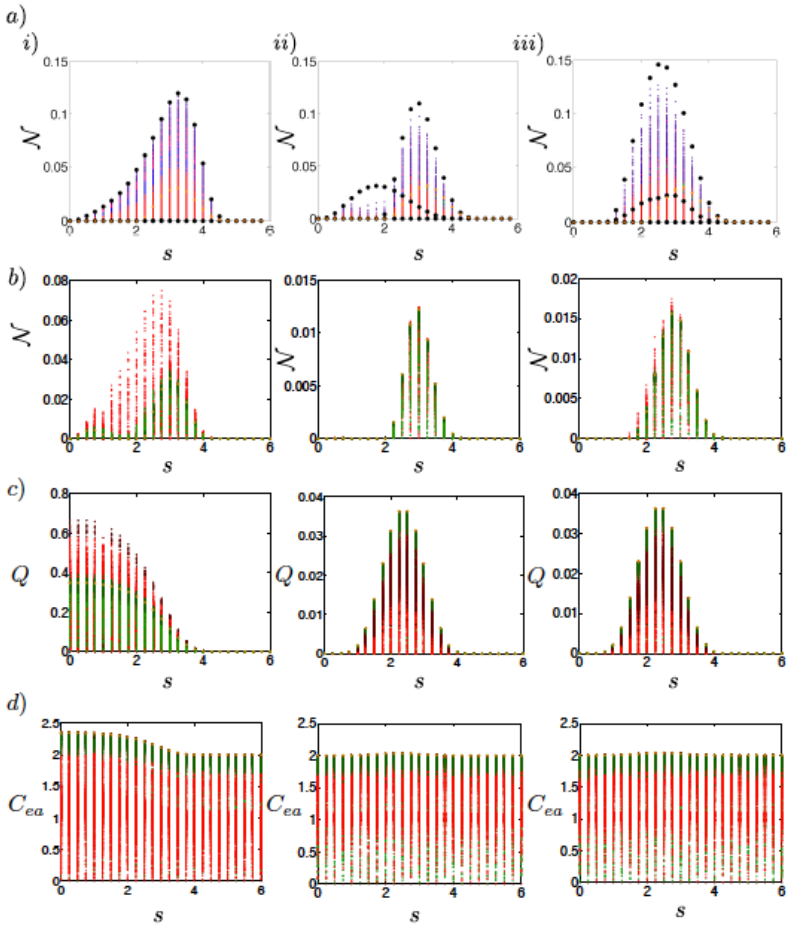

Figure B.2: Non-Markovianity Measure (the largest value in each column for each plot) for common two purely dephasing qubit systems for transit times t_s i) 0.25, ii) 2 and iii) 6. We define the dynamics using a) the Breuer, Laine, Piilo Measure, b) the Luo, Fu, Song Measure, c) the Quantum Capacity Measure and d) the the Entanglement-Assisted Classical Capacity Measure. All the measures are plotted against the Ohmicity parameter s which may be modified. In general, to maximize each measure, random states are used, including maximally entangled (purple), pure (pink), mixed states (red) and product states (green). For the Breuer, Laine and Piilo measure we include combinations of mixed and pure states (blue), Bell states (black) and the tensor product state $|\pm\pm\rangle\langle\pm\pm|$ (yellow). For all other measures we include separable states other than product states (dark green), mixed states of rank 2 with eigenvalues close to $\frac{1}{2}$ (dark red), the maximally mixed state (brown). We consider a time interval $t \in [0, 20]$ in units of $\omega_c t$. Note for rows c) and d) we optimize for $t = 5$ for the Quantum Capacity Q and the Entanglement-Assisted Classical Capacity C_{ea} respectively.

Bibliography

[1] C. Addis, B. Bylicka, D. Chruciski and S. Maniscalco, *Comparative study of non-Markovianity measures in exactly solvable one and two qubit models*, Phys. Rev. A **90**, 052103 (2014).

[2] C. Addis, E-M Laine, C. Gneiting and S. Maniscalco, *The problem of coherent control in non-Markovian open quantum systems*, arXiv:1604.07998 (2016), in the process of publication.

[3] C. Addis, F. Ciccarello, M. Cascio, G. M Palma and S. Maniscalco, *Dynamical decoupling efficiency versus quantum non-Markovianity*, New J. Phys. **17** 123004 (2015).

[4] C. Addis, G. Karpat and S. Maniscalco, *Time-Invariant Discord in Dynamically Decoupled Systems*, Phys. Rev. A **92**, 062109 (2015).

[5] C. Addis, P. Haikka, S. McEndoo, C. Macchiavello and S. Maniscalco, *Two-qubit non-Markovianity induced by a common environment*, Phys. Rev. A **87**, 052109 (2013).

[6] C. Addis, G. Brebner, P. Haikka and S. Maniscalco, *Coherence trapping and information back-flow in dephasing qubits*, Phys. Rev. A **89**, 024101 (2014).

[7] C. Addis, T. Heinosaari, J. Kiukas, E-M. Laine and S. Maniscalco, *Dynamics of incompatibility of quantum measurements in open systems*, Phys. Rev. A **93**, 022114 (2016)

[8] C. Addis, G. Karpat, C Macchiavello and S. Maniscalco, *Memory effects in correlated quantum Channels*, arXiv:1607.00134 (2016), accepted for publication in Physical Review A.

[9] H.-P. Breuer and F. Petruccione, *The Theory of Open Quantum Systems*, (Oxford Univ. Press, 2007).

[10] U. Weiss, *Quantum Dissipative Systems*, 3rd. ed (World Scientific, Singapore, 2008).

[11] C. W. Gardiner and P. Zoller, *Quantum Noise* (Springer-Verlag, Berlin, 2010).

[12] M. A. Schlosshauer, *Decoherence and the Quantum-To-Classical Transition* (Springer-Verlag, Berlin, 2007).

[13] A. W. Chin, S. F. Huelga and M. B. Plenio, *Quantum Metrology in Non-Markovian Environments*, Phys. Rev. Lett. **109**, 233601 (2012).

[14] R. Vasile, S. Olivares, M. G. A. Paris and S. Maniscalco, *Continuous-variable quantum key distribution in non-Markovian channels*, Phys. Rev. A **83**, 042321 (2011).

[15] E.-M. Laine, H.-P. Breuer and J. Piilo, *Nonlocal memory effects allow perfect teleportation with mixed states*, Sci. Rep. **4**, 4620 (2014).

[16] B. Bylicka, D. Chruściński and S. Maniscalco, *Non-Markovianity and reservoir memory of quantum channels: a quantum information theory perspective*, Sci. Rep. **4**, 5720 (2014).

[17] S. F. Huelga, A. Rivas and M. B. Plenio, *Non-Markovianity-Assisted Steady State Entanglement*. Phys. Rev. Lett. **108**, 160402 (2012).

[18] R. Schmidt, A. Negretti, J. Ankerhold, T. Calarco and J. T. Stockburger, *Optimal Control of Open Quantum Systems: Cooperative Effects of Driving and Dissipation*, Phys. Rev. Lett. **107**, 130404 (2011).

[19] M. Thorwart, J. Eckel, J. H. Reina, P. Nalbach, S. Weiss, *Enhanced quantum entanglement in the non-Markovian dynamics of biomolecular excitons*, Chem. Phys. Lett. **478**, 234 (2009).

[20] G. R. Fleming, S. F. Huelga and M. B. Plenio, *Focus on quantum effects and noise in biomolecules*, New J. Phys. **13**, 115002 (2011).

[21] A. Rivas, S. F. Huelga and M. B. Plenio, *Entanglement and Non-Markovianity of Quantum Evolutions*, Phys. Rev. Lett. **105**, 050403 (2010).

[22] H.-P. Breuer, E.-M. Laine and J. Piilo, *Measure for the Degree of Non-Markovian Behaviour of Quantum Processes in Open Systems*, Phys. Rev. Lett. **103**, 210401 (2010).

[23] E.-M. Laine, J. Piilo and H-P. Breuer, *Measure for the non-Markovianity of quantum processes*, Phys. Rev. A **81**, 062115 (2010).

[24] S. Luo, S. Fu, S and H. Song, *Quantifying non-Markovianity via correlations*, Phys. Rev. A **86**, 044101 (2012).

[25] J. Luczka, *Spin in contact with thermostat: Exact reduced dynamics*, Physica A **167**, 919 (1990).

[26] G. M. Palma, K.-A. Suominen and A. K. Ekert, *Quantum Computers and Dissipation*, Proc. Roy. Soc. Lond. A **452** 567 (1996).

[27] J. H. Reina, L. Quiroga and N. F. Johnson, *Decoherence of quantum registers*, Phys. Rev. A **65**, 032326 (2002).

[28] S. John and T. Quang, *Spontaneous emission near the edge of a photonic band gap*, Phys. Rev. A **50**, 17641769 (1994).

[29] P. Facchi, S. Tasaki, S. Pacazio, H. Nakazato, A.Tokuse and D. A. Lidar, *Control of decoherence: Analysis and comparison of three different strategies*. Phys. Rev. A **71** 022302 (2005).

[30] P. Facchi, H. Nakazato and S. Pacazio, *From the quantum Zeno to the inverse quantum Zeno effect*, Phys. Rev. Lett. **86** 2699-2703 (2001).

[31] P. Facchi, D. A. Lidar and S. Pascazio, *Unification of dynamical decoupling and the quantum Zeno effect*, Phys. Rev. A **69** 032314 (2004).

[32] L. Viola and S. Lloyd, *Dynamical suppression of decoherence in two-state quantum systems*, Phys. Rev. A **58**, 2733 (1998).

[33] L. Viola, E. Knill and S. Lloyd, *Dynamical Decoupling of Open Quantum Systems*, Phys. Rev. Lett. **82** 2417 (1998).

[34] S. Sauer, C. Gneiting and A. Buchleitner, *Optimal Coherent Control to Counteract Dissipation*, Phys. Rev. Lett. **111**, 030405 (2013).

[35] B. Recht, Y. Maguire, S. Lloyd, I.L. Chuang, N.A. Gershenfeld, *Using unitary operations to preserve quantum states in the presence of relaxation*, arXiv:quant-ph/0210078 (2002).

[36] D. Sugny, C. Kontz and H. R. Jauslin, *Time-optimal control of a two-level dissipative quantum system*, Phys. Rev. A **76**, 023419 (2007).

[37] D. J. Tannor and A. Bartana, *On the Interplay of Control Fields and Spontaneous Emission in Laser Cooling*, J. Phys. Chem. A **103**, 10359 (1999).

[38] S. Lloyd and L. Viola, *Engineering quantum dynamics*, Phys. Rev. A **65**, 010101 (R) (2001).

[39] R. Roloff, M. Wenin and W. Pötz, *Optimal Control for Open Quantum Systems: Qubits and Quantum Gates*, J. Comput. Theor. Nanosci., **6**, 1837 (2009).

[40] A. Carlini, A. Hosoya, T. Koike and Y. Okudaira, *Time-Optimal Quantum Evolution*, Phys. Rev. Lett. **96**, 060503 (2006).

[41] A. Carlini, A. Hosoya, T. Koike and Y. Okudaira, *Time optimal quantum evolution of mixed states*, J. Phys. A: Math. Theor. **41** 045303 (2008).

[42] T. Caneva, M. Murphy, T. Calarco, R. Fazio, S. Montangero, V. Giovannetti, and G. E. Santoro, *Optimal Control at the Quantum Speed Limit*, Phys. Rev. Lett. **103**, 240501 (2009).

[43] P. Rebentrost, I. Serban, T. Schulte-Herbrüggen, and F. K. Wilhelm, *Optimal Control of a Qubit Coupled to a Non-Markovian Environment*, Phys. Rev. Lett. **102**, 090401 (2009).

[44] M. Lapert, Y. Zhang, M. Braun, S. J. Glaser and D. Sugny, *Singular Extremals for the Time-Optimal Control of Dissipative Spin $\frac{1}{2}$ Particles*, Phys. Rev. Lett. **104**, 083001 (2010).

[45] B. Hwang and H-S. Goan, *Optimal control for non-Markovian open quantum systems* , Phys. Rev. A **85**, 032321 (2012).

[46] D. M. Reich, N. Katz, C. P. Koch, *Exploiting Non-Markovianity of the Environment for Quantum Control*, Sci. Rep. **5**, 12430 (2015).

[47] J-S Tai, K-T Lin, H-S Goan, *Optimal control of quantum gates in an exactly solvable non-Markovian open quantum bit system*, Phys. Rev. A **89**, 062310 (2014).

[48] V. Mukherjee, V. Giovannetti, R. Fazio, S. F. Huelga, T. Calarco, S. Montangero, *Efficiency of quantum controlled non-Markovian thermalisation*, New J. Phys. **17** 063031 (2015).

[49] T. E. Hodgson, L. Viola and I. DAmico, *Towards optimised suppression of dephasing in systems subject to pulse timing constraints*, Phys. Rev. A **81** 062321 (2010).

[50] L. Viola and S. Lloyd, *Dynamical suppression of decoherence in two-state quantum systems*, Phys. Rev. A **58** 2733 (1998).

[51] L. Viola, E. Knill E and S. Lloyd, *Dynamical Decoupling of Open Quantum Systems*, Phys. Rev. Lett. **82** 2417 (1998).

[52] R. Lo Franco, A. D'Arrigo, G. Falci, G. Compagno, E. Paladino, *Preserving entanglement and nonlocality in solid-state qubits by dynamical decoupling*, Phys. Rev. B **90**, 054304 (2014).

[53] S. Singha Roy, T. S. Mahesh, and G. S. Agarwal, *Storing entanglement of nuclear spins via Uhrig dynamical decoupling*, Phys. Rev. A **83**, 062326 (2011).

[54] F. F. Fanchini, E. F. de Lima, L. K. Castelano, *Shielding quantum discord through continuous dynamical decoupling*, Phys. Rev. A **86**, 052310 (2012).

[55] A Rosario et al, *On the relationship between non-Markovianity and entanglement protection*, J. Phys. B: At. Mol. Opt. Phys. **45** 095501 (2012).

[56] B. Bellomo, R. Lo Franco, G. Compagno*Non-Markovian Effects on the Dynamics of Entanglement*, Phys. Rev. Lett. **99**, 160502 (2007).

[57] Jian-Song Zhang and Ai-Xi Chen, *Controlling sudden transitions of bipartite quantum correlations under dephasing via dynamical decoupling.* J. Phys. B: At. Mol. Opt. Phys. **47** 21 (2014).

[58] V. Madhok and A. Datta, *Interpreting quantum discord through quantum state merging*, Phys. Rev. A **83**, 032323 (2011).

[59] D. Cavalcanti, L. Aolita, S. Boixo, K. Modi, M. Piani and A. Winter, *Operational interpretations of quantum discord*, Phys. Rev. A. **83**, 032324 (2011).

[60] A. Streltsov, H. Kampermann and D. Bruss, *Quantum Cost for Sending Entanglement*, Phys. Rev. Lett. **108**, 250501 (2012)

[61] T. K. Chuan, H. Maillard, K. Modo, T. Paterek, M. Paternostro and M. Pianai, *Quantum Discord Bounds the Amount of Distributed Entanglement*, Phys. Rev. Lett. **109**, 070501 (2012).

[62] S. Boixo, L. Aolita, D. Cavalcanti, K. Modi, A. Winter, *Quantum locking of classical correlations and quantum discord of classical-quantum states*, Int. J Quant. Inf. **9**, 1643 (2011).

[63] M. F. Cornélio, M. C. de Oliveira and F. F. Fanchni, *Entanglement Irreversibility from Quantum Discord and Quantum Deficit*, Phys. Rev. Lett. **107**, 020502 (2011).

[64] A. Streltsov, H. Kampermann and D. Bruss, *Linking Quantum Discord to Entanglement in a Measurement*, Phys. Rev. Lett. **106**, 160401 (2011).

[65] T. Werlang, C. Trippe, G. A. P. Ribeiro and G. Rigolin, *Quantum Correlations in Spin Chains at Finite Temperatures and Quantum Phase Transitions*, Phys. Rev. Lett. **105**, 095702 (2010).

[66] P. Haikka, T. H. Johnson and S. Maniscalco, *Non-Markovianity of local dephasing channels and time-invariant discord.* Phys. Rev. A **87** 010103(R) (2013)

[67] H. -P. Breuer, E. -M. Laine, J. Piilo, and B. Vacchini, *Non-Markovian dynamics in open quantum systems*, arXiv:1505.01385 (2015).

[68] E. C. G. Sudarshan, P. M. Mathews, and J. Rau, *Stochastic Dynamics of Quantum-Mechanical Systems*, Phys. Rev. **121**, 920 (1961).

[69] T. F. Jordan and E. C. G. Sudarshan, *Dynamical mappings of density operators in quantum mechanics*, Journal of Mathematical Physics **2**, 772 (1961).

[70] M. D. Choi, *Completely positive linear maps on complex matrices*, Can. J. Math. **24**, 520 (1972).

[71] W. H. Zurek, *Pointer basis of quantum apparatus: Into what mixture does the wave packet collapse?*, Phys. Rev. D **24**, 1516 (1981).

[72] W. H. Zurek, *Environment-induced superselection rules*, Phys. Rev. D **26**, 1862 (1982).

[73] W. H. Zurek, *Decoherence, einselection, and the quantum origins of the classical*, Rev. Mod. Phys. **75**, 715 (2003)

[74] A. Jamiolkowski, *Linear transformations which preserve trace and positive semidefiniteness of operators*, Rep. Math. Phys. **3** 275 (1972)

[75] M.-D. Choi, *Completely positive linear maps on complex matrices*, Lin. Alg. and Appl. **10**, 285 (1975).

[76] K. Kraus, States, *Effects and Operations* (Spring-Verlag, Berlin, 1983).

[77] C. A. Rodriguez-Rosario, K. Modi, A. Kuah, A. Shaji, and E. C. G. Sudarshan, *Completely positive maps and classical correlations*. J. Phys. A: Math Theor. **41**, 205301 (2008).

[78] A. Shabani and D. A. Lidar, *Vanishing Quantum Discord is Necessary and Sufficient for Completely Positive Maps*, Phys. Rev. Lett. **102**, 100402 (2009).

[79] C. A. Rodriguez-Rosario, K. Modi, and A. Aspuru-Guzik, *Linear assignment maps for correlated system-environment states*, Phys. Rev. A **81**, 012313 (2010).

[80] G. Lindblad, *On the generators of quantum dynamical semigroups*, Commun. Math. Phys. **48**, 119 (1976).

[81] V. Gorini, A. Kossakowski, and E. C. G. Sudarshan, *Completely positive dynamical semigroups of Nlevel systems*, J. Math. Phys. **17**, 821 (1976).

[82] M. M. Wolf and J. I. Cirac, *Dividing Quantum Channels*, Commun. Math. Phys. **279**, 147 (2008).

[83] D. Walls and G. Milburn, *Quantum Optics* (Springer-Verlag, Berlin, 1994).

[84] C. W. Lai, P. Malentinsky, A. Badolato and A. Imamogula, *Knight-Field-Enabled Nuclear Spin Polarisation in Single Quantum Dots*, Phys. Rev. Lett. **96**, 167403 (2006).

[85] M. H. Devoret, A. Wallraff and J. M. Martinis, *Superconducting Qubits: A Short Review*, arXiv 0411174 (2004).

[86] E. Yablonovitch, *Inhibited Spontaneous Emission in Solid-State Physics and Electronics*, Phys. Rev. Lett. **58**, 2059 (1987).

[87] P. Lambropoulos, G. M. Nikolopoulos, T. R. Nielsen and S. Bay, *Fundamental quantum optics in structured reservoirs*, Rep. Prog. Phys. **63**, 455 (2000).

[88] A. Rivas, S. F. Huelga, and M. B. Plenio, *Quantum non-Markovianity: characterization, quantification and detection*, Rep. Prog. Phys. **77**, 094001 (2014).

[89] S. Maniscalco, *Limits in the characteristic-function description of non-Lindblad-type open quantum systems*, Phys. Rev. A **72**, 024103 (2005).

[90] S. Barnett and S. Stenholm, *Hazards of reservoir memory*, Phys. Rev. A **64**, 033808 (2001).

[91] B. J. Dalton, Stephen M. Barnett, and B. M. Garraway, *Theory of pseudomodes in quantum optical processes*, Phys. Rev. A **64**, 053813 (2001).

[92] F. Intravaia, S. Maniscalco, and A. Messina, *Density-matrix operatorial solution of the non-Markovian master equation for quantum Brownian motion*, Phys. Rev. A **67**, 042108 (2013).

[93] S. Nakajima, *On Quantum Theory of Transport Phenomena: Progress of Steady Diffusion*, Progr. Theor. Phys. **20**, 948-959 (1958).

[94] R. Zwanzig, *Ensemble Method in the Theory of Irreversibility*, J. Chem. Phys. **33**, 1338 (1960).

[95] R. Vasile, S. Maniscalco, M. G. A. Paris, H.-P. Breuer and J. Piilo, *Quantifying non-Markovianity of continuous-variable Gaussian dynamical maps*, Phys. Rev. A **84**, 052118 (2011).

[96] X.-M. Lu, X. Wang and C.P. Sun, *Quantum Fisher information flow and non-Markovian processes of open systems*, Phys. Rev. A **82**, 042103 (2010).

[97] S. Lorenzo, F. Plastina, and M. Paternostro, *Geometrical characterisation of non-Markovianity*, Phys. Rev. A **88**, 020102(R) (2013).

[98] P. Haikka, J. D. Cresser, and S. Maniscalco, *Comparing different non-Markovianity measures in a driven qubit system*, Phys. Rev. A **83**, 012112 (2011).

[99] B. Vacchini, A. Smirne, E.-M. Laine, J. Piilo, and H.-P. Breuer, *Markovian and non-Markovian dynamics in quantum and classical systems*, New J. Phys. **13**, 093004 (2011).

[100] D. Chruscinski, A. Kossakowski, and A. Rivas, *Measures of non-Markovianity: Divisibility versus backflow of information*, Phys. Rev. A **83**, 052128 (2011).

[101] J. Piilo, S. Maniscalco, K. Harkonen, K.-A. Suominen, *Non-Markovian Quantum Jumps*, Phys. Rev. Lett. **100**, 180402 (2008).

[102] S. Wissmann, A. Karlsson, E.-M. Laine, J. Piilo, H.-P. Breuer, *Optimal state pairs for non-Markovian quantum dynamics*, Phys. Rev. A **86**, 062108 (2012).

[103] D. Petz, *Monotone Metrics on Matrix Spaces*, Linear Algebra Appl. 244, **81** (1996).

[104] D. Chruściński and S. Maniscalco, *Degree of Non-Markovianity of Quantum Evolution*, Phys. Rev. Lett. **112**, 120404 (2014).

[105] B. Schumacher and M. A. Nielsen, *Quantum data processing and error correction*. Phys. Rev. A **54**, 26292635 (1996).

[106] A. S. Holevo and V. Giovannetti, *Quantum channels and their entropic characteristics*, Rep. Prog. Phys. **75**, 046001 (2012).

[107] S. Lloyd, *Capacity of the noisy quantum channel*, Phys. Rev. A **55**, 16131622 (1997).

[108] I. Devetak and P. W. Shor, *The Capacity of a Quantum Channel for Simultaneous Transmission of Classical and Quantum Information*, Commun. Math. Phys. **256**, 287-303 (2005).

[109] P. Haikka, S. McEndoo, G. De Chiara, M. Palma, S. Maniscalco, *Quantifying, characterizing, and controlling information flow in ultracold atomic gases*, Phys. Rev. A **84**, 031602 (2011).

[110] F. F. Fanchini, G. Karpat, L. K. Castelano and D. Z. Rossatto, *Probing the degree of non-Markovianity for independent and common environments*, Phys. Rev. A **88**, 012105 (2013).

[111] E.-M. Laine, H.-P. Breuer, J. Piilo, C.-F. Li, and G.-C. Guo, *Nonlocal Memory Effects in the Dynamics of Open Quantum Systems*, Phys. Rev. Lett. **108**, 210402 (2012).

[112] Z. He, J. Zou, L. Li, and Bin Shao, *Effective method of calculating the non-Markovianity for single-channel open systems*, Phys. Rev. A **83**, 012108 (2011).

[113] I. Devetak and P. W. Shor, *The Capacity of a Quantum Channel for Simultaneous Transmission of Classical and Quantum Information*, Commun. Math. Phys. **256**, 287-303 (2005).

[114] S. McEndoo, P. Haikka, G. De Chiara, M. Palma, S. Maniscalco, *Entanglement control via reservoir engineering in ultracold atomic gases.*, EPL **101** 60005 (2013).

[115] M. A. Cirone, G. De Chiara, G. M. Palma and A. Recati, *Collective decoherence of cold atoms coupled to a BoseEinstein condensate*, New J. Phys. **11**, 103055 (2009).

[116] I. S. Gradshteyn and I. M. Ryzhik, *Table Integral, Series,and Products* (Academic, New York, 1980), p. 931.

[117] H.-S. Zeng, N. Tang, Yan-Ping Zheng, and Guo-You Wang, *Equivalence of the measures of non-Markovianity for open two-level systems*, Phys. Rev. A **84**, 032118 (2011).

[118] R. Vasile, F. Galve and Roberta Zambrini, *Spectral origin of non-Markovian open-system dynamics: A finite harmonic model without approximations*, Phys. Rev. A **89**, 022109 (2014).

[119] V. Giovannetti and R. Fazio, *Information-capacity description of spin-chain correlations*, Phys. Rev. A **71**, 032314 (2005).

[120] G. Benenti, A. D' Arrigo and G. Falci, emphEnhancement of Transmission Rates in Quantum Memory Channels with Damping, Phys. Rev. Lett. **103**, 020502 (2009).

[121] M. Wilde, *Quantum Information Theory*, (Cambridge Univ. Press, 2013).

[122] B. Bellomo, R. Lo Franco, and G. Compagno, *Non-Markovian Effects on the Dynamics of Entanglement*, Phys. Rev. Lett. **99**, 160502 (2007).

[123] R. Lo Franco, B. Bellomo, S. Maniscalco and G. Compagno, *Dynamics of quantum correlations in two-qubit systems within non-Markovian environments*, Int. J. Mod. Phys. B **27**, 1245053 (2013).

[124] L. Mazzola, S. Maniscalco, J. Piilo, K.-A. Suominen and B. M. Garraway, *Sudden death and sudden birth of entanglement in common structured reservoirs*, Phys. Rev. A **79**, 042302 (2009).

[125] J. T. Barreiro *et al*, *An open-system quantum simulator with trapped ions*, Nature **470** , 486-491 (2011).

[126] M. J. Biercuk *et al*, *Optimised dynamical decoupling in a model quantum memory*, Nature **458**, 996-1000 (2009).

[127] B.-H. Liu *et al*, *Experimental control of the transition from Markovian to non-Markovian dynamics of open quantum systems*, Nature Phys. **7**, 931934 (2011).

[128] S. Cialdi, D. Brivio, E. Tesio and M. G. A. Paris, *Programmable entanglement oscillations in a non-Markovian channel*, Phys. Rev. A **83**, 042308 (2011).

[129] D. Chruściński, A. Kossakowski, *Witnessing non-Markovianity of quantum evolution*, Eur. Phys. J. D. **68** 7 (2014).

[130] L. Viola and S. Lloyd, *Dynamical suppression of decoherence in two-state quantum systems*, Phys. Rev. A **58**, 2733 (1998).

[131] L. Viola, E. Knill and S. Lloyd, *Dynamical Decoupling of Open Quantum Systems*, Phys. Rev. Lett. **82**, 2417 (1998).

[132] J. T. Barrieiro *et al*, *An Open-System Quantum Simulator with Trapped Ions*, Nature **470**, 486-491 (2011).

[133] M. J. Biercuk *et al*, *Optimised dynamical decoupling in a model quantum memory*, Nature **458**, 996-1000 (2009).

[134] B.-H. Liu *et al*, *Experimental control of the transition from Markovian to non-Markovian dynamics of open quantum systems*, Nature Physics **7**, 931934 (2011).

[135] B-H Liu, L. Li, Y-F. Huang, C-F. Li, G-C. Guo, E-M. Laine, H-P Breuer, J. Piilo, *Experimental control of the transition from Markovian to non-Markovian dynamics of open quantum systems*, Nature Phys. **7**, 931-934 (2011).

[136] T. J. G. Apollaro, C. Di Franco, F. Plastina, and M. Paternostro, *Memory-keeping effects and forgetfulness in the dynamics of a qubit coupled to a spin chain*, Phys. Rev. A **83**, 032103 (2011).

[137] S. Sauer, Dissertation, *Entanglement in periodically driven quantum systems*, Albert-Ludwigs-Universität Freiburg (2013).

[138] T. E. Hodgson, L. Viola and I. D'Amico, *Towards optimised suppression of dephasing in systems subject to pulse timing constraints*, Phys. Rev. A **81**, 062321 (2010).

[139] T. E. Hodgson, L. Viola, and I. DAmico, *Decoherence-protected storage of exciton qubits through ultrafast multipulse control*, Phys. Rev. B **78**, 165311 (2008).

[140] A. Smirne, J. Kolodynski, S. F. Huelga, R. Demkowicz-Dobrzanski, *The ultimate precision limits for noisy frequency estimation*, Phys. Rev. Lett. **116**, 120801 (2016).

[141] E. L. Hahn, *Spin Echoes*, Phys. Rev. **80**, 580 (1950)

[142] K. Khodjasteh and D. A. Lidar, *Fault-Tolerant Quantum Dynamical Decoupling*, Phys. Rev. Lett, **95**, 180501 (2005).

[143] K. Khodjasteh and D.A. Lidar, *Performance of deterministic dynamical decoupling schemes: Concatenated and periodic pulse sequences*, Phys. Rev. A **75**, 062310 (2007).

[144] U. Haeberlen, *High Resolution NMR in Solids: Selective Averaging* (Academic Press, New York) (1976).

[145] C. P. Slichter, *Principles of Magnetic Resonance* (Springer-Verlag, New York) (1992).

[146] H. Y. Carr and E. M. Purcell, *Effects of Diffusion on Free Precession in Nuclear Magnetic Resonance Experiments*, Phys, Rev. **94** 630 (1954).

[147] S. Meiboom and D. Gill, *Modified SpinEcho Method for Measuring Nuclear Relaxation Times*, Rev. Sci. Instrum **29** 688 (1958).

[148] U. Haeberlen and J. S Waugh, *Coherent Averaging Effects in Magnetic Resonance*, Phys. Rev. **175**, 453 (1968).

[149] C. Arenz, R. Hillier, M. Fraas, D. Burgarth, *Distinguishing decoherence from alternative quantum theories by dynamical decoupling*, Phys. Rev. A **92** 022102 (2015).

[150] G. S. Uhrig, *Keeping a Quantum Bit Alive by Optimised π-Pulse Sequences*, Phys. Rev. Lett. **98** 100504 (2007).

[151] G. S. Uhrig, *Exact results on dynamical decoupling by π pulses in quantum information processes*, New J. Phys. **10** 083024 (2008).

[152] M. J. Biercuk *et al*, *Optimised dynamical decoupling in a model quantum memory*, Nat. **458** 996-1000 (2008).

[153] H. Uys, M. J. Biercuk and J. J. Bollinger, *Optimised Noise Filtration through Dynamical Decoupling*, Phys. Rev. Lett. **103**, 040501 (2009).

[154] Ł. Cywiński, R. M. Lutchyn, C. P. Nave and S. Das Sarma, *How to Enhance Dephasing Time in Superconducting Qubits*, Phys. Rev. B **77** 174509 (2008).

[155] Y. Nakamura, A. Pashkin, T. Yamamoto and J. S. Tsai, *Charge Echo in a Cooper-Pair Box*, Phys. Rev. Lett. **88**, 047901 (2002).

[156] F. Yoshihara, K. Harrabi, A. O. Niskanen, Y. Nakamura and J. S. Tsai, *Decoherence of Flux Qubits due to 1/f Flux Noise*, Phys. Rev. Lett. **97**, 167001 (2006).

[157] Kakuyanagi K *et al*, *Dephasing of a Superconducting Flux Qubit*, Phys. Rev. Lett. **98**, 047004 (2007).

[158] R. C. Bialcazk, *et al*, *1/f Flux Noise in Josephson Phase Qubits*, Phys. Rev. Lett. **99** ,187006 (2007).

[159] Y. A. Pashkin, O. Astafiev, T. Yamamoto, Y. Nakamura and J. S. Tasi, *Josephson charge qubits: a brief review*, Quantum Inf. Process. **8**, 55 (2009).

[160] X. Hu and S. Das Sarma, *Charge-Fluctuation-Induced Dephasing of Exchange-Coupled Spin Qubits*, Phys. Rev. Lett. **96**, 100501 (2006).

[161] G. Ramon and X. Hu, *Decoherence of spin qubits due to a nearby charge fluctuator in gate-defined double dots*. Phys. Rev. B **81**, 045304 (2010).

[162] I. Almog *et al*, *Direct Measurement of the System-Environment Coupling as a Tool For Understanding Decoherence and Dynamical Decoupling*, J. Phys. B: At. Mol. Opt. Phys. **44** 154006 (2011).

[163] N. Gisin, I. C. Percival, *Quantum State Diffusion: from Foundations to Applications*, arXiv 9701024 (1997).

[164] J. Dalibard, Y. Castin, and K. Molmer, *Wave-function approach to dissipative processes in quantum optics*, Phys. Rev. Lett. **68**, 580 (1992).

[165] B. Bylicka, M. Tukiainen, J. Piilo, D. Chruscinski, S. Maniscalco, *Thermodynamic meaning and power of non-Markovianity*. arXiv:1504.06533 (2015).

[166] Gilles, Brassard, *Quantum cryptography: Public-key distribution and coin tossing*, Proceedings of IEEE International Conference on Computers, Systems and Signal Processing 1984. IEEE Computer Society. pp.175-179, (1984).

[167] M.A. Nielsen and I.L. Chuang, *Quantum Computation and Quantum Information*, (Cambridge, Cambridge University Press, 2000).

[168] P. W. Shor, *Algorithms for quantum computation: Discrete logarithms and factoring*, in Proceedings of the 35th Annual Symposium on Foundations of Computer Science, IEEE Computer Society Press, Los Alamitos, CA, pp. 124D134, (1994).

[169] A. Einstein, B. Podolsky, N Rosen, *Can Quantum-Mechanical Description of Physical Reality Be Considered Complete?*, Phys. Rev. **47** 777780 (1935).

[170] R. Horodecki, P. Horodecki, M. Horodecki, and K. Horodecki, *Quantum entanglement*, Rev. Mod. Phys. **81**, 865 (2009).

[171] C.H. Bennett, D.P. DiVincenzo, J.A. Smolin and W.K. Wootters, *Mixed state entanglement and quantum error correction*, Phys. Rev. A **54** 3824 (1996).

[172] S. Hill and W.K. Wootters, *Entanglement of a pair of quantum bits*, Phys. Rev. Lett. **78** 5022 (1997).

[173] W.K. Wootters, *Entanglement of formation of an arbitrary state of two qubits*, Phys. Rev. Lett. **80** 2245 (1998).

[174] W.K. Wootters, *Entanglement of formation and concurrence*, Quantum Information and Computation **1** 27 (2001).

[175] K. Modi, A. Brodutch, H. Cable, T. Paterek, and V. Vedral, *The classical-quantum boundary for correlations: Discord and related measures*, Rev. Mod. Phys. **84**,1655 (2012).

[176] H. Ollivier and W. H. Zurek, *Quantum Discord: A Measure of the Quantumness of Correlations*. Phys. Rev. Lett. **88**, 017901 (2001).

[177] L. Henderson, and V. Vedral, *Classical, quantum and total correlations*. J. Phys. A **34**, 6899 (2001).

[178] S. Luo. *Quantum discord for two-qubit systems*, Phys. Rev. A **77**, 042303 (2008).

[179] M. Ali, A. R. P. Rau and G. Alber, *Quantum discord for two-qubit X states*, Phys. Rev. A **81** 042105 (2010).

[180] P. Giorda and M. Paris, *Gaussian Quantum Discord*, Phys. Rev. Lett. **105**, 020503 (2010).

[181] G. Adesso and A. Datta, *Quantum versus classical correlations in Gaussian states*, Phys. Rev. Lett. **105**, 030501 (2010).

[182] T. Werlang, S. Souza, F. F. Fanchini, C. J. Villas-Boas, *Robustness of quantum discord to sudden death*, Phys. Rev. A **80**, 024103 (2009).

[183] J. Maziero, L. C. Celeri, R. M. Serra, V. Vedral, *Classical and quantum correlations under decoherence*, Phys. Rev. A **80**, 044102 (2009).

[184] F. F. Fanchini, T.Werlang, C. A. Brasil, L. G. E. Arruda, A. O. Caldeira, *Non-Markovian dynamics of quantum discord*, Phys. Rev. A **81**, 052107 (2010).

[185] R. Vasile, P. Giorda, S. Olivares, M. G. A. Paris, and S. Maniscalco, *Nonclassical correlations in non-Markovian continuous-variable systems*, Phys. Rev. A **82**, 012313 (2010).

[186] T. Werlang, S. Souza, F. F. Fanchini and C. J. Villas Boas, *Robustness of quantum discord to sudden death*, Phys. Rev. A **80**, 024103 (2009).

[187] T. Yu and J. H. Eberly, *Finite-Time Disentanglement Via Spontaneous Emission*, Phys. Rev. Lett. **93**, 140404 (2004)

[188] T. Yu and J. H. Eberly, *Quantum Open System Theory: Bipartite Aspects*, Phys. Rev. Lett. **97**, 140403

[189] L. Mazzola, J. Piilo and S. Maniscalco, *Sudden Transition between Classical and Quantum Decoherence*. Phys. Rev. Lett **104** 200401 (2010).

[190] L. Mazzola, J. Piilo, and S. Maniscalco, *Frozen discord in non-Markovian dephasing channels*, Int. J. Quant. Inf., **09** 981-991 (2011).